Large Eddy Simulation of Fuel Spray Combustion

Armin Wehrfritz

Aalto University

Large Eddy Simulation of Fuel Spray Combustion

Armin Wehrfritz

A doctoral dissertation completed for the degree of Doctor of Science (Technology) to be defended, with the permission of the Aalto University School of Engineering, at a public examination held at the lecture hall 216 (K1) of the school on 14 October 2016 at 12.

Aalto University
School of Engineering
Department of Mechanical Engineering
Thermodynamics and Combustion Technology

Supervising professor
Assistant Professor Ville Vuorinen, Aalto University, Finland

Thesis advisor
Doctor Ossi Kaario, Aalto University, Finland

Preliminary examiners
Doctor Joseph Oefelein, Sandia National Laboratories, USA
Doctor Sibendu Som, Argonne National Laboratories, USA

Opponents
Professor Andreas Kempf, University Duisburg-Essen, Germany

NORDIC ECOLABEL

441   697
Printed matter

Abstract

Combustion is the main source for energy today and in the foreseeable future. It is used in a wide range of applications for power generation and transportation systems, such as internal combustion engines. In order to improve the efficiency of such systems and to reduce the emission of pollutants, a better understanding of the physical and chemical processes related to combustion is required. Fuel sprays play a major role in combustion systems like diesel engines, which is the topic of this thesis. Large Eddy Simulation (LES) constitutes an advanced computational method that has gained more attention in the recent years, as it allows for detailed investigations of the unsteady flow and combustion phenomena that occur in internal combustion engines.

The present dissertation belongs to the field of computational physics, more precisely to computational fluid dynamics and combustion. For the research this thesis comprises, the LES method is employed to investigate turbulent spray combustion in the context of diesel engines. A challenge arises from the description of the complex chemical reactions that take place during the oxidation of fuels used in such engines. The approach to address this in the present work is based on the Flamelet Generated Manifold (FGM) method, which allows to take a detailed description of these reactions into account while the computational cost remains feasible. The objectives of the dissertation are to explore and implement modeling approaches which allow to investigate high-velocity fuel sprays, and specifically their ignition and combustion characteristics, in LES. The investigated spray combustion cases correspond to Spray A, a reference case defined within the Engine Combustion Network (ECN).

The resolution of the computational mesh and the implications of modeling fuel sprays in LES were first studied in non-reacting simulations. The results indicate that an adequate mesh resolution is crucial to the simulation approach. Investigations of canonical combustion systems with two chemical mechanisms show that the mechanism significantly affects the prediction of the ignition timing. The results of the turbulent spray combustion simulations give insight into the ignition process and flame stabilization. A comparison of the results from LES and novel experimental data of hydroxyl and formaldehyde show a good agreement. The results further show that the chosen approach towards the simulation of turbulent spray flames is suitable and allows for a detailed analysis of the unsteady processes. An important achievement of this work is the implementation of the FGM method in the open-source flow solver OpenFOAM.

Keywords Large Eddy Simulation, Flamelet Generated Manifold, combustion, spray, engine

Preface

Carrying out the research and studies that lead to this doctoral dissertation gave me a great opportunity to learn and to gain experience in many regards. This does not only concern the topics of my research like fluid mechanics, combustion or numerical simulation, but also the planing and publishing of scientific research, and most importantly collaborating with fellow researchers. Many people have contributed to the realization of this dissertation and I am grateful for the help and support I received.

I am very grateful that I had the chance to work in the Thermodynamics and Combustion Technology research group at Aalto University. The research group is lead by Prof. Martti Larmi, my first supervisor, who has contributed greatly to my knowledge of internal combustion engines and the academic work life.

I am especially thankful for Prof. Ville Vuorinen with whom I worked closely during the course of my doctoral studies, and who finally became my supervisor. I very much appreciate that I had the opportunity to work with Large Eddy Simulation, and I am very grateful for all his guidance regarding fluid mechanics, high-performance computing and many other topics related to this research project.

I am very grateful to my instructor Dr. Ossi Kaario for guiding my research, and especially for initiating the spray research project concerned with the ECN target conditions. Also for the proof-reading of my reports and publications and the valuable comments I am very grateful.

My research visit to TU Eindhoven, The Netherlands was a great experience, not only because of the knowledge I gained on combustion research, but also because of the people I worked with. Most notably Prof. Bart Somers, whose guidance on combustion modeling and spray combustion research contributed to the success of this work.

My sincerest thanks to the pre-examiners, Dr. Joseph Oefelein and Dr. Sibendu Som, for their time and effort to read and comment on my dissertation. Their constructive feedback helped to improve the quality of this dissertation. Similarly, I am grateful to Prof. Andreas Kempf for

arranging the time to act as my opponent in the public defense.

I would like to express my sincere gratitude to my friends and colleagues that were part of this journey. This concerns especially my office mates at Aalto University: Jukka-Pekka, Karri, Heikki, Mahdi, it has been a pleasure to work with you and I enjoyed the interesting discussions on all kind of topics, be it research related or not. But also the people that made my stay in Eindhoven such a pleasant experience shall not be left unmentioned: Alessio, Francisco, Cemil, Ulaş, Shridar, it was great fun to work with you, as well as spending time outside of work.

I would like to thank my parents, Regine and Gerhard, for their constant support and encouragement throughout my life. Not any less to mention the cheering conversations and advice from my siblings, Holger and Carolin, who more than once reminded me that this thesis is not everything in life.

To conclude, I want to thank Tiia for listening to my endless stories about work, life, or anything else that comes to my mind. You kept me on track throughout this, sometimes difficult, journey with your always positive attitude. Thank you!

Espoo, September, 2016,

Armin Wehrfritz

Contents

List of Publications

This thesis consists of an overview and of the following publications which are referred to in the text by their Roman numerals.

I Armin Wehrfritz, Ville Vuorinen, Ossi Kaario and Martti Larmi. Large Eddy Simulation of High-Velocity Fuel Sprays: Studying Mesh Resolution and Breakup Model Effects for Spray A. *Atomization and Sprays*, 23 (5), 419–442, doi: 10.1615/AtomizSpr.2013007342, 2013.

II Armin Wehrfritz, Ville Vuorinen, Ossi Kaario and Bart Somers. Large Eddy Simulation of *n*-dodecane spray flames using Flamelet Generated Manifolds. *Combustion and Flame*, 167, 113–131, doi: 10.1016/j.combustflame.2016.02.019, 2016.

III Heikki Kahila, Armin Wehrfritz, Ville Vuorinen, Ossi Kaario, Mahdi Ghaderi Masouleh, Noud Maes and Bart Somers. Large Eddy Simulation on the Influence of Injection Pressure in Reacting Spray A. *Combustion and Flame*, submitted, 2016.

Author's Contribution

Publication I: "Large Eddy Simulation of High-Velocity Fuel Sprays: Studying Mesh Resolution and Breakup Model Effects for Spray A"

The author was the lead author, carried out the simulations and post-processed the data. The work was initiated by the co-authors and the applied modeling concepts are based on previous research of V. Vuorinen and O. Kaario. The author was responsible for the case setup, particularly the mesh generation, choice of the mesh resolution and the flow solver settings, with the guidance of V. Vuorinen and O. Kaario. The author was mainly responsible for the analysis of the results and writing of the article, with constructive feedback and suggestions for improvements by the co-authors.

Publication II: "Large Eddy Simulation of *n*-dodecane spray flames using Flamelet Generated Manifolds"

The author was fully responsible for the design of the research in this article. The author developed and implemented the spray combustion simulation approach using LES and FGM within the OpenFOAM framework. B. Somers provided insight and guidance on the FGM combustion model, specifically during the author's research visit at TU Eindhoven, The Netherlands. The author planned and carried out the simulations, post-processed the data and analyzed the results. The co-authors participated in the analysis and interpretation of the results. The article was mainly written by the author, except for parts of the cool flame analysis which were contributed by V. Vuorinen.

Publication III: "Large Eddy Simulation on the Influence of Injection Pressure in Reacting Spray A"

The author is responsible for the idea of the article and initiated the research. The author developed and implemented the computational framework and case setup for the simulations, was very tightly involved in all phases of the study, and contributed substantially to the analysis of the results, as well as writing of the manuscript. The simulations in this study were carried out by H. Kahila. The experimental work related to the PLIF measurements was carried out by N. Maes at TU Eindhoven. The respective data analysis and LES–PLIF comparison was done by the author (A. Wehrfritz). The POD analysis is based on previous work by V. Vuorinen and was carried out by H. Kahila in this study. All co-authors contributed to the discussion of the results and commented on the manuscript.

1. Introduction

In the following, a general introduction and motivation for combustion research is given including a phenomenological description of fuel sprays. Thereafter, the fundamental aspects of fluid motion and combustion are introduced, followed by the scope and an outline of the thesis.

1.1 Motivation and background

Over the past century, the global energy demand has been steadily growing [1]. The growing demand for energy has mostly been met with fossil energy sources and this trend is likely to continue for the foreseeable future. Despite the increasing efforts in finding alternative energy sources, several key issues remain unresolved, specifically with respect to the local availability and the storage of energy from alternative sources. Finding alternative fuels for transportation systems can be particularly challenging, since a high energy storage density is necessary for practical applications.

Liquid fuels have found widespread usage in the transportation sector, due to their availability, high energy density and the highly developed technologies of the respective combustion systems, such as internal combustion engines and aircraft combustors. During the last decades, it has however become evident that combustion engines have certain disadvantages. First, emissions like nitrogen oxides (NOx) and particulate matter (PM) have been shown to have harmful effects on the human health and the environment. This has been identified by the legislative bodies and has led to increasingly stringent emission limits (e.g. [2]) for the various combustion systems used in transport, power and heat generation.

Another problem related to combustion of hydrocarbon fuels obtained from fossil sources is the emission of carbon dioxide (CO_2), which is generally deemed as a greenhouse gas. Apart from the global environmental

impact, the emission of CO_2 is an indicator for the overall energy consumption, as it is a direct product of combustion of any hydrocarbon fuel. The increase of global CO_2 emissions from fossil fuels is shown in Fig. 1.1. The significant increase of CO_2 emissions from liquid sources staring in
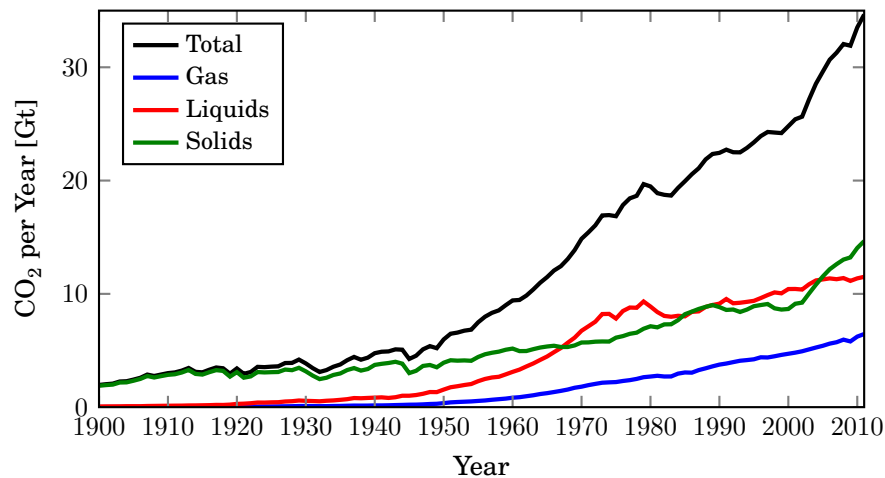
Figure 1.1 – Trend in CO_2 emissions from fossil fuel combustion. Source: Boden et al. [3]

the 1960's can in large parts be attributed to the growing energy demand in the transportation sector. With the former mentioned environmental impact of fossil fuels, the development of alternative fuel sources, as well as a more efficient usage and cleaner combustion concepts are paramount to ensure sustainable continuation for the transportation of people and goods.

Promising new combustion concepts aim at low temperature combustion (LTC) [4–6] in order to increase the fuel efficiency and to reduce harmful emissions. Particularly, in the research and development of internal combustion engines, LTC concepts have gained significant attention. The common idea of these concepts is to reduce the peak combustion temperature, due to a change in the reactivity of the fuel and/or the heat capacity of the mixture. The former is often associated with blending fuels of different reactivities. The latter can be achieved by operating the engine at very fuel-lean conditions or by a dilution of the fuel-air mixture through the recirculation of exhaust gases. With respect to the development of diesel engines, which are particularly interesting due to their high thermal efficiency, LTC concepts have been shown to significantly reduce the otherwise high NOx or PM emission. The working principle of a diesel, i.e. compression ignition (CI), engine can be found in many text books, e.g. [7, 8]. Next, the fundamentals of the mixture formation and combustion

are briefly introduced.

1.2   Diesel fuel spray physics and chemistry

Since the 1990's, the prevailing approach to the formation of a fuel-air mixture in diesel engines is the direct injection of liquid fuel into the combustion chamber. The liquid jet, or spray, that is formed when the pressurized fuel exits the injector leads to an inherently inhomogeneous mixture and involves many complex physical processes. The understanding of these processes is of key importance in the development of advanced combustion modes, such as within the LTC concepts. The main aspects of the underlying physical processes are described in the following.

Injection systems in modern diesel engines are operated at high pressures up to $250\,\mathrm{MPa}$ and the diameter of the injector nozzle is in the order of $100\,\mathrm{\mu m}$ [8, 9]. A simple Bernoulli law estimate shows that the turbulent liquid fuel jet may reach velocities of $600\,\mathrm{m\,s^{-1}}$. The liquid fuel undergoes rapid atomization due to the aerodynamic forces resulting from the large velocity difference between the ambient air and the liquid. With the disintegration of the liquid jet and the entrainment of hot ambient gas, the liquid fuel evaporates and subsequent turbulent mixing takes place. The vapor jet induced by the liquid fuel spray will further mix and chemically react with the ambient gas. A more detailed description of the processes related to liquid fuel jets and sprays is given in the textbooks [9–11] and will also be further discussed in the latter part of this thesis.

The diesel combustion process has been subject to experimental and computational research for several decades and the phenomenological understanding of the diesel combustion mode is fairly well established. The conventional diesel combustion mode can be regarded as *mixing limited*, because the process is governed by the mixture formation (i.e. fuel injection, atomization, evaporation and mixing). The fuel is injected close to the point of the highest pressure and temperature in the compression stroke of the engine. The ambient conditions (i.e. air mass and gas composition) are such that auto-ignition takes place very rapidly after favorable conditions are formed due to mixing. The combustion process following the ignition is dependent on the supply of fuel and the mixing rate. This process is called nonpremixed combustion, also referred to as combustion in a diffusion flame. This diffusion flame envelopes the fuel jet and stabilizes at a certain location downstream of the injector. The associated chemical

processes are fast and the diffusion flame is governed by high-temperature reactions. Hence, the fuel consumption rate is not limited by chemistry in this combustion mode.

The situation is different for the LTC concepts, where the different fuel reactivities or ambient conditions lead to a larger delay between injection and ignition, and hence combustion. Various approaches have been introduced, including the Homogeneous Charge Compression Ignition (HCCI), Reactivity Controlled Compression Ignition (RCCI) or Partially Premixed Combustion (PPC). In LTC concepts, the time for the fuel to mix with the ambient gases is typically longer compared to the conventional diesel combustion, which leads to a more homogenous mixture and distributed ignition locations. Thus, ignition and combustion are not anymore dominated by the fuel injection, as slow chemical reactions start to become more important, and hence rate limiting. However, because fuel is directly injected into the combustion chamber, inhomogeneities are still present and the mixture formation influences the combustion processes. A conceptual model describing the conventional diesel combustion has been proposed by Dec in 1997 [12] and later extended to include LTC concepts by a group of researchers at the Sandia National Laboratories [6, 13].

The development of combustion systems comprises several engineering disciplines and various fields of natural sciences. With the aim of developing more energy efficient combustion systems, further experimental, theoretical and computational research is needed to gain a profound understanding of the fundamental physical and chemical processes. The following paragraphs will introduce some important aspects of these processes.

1.3 Fluid motion

The motion of fluids is at the heart of many technical applications, such as combustion systems. Fluid mechanics is the field of science that deals with the motion of fluids and the beginnings date back to the 18th and 19th century, starting with Newton's laws of motion and resulting in the Navier–Stokes (NS) equations, the governing equations for fluid motion. A particularly important characteristic of a fluid is its state of motion, i.e. laminar, turbulent or the transition in between. Most fluid flows encountered in practical engineering applications and in nature are turbulent. However, in many cases especially the transition from an initially laminar

flow to a fully developed turbulent flow is of great interest and subject to active research. The onset of this transition is often determined by using a non-dimensional number, the Reynolds number Re, which is defined as the ratio of inertial to viscous forces. Flows at low Reynolds numbers are laminar, whereas Reynolds numbers of turbulent flows in practical application may easily exceed millions. The transition from an initially laminar flow in a rapid to a turbulent state is illustrated in Fig. 1.2(a). Another example is shown in Fig. 1.2(b), illustrating the interaction of an atmospheric flame with the surrounding flow field.
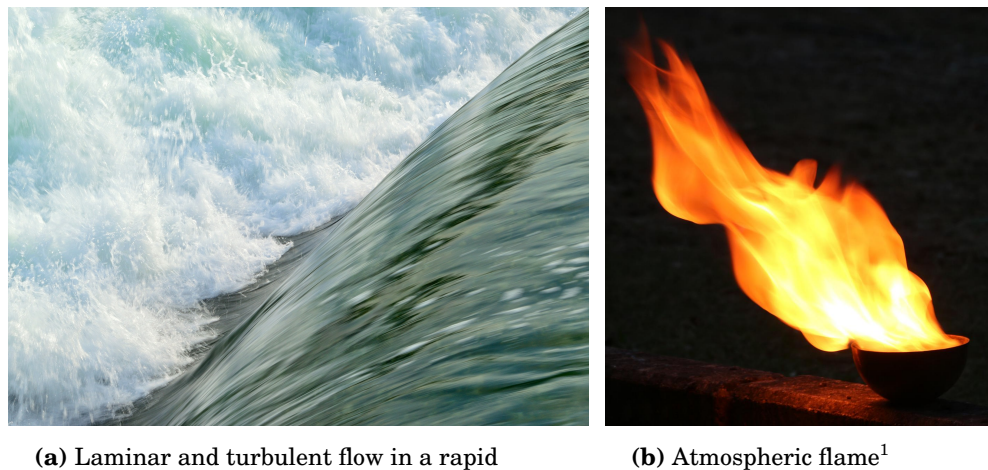
(a) Laminar and turbulent flow in a rapid   **(b)** Atmospheric flame[1]

Figure 1.2 – Illustrations of fluid motion and combustion.

Essential characteristics of turbulent flows are the chaotic motion in space and time, and high levels of vorticity. The length scales in turbulent flows range from the large scales describing the macroscopic characteristics of the flow, down to much smaller scales. The size of the structures in turbulent flows, often referred to as *eddies*, hence range over several orders of magnitudes. The large energy containing eddies induce smaller eddies, which in turn result in even smaller eddies. The turbulent kinetic energy that is brought into the system on the large scales, is transferred to smaller scales until it is dissipated into heat on the smallest scales. This transfer of energy from the large scales of motion to the small scales is referred to as the *energy cascade*. The characteristic size of a flow, often referred to as the *integral length scale* $\mathcal{L}$, is typically determined by the size of the largest energy-containing eddies. Based on dimensional analysis, Kolmogorov [14] suggested in 1941 that the size of the smallest eddies can be directly related to the rate at which the energy dissipates (ε) and the diffusivity of

---

[1]Photo: "Flame" by Oliver Feiler (CC BY-SA 4.0)

the kinetic energy ν as

$$\eta = \left(\frac{\nu^3}{\varepsilon}\right)^{\frac{1}{4}} , \qquad (1.1)$$

the *Kolmogorov length scale*. The eddies in a turbulent flow are generally anisotropic and can only for the smallest scales be considered as isotropic. Kolmogorov [15] further postulated that the energy spectrum is proportional to $\varepsilon^{2/3}\kappa^{-5/3}$, where κ denotes the wavenumber, at scales much smaller than the energy-containing and much larger than the dissipative length scales. This is illustrated in Fig. 1.3, where a model spectrum of turbulent kinetic energy is shown. With respect to the application in diesel
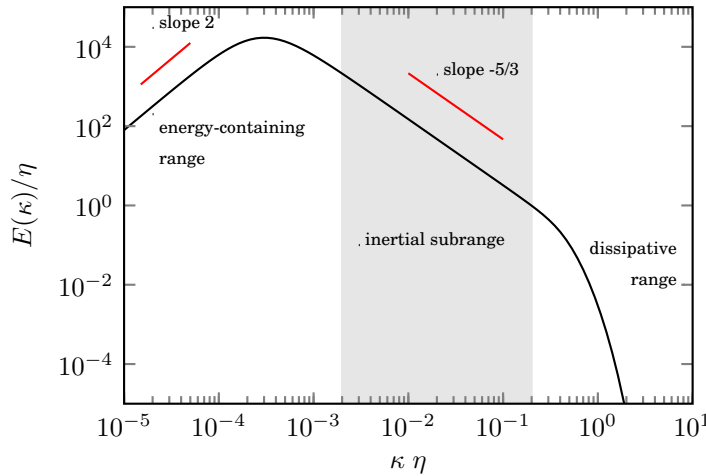
Figure 1.3 – Model energy spectrum as described in the textbook by Pope [16].

engines, the integral length scale may be in the order of $1\,\text{mm}$ and the Kolmogorov length scales in the order of $10\,\mu\text{m}$, already for low speed engines [17]. The range of length scales for engines at higher speed, which subsequently leads to higher Reynolds numbers, is significantly wider, since the ratio of integral and Kolmogorov length scale is inversely proportional to the Reynolds number $\eta/\mathcal{L} \propto Re^{-3/4}$ [16].

The Navier–Stokes equations describe the fluid motion of laminar, transitional and turbulent flows in the continuum limit, i.e. for length scales much above the mean free path of a molecule. Their solution, however, constitutes significant difficulties. In fact, analytical solutions to the NS equations only exist for a few specific cases, like the Poiseuille flow [18] or Taylor–Green vortices [19]. Because no general analytical solution is known, one needs to resort to numerical methods to obtain an approximate solution [16, 20]. This however, introduces significant challenges on its own, due to the wide range of length and time scales that has to be resolved for a comprehensive description of fluid flows. The majority of

these methods is based on discretizing the underlying partial differential equations and obtain a discretized solution.

The conceptually simplest, but computationally most expensive, approach is to choose the resolution such that the whole spectrum of fluid motion is directly resolved in space and time, i.e. Direct Numerical Simulation (DNS). This approach is still unfeasible for most turbulent flow cases and mainly restricted to simplified flow problems. To reduce the computational cost for turbulent flow calculations certain techniques are available.

An approach widely used in industry applications, but also in research, is based on the Reynolds-averaged Navier–Stokes (RANS) equations. Within the RANS approach the flow quantities are decomposed in an averaged and a fluctuation part, where only the averaged part is directly computed and the fluctuation part (i.e. the turbulent motion) is obtained from certain submodels. Hence, all turbulent scales are modeled in the RANS approach, which leads to rather low computational costs, while important characteristics of the mean flow are still captured.

A method called Large Eddy Simulation (LES), is based on the idea to resolve the large turbulent structures (eddies) directly and model only the small scale motion [21, 22]. The LES method is one of the oldest techniques to reduce the computational cost, but gained only in the recent years more attention in non-fundamental research due to the advances in computational power. With today's available computational resources, LES provides a feasible, though still challenging way to investigate turbulent flows. The conceptual differences of these three methods are illustrated in Fig. 1.4, where a quantity (e.g. temperature) obtained at a single spatial location in a turbulent flow is plotted over time. The highly fluctuating nature of such a quantity is captured only by a DNS, where the LES approach would still give a good description of the unsteady characteristics. The RANS approach would not be able to represent the turbulent characteristics, but still provide a good approximation of the mean quantities.

1.4 Combustion

In chemically reacting flows, and specifically in combustion processes, the composition of the fluid changes due to chemical reactions and mixing. Combustion processes are further characterized by a high heat release stemming from the exothermic chemical reactions. This further leads to significant changes in temperature and thermophysical properties, such as
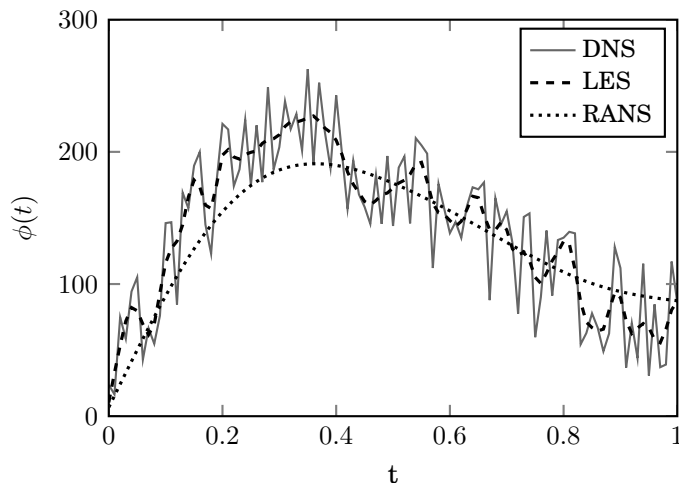
Figure 1.4 – Comparison of a quantity representing data obtained from DNS, LES and RANS simulations.

viscosity or heat capacity, and subsequently has to be taken into account in the mathematical description of reacting flows [23, 24].

Given a homogenous mixture composition, the rate at which fuel and oxidizer react with each other and form the combustion products is governed by elementary reactions between many chemical species. The rate data for the elementary reactions are typically obtained in well defined experiments and compiled to tables, the so-called elementary reaction mechanisms. Detailed reaction mechanisms for even simple configurations like hydrogen-oxygen involve 9 species and 19 reactions [25]; typical fuels used in industrial combustion devices, such as methane, may already concern up to 53 species and 325 reactions [26]. Long-chained hydrocarbon fuels like n-heptane and n-dodecane result in mechanisms with several thousand species and multiple times more reactions [27–29]. An overview of the number of species and reactions in hydrocarbon reaction mechanisms was given by Lu and Law [30] and an extended version is shown in Fig. 1.5.

Each elementary reaction can mathematically be described by a differential equation (see Section 3.1.3) involving several chemical species, which yields a coupled system of differential equations for an elementary reaction mechanism. The nature of chemical reactions in combustion processes imposes significant challenges to the solution of this differential equation system, due to (1) the typically great number of chain reactions and (2) the wide range of time scales for the elementary reactions. These characteristics lead to a highly coupled and typically stiff system of differential equations [23]. The solution of this system requires robust, and yet accu-
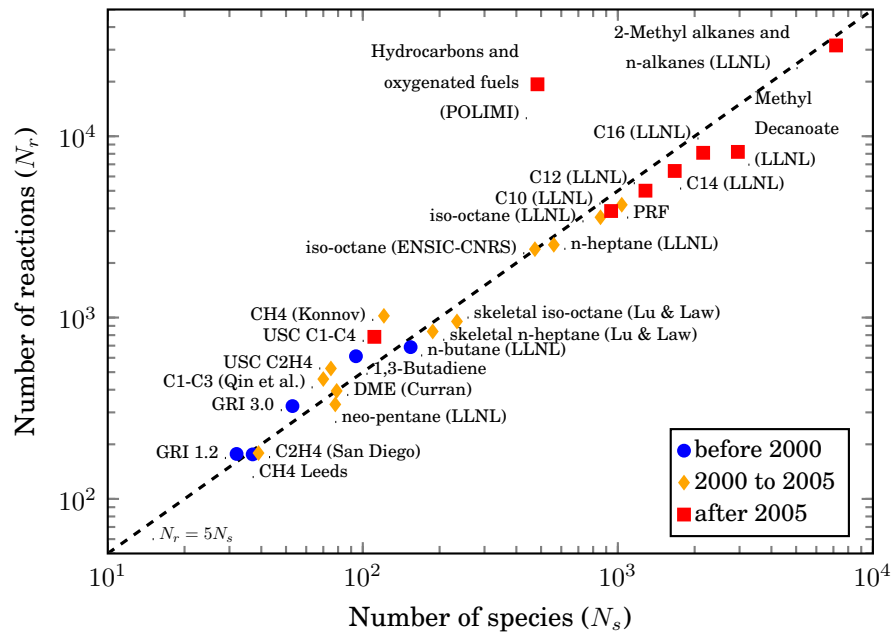
Figure 1.5 – Number of species and reactions in hydrocarbon fuel reaction mechanisms.

rate, numerical methods. Thus, to avoid instabilities in the solution either implicit or explicit methods with extremely small time steps have to be applied [31, 32]. Both methods impose high computational requirements, especially for large reaction mechanisms, and thus a direct solution of the full chemical system is unfeasible for practical combustion systems. This holds especially true for multi-dimensional simulations where additional conservation equations would have to be solved for each species. It should be further noted that the chemical reactions take place at a molecular level, i.e. at length scales typically well below the Kolmogorov length scale. In general, these restrictions motivate the use of simplified reaction mechanisms and combustion modeling approaches with various degrees of detail and complexity, ranging from simple phenomenological models to accurate approximations of the molecular diffusion and reaction processes.

1.5 Objectives and scope of the thesis

The objectives of the present thesis are to explore and implement modeling approaches, which allow to investigate high-velocity fuel sprays, and specifically their ignition and combustion characteristics, using LES. The spray combustion cases to be investigated are relevant to conventional diesel combustion, as well as LTC concepts in internal combustion engines.

The research topics are further divided into three topics for which several

research questions are formulated as follows:

1. Implications of modeling fuel sprays in LES (Publication I):

    - What is an adequate mesh resolution for high-velocity fuel spray LES?

    - What is the sensitivity of droplet breakup modeling to integral spray quantities and mixture formation?

2. Turbulent combustion simulation of n-dodecane fuel sprays (Publication II):

    - Which chemical mechanisms are suitable for n-dodecane spray flames?

    - Can the complex unsteady characteristics of spray ignition be captured for different ambient conditions relevant to LTC?

3. Effect of flow and turbulence on ignition and flame stabilization (Publication III):

    - How are the ignition characteristics influenced by the spray injection velocity?

    - What are the requirements to predict the spray flame stabilization under different turbulence levels?

To address these research questions, a well defined reference case is chosen and two parameter studies are carried out. For the numerical computations, certain modeling approaches for the fuel spray and combustion are chosen and implemented within the LES context.

1.6 Outline

In the previous sections, a rather general background and motivation for engine combustion research has been given, followed by an outline of the fundamental challenges in the research field and the objectives of the present research. The remainder of the thesis is structured as follows:

A literature review on diesel spray combustion is given in Chapter 2, including a discussion on diesel surrogates and the respective chemical mechanisms.

In Chapter 3 the governing equations and methods are given. Sections 3.2 and 3.3 focus thereby on the modeling of fuel sprays in LES. The various aspects of combustion modeling are introduced in Sections 3.5 - 3.7.

Thereafter, the main results of the research conducted in the course of the present thesis are presented in Chapter 4. The Chapter is structured such that the first section (4.1) summarizes the results of the non-reacting spray LES, corresponding to Publication I. The results address the research questions of the first topic defined in Section 1.5. Then, in Section 4.2 the results from canonical combustion configurations are analyzed, which were originally published in Publication II. The results of the various turbulent spray combustion cases are presented in Section 4.3, corresponding to the two parameter studies in Publication II and III. The results from Publication II address thereby the research questions of topic 2 and results from Publication III aim at the questions raised under topic 3.

The conclusions of this doctoral thesis are given in Chapter 5, including a brief summary of the major findings and recommendations for future studies. The list of references closes this summary part and the Publication I–III are attached at the end of this thesis.

2. Literature review

In order to develop and validate advanced computational models with the goal to establish predictive modeling capabilities, well defined and accurately measured experimental data are necessary. In a similar manner as in the series of workshops on Turbulent Nonpremixed Flames (TNF) [33], where accurate and extensive experimental data were used to validate canonical atmospheric jet flames, the Engine Combustion Network (ECN) [34] was established for collaboration on turbulent spray flames under engine operating conditions. While the two collaborative efforts share the same principles, significant differences can be found in the physical and chemical conditions. For instance, the large injection velocity of liquid fuel in diesel engines (typically in the order of $500\,\mathrm{m\,s^{-1}}$) results in a high-momentum jet, which subsequently leads to a substantially larger flame lift-off for diesel spray flames compared to laboratory jet flames. Further differences arise from the elevated ambient pressure and the long-chained hydrocarbon fuels. Hence there is a need for well defined measurements under conditions relevant to diesel engines in order to gain a deeper understanding of the physical and chemical processes and to provide validation data for the computational model development.

In the following, a review of the literature concerning diesel spray combustion is given. In Section 2.1 possible surrogates for diesel fuel and the respective chemical mechanisms are discussed, followed by a review of computational studies on the ECN target conditions in Section 2.2. The spray combustion modeling approach chosen for the present thesis is then discussed in Section 2.3 and the investigated spray conditions are briefly introduced in Section 2.4.

2.1 Diesel surrogates and chemical reaction mechanisms

The chemical composition of commonly available diesel fuel is complex and hence its thermophysical and chemical properties are difficult to access. In order to accurately define the fuel properties for experimental and computational combustion research, surrogate fuels, such as the Primary Reference Fuels (PRF) for gasoline [35], are widely used. Diesel fuels have been represented by n-heptane in a wide range of experimental [36–38] and computational studies [39–51] and hence also the first target conditions within the ECN were using n-heptane. A particular advantage of n-heptane is the availability of tractable and widely tested chemical mechanisms; comprehensive lists of n-heptane studies can be found in [45, 46]. However, the carbon chains of typical diesel fuel components range from 10 to 25 carbon atoms [52] and hence the thermophysical properties, especially with respect to evaporation and boiling, are not well represented by n-heptane. As a more suitable surrogate for diesel fuel, n-dodecane was identified due to the longer carbon chain and the well defined thermophysical properties [52]. A set of target conditions using n-dodecane, named *Spray A*, was defined to study canonical spray flames within the ECN [53, 54]. Extensive experimental data for Spray A are available, including parametric variations for ambient temperature, density and oxygen concentration, as well as injection pressure [55–60]. Several modeling studies of the Spray A case have been carried out [46, 61–69], using various turbulence and combustion modeling approaches. However, the lack of accurate and yet computationally affordable chemical mechanisms for n-dodecane has been identified as a key issue and is still subject to ongoing research by several groups.

To the present day, the most comprehensive descriptions of hydrocarbon oxidation are given by two independently developed chemical kinetic mechanisms: (1) The detailed mechanism for 2-methyl-alkanes up to C20 and n-alkanes up to C16 by Sarathy et al. [27, 28], and (2) the detailed and lumped mechanism for hydrocarbon and oxygenated fuels by Ranzi et al. [29]. Due to the large amount of species and reactions in these detailed descriptions, reduced mechanisms have to be considered, even for flamelet calculations.

In the present study two recently developed mechanisms are evaluated for Spray A: (1) the 257-species/1521-reaction mechanism by Narayanaswamy et al. [70] (hereafter referred to as Stanford mechanism) and (2) the 130-

species/2395-reaction mechanism by Ranzi et al. [71] (hereafter referred to as POLIMI mechanism). The mechanisms were respectively derived from the above mentioned, detailed mechanisms with thousands of species and multiple times more reactions. The reduction strategies involve in both cases a multi-stage automatic species and reaction elimination and chemical lumping of species. The differences between the reduced mechanisms stem from the different initial mechanisms and the particular reduction strategy. Where Narayanaswamy et al. [70] obtained their mechanism from a reduction of the detailed n-dodecane mechanism by Sarathy et al. [27] and a subsequent lumping of species, Ranzi et al. [71] applied first a lumping procedure to their own detailed mechanism [29] and then a species and reaction reduction. For a detailed description of the respective procedures, it is referred to the original publications. It is noteworthy that both, Narayanaswamy et al. [70] and Ranzi et al. [71], emphasize the crucial role of the lumping procedure with respect to the ignition delay times.

Alternative reduced mechanisms for n-dodecane have been developed e.g. by Som et al. [61] (103 species/370 reactions) and Luo et al. [62] (106 species/420 reactions), where the latter has also been employed in a further reduced version [66]. These mechanisms are derived from the detailed mechanism by Westbrook et al. [72], which served also as a starting point for the development of the detailed mechanisms by Sarathy et al. [27]. Their clear benefit is the significantly reduced size, which makes them applicable for multi-dimensional simulations using a direct chemistry integration (e.g. [67, 68]).

2.2 Multi-dimensional spray simulations

The development of the skeletal n-dodecane mechanism by Luo et al. [62] targeted specifically the Spray A conditions and the study included three-dimensional spray simulations using unsteady RANS turbulence modeling. This mechanism was also used by D'Errico et al. [63] comparing a well-mixed and the multiple Representative Interactive Flamelet (mRIF) combustion model for different ambient temperatures and oxygen concentrations of the Spray A conditions. The study employed a RANS based solver and in case of the mRIF model a presumed Probability Density Function (PDF) turbulence-chemistry interaction approach was used. It was found that generally a better agreement with experimental re-

sults was achieved for the mRIF model compared to the well-mixed model. A more comprehensive study with respect to Spray A parameter variations was conducted by Kundu et al. [64] using a similar RANS/mRIF approach. Several presumed PDFs were investigated and the mechanism by Luo et al. was compared to an earlier version with 103-species and 370-elementary reactions by Som et al. [61]. The latter mechanism was also used by Bhattacharjee and Haworth [46] in a parameter study for the Spray A case using a two-dimensional RANS approach in combination with a Transported Probability Density Function (TPDF) method to model the reaction-diffusion processes. Similarly, Pei et al. [66] carried out a comprehensive parameter study of the Spray A conditions using a further reduced version of the mechanism by Luo et al. with 88-species. For the turbulence and reaction-diffusion modeling a two-dimensional RANS/TPDF approach was employed. In fact, most of the computational studies of spray combustion within the ECN have been based on the unsteady RANS approach with various combustion models.

The majority of the computational Spray A studies report ignition delay times and lift-off length predictions, but detailed investigations of spray ignition characteristics have mainly been carried out for n-heptane sprays. Most notably, the studies by Bhattacharjee and Haworth [46], Bajaj et al. [47], Irannejad et al. [50] investigated n-heptane spray ignition and provide a detailed analysis of ignition location and mixture conditions. The reasoning behind this can be mainly attributed to the widely tested chemical mechanisms for n-heptane and the uncertainties in the mechanisms used in the previous n-dodecane spray studies [46, 67].

Only very recently, LES studies of the ECN target conditions have been carried carried out, where the studies by Bekdemir et al. [42], Tillou et al. [48], Irannejad et al. [50], Ameen and Abraham [73] investigate the n-heptane spray conditions. Bekdemir et al. [42] used the Flamelet Generated Manifold (FGM) model together with a Smagorinsky type LES model and employed a computational mesh with a minimum cell size of $80\,\mu m$ near the nozzle exit which was gradually increased to $800\,\mu m$ further downstream. The ignition and flame characteristics were well captured, demonstrating the potential of the FGM method for LES of diesel spray flames. Similarly, Tillou et al. [48] simulated the n-heptane spray conditions using the same LES solver (AVBP [74]) and a tabulated chemistry model was employed for the combustion modeling. A similar computational mesh as in [42] was used with a lower cell count and 15 realizations

were carried out in order to assess the variability of the spray combustion processes. The results showed a low sensitivity of the ignition delay time to the spray variability, but up to $10\,\%$ variation of the heat release rate in the later combustion stages. The study by Ameen and Abraham [73] investigated an n-heptane gas jet under diesel engine conditions, however, with four times smaller injection velocity than for typical diesel fuel sprays. The computational model was based on a Smagorinsky LES model coupled with an unsteady Flamelet Progress Variable (UFPV) model and a computational grid size ranging from $50\,\mu m$ to $100\,\mu m$ in axial and $20\,\mu m$ to $34\,\mu m$ in radial direction. The results showed significant differences in the transient behavior between the LES and accompanied RANS simulations, however the fundamental physics affecting the flame lift-off length were found to be the same. Irannejad et al. [50] carried out an LES study of the ECN n-heptane spray conditions using the Filtered Mass Density Function (FMDF) approach to assess the effect of turbulence-chemistry interaction. The employed grid size was $100\,\mu m$ in the core spray flame region. Important findings were that auto-ignition first occurred in the fuel-rich regions and that the flame lift-off was strongly dependent on the spray parameters and ambient conditions.

One of the few LES studies of the ECN Spray A target conditions was carried out by Gong et al. [67] who employed a chemistry coordinated mapping (CCM) method and the 103-species mechanism by Som et al. to model the combustion process. A uniform mesh with a cell size of $250\,\mu m$ was adopted. The effect of the low-temperature reactions on the mixing was investigated and the simulation approach was able to capture the two-stage ignition behavior. However, the ignition delay times were not reported in this study, but the authors remarked that the delayed pressure rise may be partly due to uncertainties in the chemical mechanism. Very recently, Pei et al. [68] utilized LES and finite rate chemistry to investigate the effect of multiple realizations for Spray A conditions at several ambient temperatures. A dynamic structure LES model was employed together with a multi-zone model to accelerate the chemistry calculations. An adaptive mesh refinement was used with a minimum cell size of $62.5\,\mu m$. Due to the relatively fine mesh resolution and detailed chemistry calculations, the ignition delay predictions agreed very well with experimental data for the higher ambient temperatures. The differences in ignition delay for the lower temperatures were attributed to the chemical mechanism. In line with the findings by Tillou et al. [48], the ignition delay showed

a low sensitivity to the spray variability, however for the lift-off length predictions several realizations were found to be necessary. The observed differences in lift-off length between the LES and experimental data was partially attributed to an insufficient number of LES realizations, owing to the high computational cost of these calculations. The latest LES study on the ignition characteristics of the Spray A baseline case was carried by Hakim et al. [69]. The study employs a high-fidelity simulation approach for the turbulent flow description using real-gas thermodynamics and a cell size of approximately $2\,\mu$m in the injector vicinity. The chemistry model is based on a 2-step mechanism with variable Arrhenius coefficients that were calibrated using Bayesian inference to match the auto-ignition times in homogenous reactors. The results showed that the modeling approach predicts accurately the complex processes related to turbulent mixing and ignition, where the authors emphasize the importance of the accurate description of the mixing processes. The simulation did not cover the flame development or flame stabilization.

It should be mentioned that the latter two LES studies were published after the research for the present thesis was carried out.

2.3   Current modeling approach

The substantial progress in LES of diesel spray flames has motivated the research for the current thesis. Various research questions regarding the modeling of diesel spray flames remain however still open, specifically regarding the accurate prediction of ignition and flame stabilization. The further, systematic investigations of parametric variations in ambient conditions or injection properties are lacking, especially regarding LES. Such parametric variations impose various challenges for high-fidelity numerical combustion simulations, especially since the computational requirements may significantly limit the realizable spatial and temporal resolution and/or the description of the chemical kinetics. In the present thesis, a high-fidelity LES approach is chosen to describe the turbulent fluid motion in combination with a tabulated chemistry approach employing detailed chemical kinetics, namely the Flamelet Generated Manifold approach. One of the main advantages of the FGM combustion model is the low computational cost, while detailed chemical kinetics can be taken into account. This makes the FGM combustion model particularly well suited for LES, where the required spatial and temporal resolution imposes

already a high computational cost. On the other hand, LES offers a tool to investigate the unsteady processes during the ignition of turbulent fuel sprays [42, 48, 73]. The low additional cost of the FGM combustion model compared to the non-reacting fuel spray simulations allows further for systematic investigations of parametric variations, which are essential in gaining a deeper understanding of the fundamental processes. Another noteworthy feature of the FGM combustion model is the easy access to the full species composition, during run-time of the LES as well as for post-processing.

2.4   Experimental reference case

The spray cases investigated in the present thesis correspond to the experimental Spray A conditions with $900 \, \mathrm{K}$ and $22.8 \, \mathrm{kg/m^3}$ ambient gas temperature and density, respectively. For the non-reacting spray research an inert ambient gas composition ($0 \, \%$ oxygen) is used. The experimental validation data were measured at the Sandia National Laboratories in a constant-volume pre-burn combustion chamber. Hence, the target ambient temperature, oxygen composition and pressure are achieved by a premixed combustion of acetylene, hydrogen, oxygen and nitrogen prior to the n-dodecane injection. For the simulations idealized initial conditions are chosen, i.e. gradients or fluctuations in the ambient mixture composition, temperature or velocity are not considered in the present setup. For the spray combustion investigations, three ambient oxygen concentrations ($21 \, \%$ $15 \, \%$ and $13 \, \%$) are considered in this thesis. The respective gas compositions, corresponding to the nominal experimental values measured at Sandia, are listed in Table 2.1. The injection pressure in Publication I and

Table 2.1 – Ambient molar gas compositions for the Sandia constant-volume chamber

O_2 (%)	N_2 (%)	CO_2 (%)	H_2O (%)
21	69.33	6.11	3.56
15	75.15	6.23	3.62
13	77.10	6.26	3.64
0	89.71	6.52	3.77

II is kept at $150 \, \mathrm{MPa}$. In Publication III an injection pressure variation for

the reacting ($15\,\%$ O_2) and non-reacting ($0\,\%$ O_2) conditions is carried out and the corresponding n-dodecane injection parameters are listed in Table 2.2.

Table 2.2 – Fuel injection parameters

Injection pressure (MPa)	50	100	150
Average injection velocity^a (m/s)	320.4	468.3	579.6
Nozzle diameter (μm)		90	
Fuel temperature (K)		363	

^{a}Calculated from the injection rate profile.

3. Methods

3.1 Governing equations

The mathematical description of fluid motion is given by the Navier–Stokes equations. In the following the conservation equations and constitutive relations for a reactive mixture of thermally perfect gases are given. Further, certain fundamental aspects of turbulent nonpremixed combustion modeling are provided. Detailed derivations of these equations can be found in standard textbooks, e.g. by Kundu and Cohen [18], and Poinsot and Veynante [75].

3.1.1 Navier–Stokes equations

The equations for mass (3.1) and momentum (3.2) conservation read

$$\frac{\partial \rho}{\partial t} + \frac{\partial \rho u_j}{\partial x_j} = 0 \tag{3.1}$$

$$\frac{\partial \rho u_i}{\partial t} + \frac{\partial (\rho u_i u_j)}{\partial x_j} = \frac{\partial}{\partial x_j} \left(-p\delta_{ij} + \sigma_{ij} \right) + \rho g_i \ , \tag{3.2}$$

where ρ, u_i, p and σ_{ij} denote the density, velocity, pressure and viscous stress tensor, respectively. Using *Stokes' hypothesis*, the viscous stress tensor for a *Newtonian* fluid is defined as

$$\sigma_{ij} = \mu \left(\frac{\partial u_i}{\partial x_j} + \frac{\partial u_j}{\partial x_i} - \frac{2}{3} \frac{\partial u_i}{\partial x_j} \delta_{ij} \right) \ , \tag{3.3}$$

where μ is the dynamic viscosity of the mixture. In reactive flows, the composition of the mixture is of interest and hence the conservation equation for total mass is complemented by transport equations for the species mass fractions $Y_\alpha = \rho_\alpha / \rho$, with ρ_α denoting the mass density of species α. The density of the mixture is thus given as the sum of partial densities $\rho = \sum_{\alpha=1}^{N_s} \rho_\alpha$, where N_s is the number of species. The transport equations

for the species mass fractions $Y_\alpha (\alpha = 1 \ldots N_s)$ read

$$\frac{\partial \rho Y_\alpha}{\partial t} + \frac{\partial (\rho Y_\alpha u_j)}{\partial x_j} + \frac{\partial (\rho Y_\alpha V_{j,\alpha})}{\partial x_j} = \dot{\omega}_\alpha \, , \qquad (3.4)$$

where $V_{j,\alpha}$ denotes the diffusion velocity and $\dot{\omega}_\alpha$ the chemical source term for species α. The exact solution for the diffusion velocity is given by a complex system of equations, accounting for various phenomena of differential diffusion. The Hirschfelder and Curtiss approximation is considered as the best first-order approximation to the exact solution [75]:

$$V_{j,\alpha} X_\alpha = -D_\alpha \frac{\partial X_\alpha}{\partial x_j} \qquad (3.5)$$

Here, the species mole fractions $X_\alpha = n_\alpha/n$ are used, where n_α denotes the number of moles of species α and n the total number of moles. For perfect gases, the mole and mass fractions are related by $X_\alpha = Y_\alpha \frac{M}{M_\alpha}$, where M_α are the species molar masses and $M = \dfrac{1}{\sum_{\alpha=1}^{N_s} \frac{Y_\alpha}{M_\alpha}}$ the mixture-averaged molar mass. The mixture-averaged species diffusion coefficients D_α can be expressed in terms of the binary diffusion coefficients $\mathcal{D}_{\alpha\beta}$[1] as $D_\alpha = \frac{1-Y_\alpha}{\sum_{\alpha \neq \beta}^{N} X_\alpha/\mathcal{D}_{\alpha\beta}}$. Rearranging equation (3.5) yields

$$\begin{aligned}
V_{j,\alpha} Y_\alpha &= -D_\alpha \frac{M_\alpha}{M} \frac{\partial X_\alpha}{\partial x_j} \\
&= -D_\alpha \frac{M_\alpha}{M} \frac{\partial}{\partial x_j} \left(\frac{M}{M_\alpha} Y_\alpha \right) \\
&= -D_\alpha \left(\frac{\partial Y_\alpha}{\partial x_j} + Y_\alpha \frac{\partial}{\partial x_j} \ln(M) \right) \\
&\approx -D_\alpha \frac{\partial Y_\alpha}{\partial x_j} \, .
\end{aligned} \qquad (3.6)$$

Furthermore the species diffusion coefficients D_α can be expressed in terms of the Lewis number Le_α, heat conductivity λ and heat capacity c_p as

$$D_\alpha = \frac{1}{Le_\alpha} \frac{\lambda}{\rho c_p} \, . \qquad (3.7)$$

In many turbulent combustion processes molecular transport phenomena play a minor role and hence the above introduced simplifications are well justified. The further, differential diffusion effects can often be neglected in nonpremixed combustion configurations and hence a unity Lewis number assumption for all species is widely used [23, 24]. Hence, if not otherwise stated, the assumption of unity Lewis number is used throughout this thesis and the equations are presented accordingly. Substituting equation

---

[1]Note that also the binary diffusion coefficients are only an approximation to the generalized diffusion coefficients $D_{\alpha\beta}$, which depend explicitly on the mixture composition.

(3.6) into equation (3.4) and using the unity Lewis number assumption yields

$$\frac{\partial \rho Y_\alpha}{\partial t} + \frac{\partial \left(\rho Y_\alpha u_j\right)}{\partial x_j} = \frac{\partial}{\partial x}\left(\frac{\lambda}{c_p}\frac{\partial Y_\alpha}{\partial x_j}\right) + \dot{\omega}_\alpha \ , \tag{3.8}$$

The energy conservation in terms of total enthalpy $h_t = h + \frac{u_j u_j}{2}$ with h denoting the absolute enthalpy reads

$$\frac{\partial \left(\rho h_t\right)}{\partial t} + \frac{\partial \left(\rho h_t u_j\right)}{\partial x_j} = \frac{\partial p}{\partial t} - \frac{\partial q_j}{\partial x_j} + \frac{\partial \left(\sigma_{ij} u_j\right)}{\partial x_i} + \rho u_j g_j \ . \tag{3.9}$$

A widely used approximation for the energy flux q_j is given by *Fourier's law* $q_j = -\lambda \frac{\partial T}{\partial x_j}$, where T denotes the temperature. To close the system of $N_s + 5$ equations and $N_s + 7$ unknown variables, the caloric and thermal equation of state

$$h = \sum_{\alpha=1}^{N_s} Y_\alpha h_\alpha = \sum_{\alpha=1}^{N_s} Y_\alpha \left(h_{0,\alpha} + \int_{T_0}^{T} c_{p,\alpha}(T^*)\, dT^*\right) \ , \tag{3.10}$$

$$p = \rho \frac{\mathcal{R}}{M} T \tag{3.11}$$

are used, where $\mathcal{R}$ denotes the universal gas constant. It should be noted that the *ideal gas law* (Eq. 3.11) is a widely used approximation, but recent studies [76–83] show that a *real gas* equation of state may be needed to correctly predict the complex phenomena related to the phase transition of diesel fuel sprays at supercritical conditions.

3.1.2 Thermodynamic and transport properties

In general, the thermodynamic and transport properties for a single species are temperature and pressure dependent, where the pressure dependency can typically be neglected for perfect gases. For a multi-component mixture the thermodynamic properties can simply be obtained by mass-averaging (e.g. $c_p = \sum_{\alpha=1}^{N_s} Y_\alpha c_{p,\alpha}$), whereas the evaluation of the transport properties is fairly complex and computationally expensive. Several simplified formulations have been proposed to approximate the transport properties, where the semi-empirical expression by Wilke [84] is adopted here for the mixture viscosity:

$$\mu = \sum_{\alpha=1}^{N_s} \frac{\mu_\alpha}{1 + 1/X_\alpha \sum_{\alpha=1,\alpha\neq\beta}^{N_s} X_\beta \Phi_{\alpha\beta}} \tag{3.12}$$

Here, μ_α is the single species viscosity and $\Phi_{\alpha\beta}$ is given by

$$\Phi_{\alpha\beta} = \frac{1}{\sqrt{8}}\left(1 + \frac{M_\alpha}{M_\beta}\right)^{-\frac{1}{2}}\left(1 + \left(\frac{\mu_\beta}{\mu_\alpha}\right)^{\frac{1}{2}}\left(\frac{M_\beta}{M_\alpha}\right)^{\frac{1}{4}}\right)^2 \ .$$

A semi-empirical expression for the mixture-averaged heat conductivity is given by Mathur and Saxena [85] and reads

$$\lambda = \frac{1}{2} \left(\sum_{\alpha=1}^{N_s} X_\alpha \lambda_\alpha + \left(\sum_{\alpha=1}^{N_s} X_\alpha / \lambda_\alpha \right)^{-1} \right) , \qquad (3.13)$$

with the species heat conductivity λ_α.

For a single species the thermodynamic properties are cast in a polynomial form[2]

$$\frac{C_p}{\mathcal{R}} = a_1 + a_2 T + a_3 T^2 + a_4 T^3 + a_5 T^4$$

$$\frac{H}{\mathcal{R}T} = a_1 + \frac{a_2}{2} T + \frac{a_3}{3} T^2 + \frac{a_4}{4} T^3 + \frac{a_5}{5} T^4 + \frac{a_6}{T}$$

$$\frac{S}{\mathcal{R}} = a_1 \ln T + a_2 T + \frac{a_3}{2} T^2 + \frac{a_4}{3} T^3 + \frac{a_5}{4} T^4 + a_7 ,$$

where C_p, H and S have units J/(molK), $\mathrm{J\,mol}^{-1}$ and J/(molK), respectively. The coefficients $a_1 \ldots a_7$ are tabulated for virtually all relevant species in combustion processes and generally available [86].

Viscosity and conductivity are expressed in terms of binary diffusion coefficients. However, since diffusivity is not an intrinsic property, the binary diffusion coefficients must be evaluated from Lennard–Jones potentials of the two considered species, which in turn permits a generally valid tabulation of transport properties. In practical computations, the Lennard–Jones potentials are evaluated for the specific mixture and the transport properties are fitted for each species α to a polynomial form:

$$\ln(\mu_\alpha) = \sum_{n=1}^{N_p} a_{n,\alpha} \ln(T)^{n-1} \quad \text{with } \alpha = 1 \ldots N_s$$

$$\ln(\lambda_i) = \sum_{n=1}^{N_p} b_{n,\alpha} \ln(T)^{n-1} \quad \text{with } \alpha = 1 \ldots N_s$$

$$\ln(\mathcal{D}_{\alpha\beta}) = \sum_{n=1}^{N_p} d_{n,\alpha\beta} \ln(T)^{n-1} \quad \text{with } \alpha = 1 \ldots N_s , \ \beta = 1 \ldots N_s , \ \alpha \neq \beta$$

3.1.3 Chemical kinetics

The chemical source term $\dot{\omega}_\alpha$ appearing in Eq. 3.8 accounts for the rate of change in species mass due to chemical reactions. In the present formulation of the transport equations, this source term is the only explicit link between the flow quantities and the combustion chemistry.

In gas combustion this source term is computed from reaction rates of the elementary chain reactions. In general, any elementary reaction can

---

[2]often referred to as NASA polynomials

be written in the form

$$\nu_1' \mathcal{A}_1 + \nu_2' \mathcal{A}_2 + \ldots + \nu_{N_s}' \mathcal{A}_{N_s} \longrightarrow \nu_1'' \mathcal{A}_1 + \nu_2'' \mathcal{A}_2 + \ldots + \nu_{N_s}'' \mathcal{A}_{N_s} ,$$
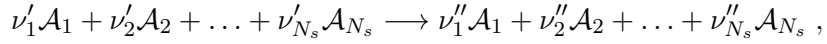
where ν_α' and ν_α'' denote the stoichiometric coefficients of the involved species $\mathcal{A}_\alpha$. In combustion modeling the reverse reactions play often an important role and hence a compact way to denote a coupled system of N_r elementary reactions is

$$\sum_{\alpha=1}^{N_s} \nu_{\alpha,l}' \mathcal{A}_\alpha \rightleftharpoons \sum_{\alpha=1}^{N_s} \nu_{\alpha,l}'' \mathcal{A}_\alpha , \quad \text{with } l = 1 \ldots N_r$$

and $\rightleftharpoons$ indicating the reversible nature. The net reaction rate for a single elementary reaction l is given by

$$q_l = k_l^f \prod_{\alpha=1}^{N_s} [\mathcal{A}_\alpha]^{\nu_{\alpha,l}'} - k_l^r \prod_{\alpha=1}^{N_s} [\mathcal{A}_\alpha]^{\nu_{\alpha,l}''} ,$$

where $[\mathcal{A}_\alpha] = \rho \frac{Y_\alpha}{M_\alpha}$ denotes the molar concentration of species $\mathcal{A}_\alpha$. Here k_l^f and k_l^r are the rate coefficients of the forward and backward reaction, respectively. For typical reactions in gaseous combustion processes the rate coefficients are determined by an Arrhenius type expression,

$$k = AT^b e^{-E_a/\mathcal{R}T} \tag{3.14}$$

with A and b being constants of the temperature dependent pre-exponential factor and E_a the activation energy of the reaction. It should be noted that alternative rate expressions may also be used, for instance, to account for a direct pressure dependency. Finally, the chemical source term $\dot{\omega}_\alpha$ of species α reads

$$\dot{\omega}_\alpha = M_\alpha \sum_{l=1}^{N_r} \left(\nu_{\alpha,l}'' - \nu_{\alpha,l}' \right) q_l . \tag{3.15}$$

3.1.4 Mixture fraction

The mass of chemical species in a system can change due to chemical reactions and hence species mass fractions are not suited to describe the state of mixing in reactive flows. The local mixture composition can be consistently defined by introducing a conserved[3] scalar Z, the *mixture fraction*. Several definitions of the mixture fraction exist, where a general and consistent way of defining it is based on the mass conservation of the chemical elements. The element mass fraction, defined as the ratio of the

---

[3]with respect to chemical reaction

mass of all atoms of element l in a system and the total mass $Z_l = \frac{m_l}{m}$, is related to the species mass fractions

$$Z_l = M_l \sum_{\alpha=1}^{N_s} a_{l,\alpha} \frac{Y_\alpha}{M_\alpha} \ , \tag{3.16}$$

where $a_{l,\alpha}$ is the number atoms of element l in species α and M_l the molar mass of element l. The mixture fraction may then be defined in terms of coupling functions ξ as

$$Z = \frac{\xi - \xi_0}{\xi_1 - \xi_0} \ , \tag{3.17}$$

where ξ_1 and ξ_0 denote constants evaluated in the fuel and oxidizer stream, respectively. The coupling functions ξ are defined as

$$\xi = \sum_{l=1}^{N_e} \gamma_l Z_l$$
$$= \sum_{l=1}^{N_e} \gamma_l \sum_{\alpha=1}^{N_s} \frac{a_{l,\alpha} M_l}{M_\alpha} Y_\alpha \ ,$$

where γ_l are weighting factors and commonly used values are given in Table 3.1. In the present thesis, Bilger's definition [87] of the weight factors

Table 3.1 – Commonly used weight factors γ_l.

	Bilger et al. [87]	C	H	O
γ_C	$2/W_C$	1	0	0
γ_H	$0.5/W_H$	0	1	0
γ_O	$-1/W_O$	0	0	1
γ_N	0	0	0	0

is used because the stoichiometric conditions can be readily obtained as $Z_{st} = Z(\xi = 0)$. A straightforward definition of the widely used fuel-oxidizer equivalence ratio ϕ is then given by

$$\phi = \frac{Z}{1-Z} \frac{1 - Z_{st}}{Z_{st}} \ . \tag{3.18}$$

The conservation equation for Z follows directly from the definition of ξ and reads

$$\frac{\partial \rho Z}{\partial t} + \frac{\partial (\rho Z u_j)}{\partial x_j} = \frac{\partial}{\partial x} \left(\frac{\lambda}{c_p} \frac{\partial Z}{\partial x_j} \right) \ , \tag{3.19}$$

where the unity Lewis number assumption is again used. It should be emphasized that the mixture fraction has no source term due to chemical reactions.

3.2 Large Eddy Simulation

In LES, the turbulent flow is decomposed into coherent large scales, which are directly resolved, and small, unresolved scales. Considering a physical quantity in a turbulent flow, the instantaneous value $\Psi(\vec{x}, t)$ can be expressed by its mean $\overline{\Psi(\vec{x}, t)}$ and fluctuating $\Psi'(\vec{x}, t)$ parts:

$$\Psi(\vec{x}, t) = \overline{\Psi(\vec{x}, t)} + \Psi'(\vec{x}, t)$$

The mean value in an LES is obtained from the filter operation

$$\overline{\Psi(\vec{x}, t)} = G * \Psi = \int G(\vec{x}, \vec{\zeta}, \Delta) \Psi(\vec{\zeta}, t) d\vec{\zeta} \, ,$$

where G is a spatial low-pass filter of constant width Δ. With respect to variable density flows, a mass-weighted, i.e. *Favre*, filtering is introduced as

$$\widetilde{\Psi} = \frac{\overline{\rho \Psi}}{\overline{\rho}} = \frac{1}{\overline{\rho}} \int \rho(\vec{x}, t) G(\vec{x}, \vec{\zeta}, \Delta) \Psi(\vec{\zeta}, t) d\vec{\zeta} \, .$$

Applying the filter operation to the governing equations describing the conservation of mass, momentum and energy (Section 3.1), the Favre-filtered equations read

$$\frac{\partial \overline{\rho}}{\partial t} + \frac{\partial \overline{\rho} \widetilde{u}_j}{\partial x_j} = \overline{S_\rho} \tag{3.20}$$

$$\frac{\partial \overline{\rho} \widetilde{u}_i}{\partial t} + \frac{\partial \left(\overline{\rho} \widetilde{u}_i \widetilde{u}_j \right)}{\partial x_j} = \frac{\partial}{\partial x_j} \left(-\overline{p} \delta_{ij} + \overline{\rho} \widetilde{u}_i \widetilde{u}_j - \overline{\rho \widetilde{u_i u_j}} + \overline{\sigma_{ij}} \right) + \overline{\rho} \widetilde{g}_i + \overline{S_{u,i}} \tag{3.21}$$

$$\frac{\partial \overline{\rho} \widetilde{h_t}}{\partial t} + \frac{\partial \left(\overline{\rho} \widetilde{u}_j \widetilde{h}_t \right)}{\partial x_j} = \frac{\partial \overline{p}}{\partial t} + \frac{\partial}{\partial x_j} \left(\overline{\rho} \widetilde{u}_j \widetilde{h} - \overline{\rho \widetilde{u_j h}} + \frac{\overline{\lambda}}{\overline{c_p}} \frac{\partial \widetilde{h}}{\partial x_j} \right) + \overline{S_h} \, , \tag{3.22}$$

where $\overline{\rho}$, $\widetilde{u}_i$, $\overline{p}$ and $\overline{\sigma_{ij}}$ denote the filtered density, velocity, pressure and viscous stress tensor, respectively. Here, the mechanical sources ($\frac{\partial (\overline{\sigma_{ij} u_j})}{\partial x_i}$ and $\overline{\rho u_j g_j}$) are neglected in the filtered enthalpy equation. Each equation contains a source term for mass ($\overline{S_\rho}$), momentum ($\overline{S_{u,i}}$) and energy ($\overline{S_h}$) that incorporates the interaction of the continuous (gas) with the dispersed (liquid) phase and are described in Section 3.3. Mixing of the evaporated fuel and the ambient gas is describe by the mixture fraction and the respective Favre-filtered transport equation reads

$$\frac{\partial \left(\overline{\rho} \widetilde{Z} \right)}{\partial t} + \frac{\partial \left(\overline{\rho} \widetilde{u}_j \widetilde{Z} \right)}{\partial x_j} = \frac{\partial}{\partial x_j} \left(\overline{\rho} \widetilde{u}_j \widetilde{Z} - \overline{\rho \widetilde{u_j Z}} + \overline{\rho} \widetilde{D} \frac{\partial \widetilde{Z}}{\partial x_j} \right) + \overline{S_Z} \, , \tag{3.23}$$

where the spray source term for a single component fuel corresponds to the mass source term, viz. $\overline{S_Z} = \overline{S_\rho}$. It should be noted that in non-reacting LES, the species mass fractions can be directly obtained from the mixture fraction and initial gas composition, and hence no transport equations

for the species mass fractions are solved in the non-reacting LES. The treatment of the species mass fractions in the reacting LES is described in Section 3.5.

The filter operation introduces additional terms on the right-hand side of Eqs. (3.21)–(3.23) that cannot be directly expressed in terms of filtered quantities. Such terms require modeling and their role is to account for the interaction between the resolved and the unresolved, i.e. subgrid, scales. Various subgrid scale models have been introduced in literature and have been further discussed by Garnier et al. [88]. In this thesis the monotonically integrated LES (MILES) approach [89–91], also referred to as implicit LES (iLES), is applied. This turbulence modeling approach is based on the assumption that the numerical dissipation introduced by the discretization scheme acts similarly as the dissipation at the subgrid scales. Hence, the unresolved, i.e. subgrid scale, terms are treated implicitly without an explicit subgrid scale model. A comprehensive overview of the method is given in the textbook by Grinstein et al. [90]. Furthermore it is noted that the MILES approach has been successfully applied in several spray and gas jet studies [92–97].

3.3   Spray modeling

The main computational concepts for spray simulations are the Lagrangian Particle Tracking (LPT) and the Euler–Euler (E-E) method. The latter treats both the gaseous and liquid phase as continua, whereas the LPT method models the liquid phase as discrete particles [11, 98]. The E-E method is well suited for dense sprays as they occur in the near nozzle region of typical fuel sprays, but becomes unpractical in more dilute spray regions. As typical fuel sprays are characterized by a very short liquid core and fast atomization due to hot air entrainment, sprays become quickly dilute and evaporate quickly [99]. Hence the LPT method is commonly used for fuel-spray simulations [41, 43, 51, 94, 100–105] and also applied in this thesis.

3.3.1   Droplet kinematics, mass and heat transfer

Following the LPT approach [11, 98], the liquid phase is described by several equations for droplet motion, heat and mass transfer. By defining

the droplet Reynolds number

$$Re_d = \frac{|\vec{u}_g - \vec{u}_d| \, d_d \rho_g}{\mu_g}$$

and the droplet time scale

$$\tau_d = \frac{\rho_d d_d^2}{18\mu_g} \tag{3.24}$$

the equation of motion reads

$$\frac{d}{dt}\vec{u}_d = \frac{C_D}{\tau_d}\frac{Re_d}{24}\left(\vec{u}_g - \vec{u}_d\right) , \tag{3.25}$$

where the subscript d denotes the droplet and g the gas phase quantities. The empirically determined values for the drag coefficient C_D can be expressed by the relations

$$C_D = \begin{cases} \frac{24}{Re_d}\left(1 + \frac{1}{6}Re_d^{2/3}\right) & Re_d < 1000 \\ 0.424 & Re_d \geq 1000 \end{cases} .$$

The change in droplet position is then obtained from

$$\frac{d}{dt}\vec{x}_d = \vec{u}_d .$$

The mass transfer from the liquid to the gaseous phase is modeled according to the droplet vaporization correlation by Frössling [106] and hence the change in droplet mass can be expressed by $\frac{dm_d}{dt} = -\frac{m_d}{\tau_e}$ with the evaporation time scale

$$\tau_e = \frac{\rho_d d_d^2}{6 D_m \; Sh \; \rho_v \ln\left(\frac{p - p_{v,\text{inf}}}{p - p_{v,s}}\right)} . \tag{3.26}$$

The heat transfer at the droplet surface is derived from the droplet energy balance and the Ranz–Marshall correlations for the Sherwood (Sh) and Nusselt (Nu) numbers [107, 108] are applied in the equations for mass and heat transfer. The implementation of the LPT method incorporates the parcel approach, which groups physically similar droplets into a parcel and reduces therefore the computational cost significantly.

3.3.2 Droplet breakup

Various breakup models have been proposed in the literature and an overview can be found in the textbooks by Ashgriz [9] or Stiesch [11]. Two breakup models, developed and well established for RANS simulations, are utilized in an implicit LES context in the course of the present thesis. The models are briefly introduced here and a more detailed description of the mathematical relations is given in Publication I.

The Kelvin–Helmholtz Rayleigh–Taylor (KHRT) model [109] is a combination of the Kelvin–Helmholtz (KH) wave model [110] and the assumption of occurring Rayleigh–Taylor (RT) instabilities at the droplet surface. A droplet breakup time scale is then obtained from model equations for these phenomena. The Enhanced Taylor Analogy Breakup (ETAB) model [111] is based on the TAB (Taylor Analogy Breakup) model proposed by O'Rourke and Amsden [112], and hence both share the basic concept for calculating the breakup time. Following the Taylor analogy, the droplet distortion can be modeled by a one-dimensional, forced, damped, harmonic oscillator. A solution to the equation describing the motion of the oscillator leads to an expression for the droplet breakup conditions and thus a breakup time scale can be calculated.

3.4 Discretization and numerical solution

Standard methods to obtain a numerical solution for a set of partial differential equations (PDE) include the finite difference, finite element, finite volume (FV) or spectral methods. In computational fluid dynamics (CFD), the FV method has been widely applied due to its conservative properties and a comparably easy implementation for unstructured grids [20]. Specifically the latter makes the method well suited for simulations of complex geometries, as they are found in many technical applications. Using the FV method, the computational domain is divided into small *control volumes* (e.g. tetrahedra, hexahedra or polyhedra) over which the PDEs are integrated. Using the Gauss divergence theorem, the divergence terms in the volume integrals are converted to surface integrals, referred to as *fluxes* in fluid mechanics. The conservative properties of the method arise from the requirement that the flux entering a control volume has to be identical to that leaving the adjacent volume. The LES flow solver used in this thesis is implemented in the open-source CFD framework OpenFOAM [113, 114]. The code offers a general framework to solve PDEs on unstructured grids using the FV method and various spatial and temporal discretization schemes are readily available.

In LES, it is generally desirable to employ low-dissipative schemes in order to adequately describe the large scale structures of the flow and hence obtain a close approximation of the physical solution [16, 20]. However, in LES a significant challenge arises due to the under-resolved simulation of turbulence associated with the filter operation. The dissipation of tur-

bulent kinetic energy takes place at the smallest, i.e. in LES unresolved, scales, and hence dissipation has to be explicitly accounted for to avoid the accumulation of energy at the highest wave numbers (compare Fig. 1.3). This can be achieved either by an explicit model term representing the unresolved scales in Eqs. (3.21)–(3.23), or implicitly by numerical dissipation from the discretization scheme. In the present work, high-resolution schemes based on flux limiter functions are employed in the FV framework, which yields a formally second order accurate scheme. In Publication I the `limitedLinear` scheme (see e.g. [115]) from the OpenFOAM framework was used for all convection terms, whereas in Publication II and III the `Gamma` scheme by Jasak et al. [116] was used.

It has been emphasized by several authors (e.g. [117–121]) that the scalar quantities in turbulent combustion simulation, such as mixture fraction, must remain bounded, if unphysical values of density or temperature are to be avoided. Hence, the coefficients of the flux limiter functions for the convection terms in the scalar transport equations are chosen such that the scheme is Total Variation Diminishing (TVD). For a general introduction to high-resolution schemes and the concept of limiters it is referred to the textbook by Hirsch [20]. For the time integration a second order accurate backward differencing scheme is used in all simulations. The pressure-velocity-density solution algorithm employed in this thesis is based on the compressible Pressure Implicit Splitting of Operators (PISO) technique [122].

3.5 Combustion modeling

As it was outlined in Chapter 1, the solution of detailed reaction mechanisms is unfeasible in multi-dimensional simulations of turbulent combustion, and thus simplified reaction mechanisms and/or combustion modeling approaches have to be considered. Next, the basic principles related to reduced chemical models, manifolds in composition space and flamelet modeling are introduced, as they form the basis of the combustion model used in the present thesis.

3.5.1 Conventional mechanism reduction

A method to obtain a simplified reaction mechanism that has been used extensively for decades is based on quasi-steady state and partial equilibrium

assumptions for intermediate species, often referred to as *conventional systematic reduction technique*. Chemical reaction times are typically in a range from 10^{-10}s to 1s, where the small time scales correspond to "equilibrium chemistry", i.e. reactions in partial equilibrium and species in a quasi-steady state. A comparison of the chemical and physical time scales of flow, transport and turbulence is given in Fig. 3.1. The quasi-steady
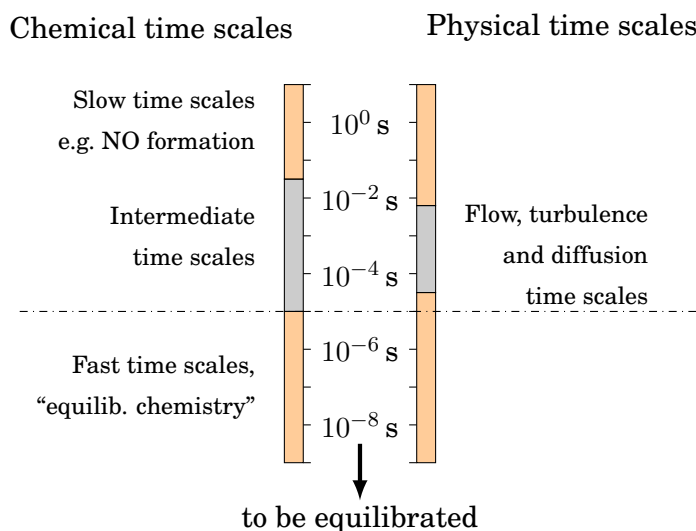
Figure 3.1 – Comparison of time scales in reacting flows [23].

state assumption for certain species allows to remove the fast chemical reactions and leads to a so-called reduced mechanism. The limited range of time scales in such a mechanism leads in turn to a significantly reduced stiffness and efficient solution of the system. However, this method requires certain insight into the reaction mechanism and the reduced mechanism is only valid for a limited range of conditions.

3.5.2 Intrinsic Low-Dimensional Manifolds

A method that aims at minimising the number of independent variables is the method of Intrinsic Low-Dimensional Manifolds (ILDM) developed by Maas and Pope [123]. The theoretical basis of this method is given by the fact that the evolution of a reactive system can be described by trajectories in the $(2 + N_s)$-dimensional state space spanned by enthalpy h, pressure p and N_s species mass fractions. After a sufficiently long enough time, the system reaches eventually an equilibrium state. The state of the reactive system at equilibrium is fully determined by the conserved quantities (absolute enthalpy, pressure and the element mass fraction), i.e. variables invariant to chemical reactions, whereas the combustion progress from unburnt to burnt is described by the evolution of the species mass

fractions.

The ILDM method relies on the fact that many of the chemical time scales involving intermediates in the reaction chain are fast and thus not rate limiting. Hence, by neglecting chemical reactions faster than the considered time scales a corresponding m-dimensional manifold, with $m < (2 + N_s)$, exists and gives an approximation of the system. To identify the fast time scales the ILDM method uses a local eigenvector analysis of the Jacobian of the differential equation system. In practical applications of the ILDM method the thermochemical quantities (e.g. temperature T or species mass fractions Y_α) are pre-calculated and tabulated as a function of the degrees of freedom, often called control variables $\Phi_1 \ldots \Phi_m$. The dimension of the database corresponds to the dimension of the manifold m. In comparison to the direct computation of detailed chemistry, where a transport equation for each species is solved together with the stiff system of differential equations, the computational cost is reduced to solving a transport equation for each control variable Φ_i and a table look-up routine for the thermochemical quantities. Details, limitations and improvements of the original ILDM method can be found in a wide range of literature, e.g. [123–128].

3.5.3 Overview of flamelet models

Another group of methods to reduce the computational load of combustion simulation is based on the laminar flamelet concept. The theoretical background for the flamelet concept to treat a turbulent diffusion flame as a statistical ensemble of laminar diffusion flames was given by Williams [129]. The concept was subsequently generalized to view a multi-dimensional flame locally as an ensemble of laminar one-dimensional flames, the so-called flamelets [130–137]. A range of combustion models are based on the flamelet concept, e.g. the *G-equation* [138] and *Reactive Interactive Flamelet (RIF)* [139] model.

The definition of a flamelet further implies that the trajectory in state space of a multi-dimensional flame will be close to the trajectory found from a corresponding one-dimensional flame. Using this implication allows to construct low-dimensional manifolds from flamelet solutions, which is the basis for the *Flamelet Generated Manifold (FGM)* approach developed by van Oijen and de Goey [140]. The FGM method can be seen as an extension of the ILDM method to include convection and diffusion effects and hence broadens the applicability of the method. The *Flamelet Prolonged ILDM*

(FPI), independently developed by Gicquel et al. [141], is based on the same assumptions as the FGM method. For nonpremixed combustion, the *Flamelet Progress Variable (FPV)* method developed by Pierce and Moin [142], and further extended by Ihme et al. [143], leads to a tabulated chemistry approach, where the thermochemical quantities are similarly obtained from flamelet calculations. The common characteristic of these methods is that the high-dimensional thermochemical state space obtained from flamelet calculations is projected onto a low-dimensional manifold.

3.5.4 Nonpremixed flamelets

Different formulations of the flamelet equations exist for various canonical flame configurations. A commonly used setup for nonpremixed combustion problems is given by the opposed flow, strained flame problem, where the fuel and oxidizer flows mix and form a reaction zone as depicted in Figure 3.2. Starting from a two-dimensional description of the reacting
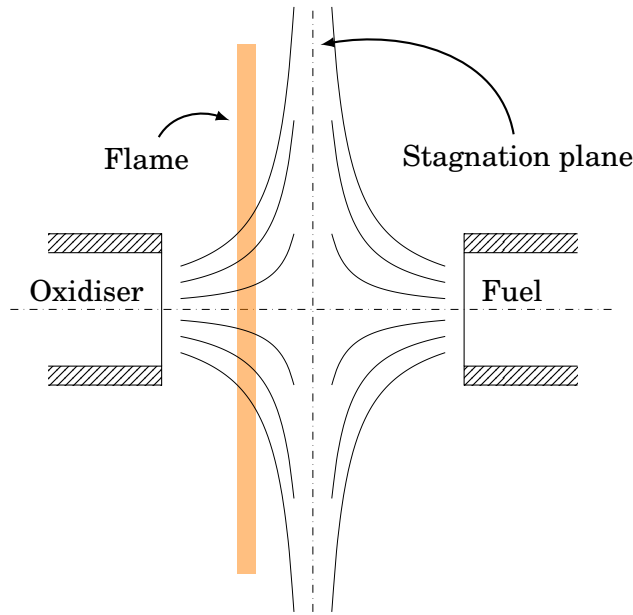
Figure 3.2 – Schematic setup of a counterflow flame.

Navier–Stokes equations, Kee et al. [144] showed that the problem can be reformulated in one-dimension by introducing the local flame stretch rate K defined as the tangential velocity gradient

$$K(x,t) := \frac{\partial v}{\partial y} \; .$$ (3.27)

It should be noted that K is solely depending on the spatial coordinate x and time t, and its definition allows for the derivation of a transport equation (see Appendix A). Here the unsteady formulation by Stahl and

Warnatz [137] is adopted:

$$\frac{\partial \rho}{\partial t} + \frac{\partial \rho u}{\partial x} = -\rho K$$

$$\frac{\partial \rho Y_\alpha}{\partial t} + \frac{\partial \rho u Y_\alpha}{\partial x} = \frac{\partial}{\partial x}\left(\rho D \frac{\partial Y_\alpha}{\partial x}\right) - \dot\omega_\alpha - \rho K Y_\alpha$$

$$\text{with } \alpha = 1 \dots N_s - 1 \tag{3.28}$$

$$\frac{\partial \rho h}{\partial t} + \frac{\partial \rho u h}{\partial x} = \frac{\partial}{\partial x}\left(\rho D \frac{\partial h}{\partial x}\right) - \rho K h$$

$$\frac{\partial \rho K}{\partial t} + \frac{\partial \rho u K}{\partial x} = \frac{\partial}{\partial x}\left(\mu \frac{\partial K}{\partial x}\right) + \rho_{ox}\left(\frac{\partial a(t)}{\partial t} + a(t)^2\right) - 2\rho K^2$$

The diffusion coefficient D results from the unity Lewis number assumption as $D = \frac{\lambda}{\rho c_p}$. The chemical source term in the species equations $\dot\omega_\alpha$ is computed following the relations given in Section 3.1.3. For the species mass fractions and enthalpy, Dirichlet boundary conditions are applied in the oxidizer and fuel stream. The boundary conditions for the flame stretch rate result from the assumptions used to derive the transport equation (see Appendix A), i.e. Dirichlet boundary conditions in the oxidizer ($K_{ox}(t) = a(t)$) and Neumann in the fuel stream ($\frac{\partial K}{\partial x}\big|_{fu} = 0$). The numerical solution of Eqs. (3.28) is obtained with the one-dimensional flame code CHEM1D [145, 146].

3.6 Flamelet Generated Manifolds

Based on the theoretical considerations of the ILDM method (see Section 3.5.2), a reactive system can be represented by trajectories in the $(2 + N_s)$-dimensional state space spanned by enthalpy h, pressure p and N_s species mass fractions. The basic assumption of the FGM model is that the trajectories in the state space of a multi-dimensional flame can be approximated by a trajectory found from a respective set of flamelet solutions. Further following the ILDM approach, the flamelet solutions are subsequently parametrized by a low number of control variables, which yields a so-called Flamelet Generated Manifold.

3.6.1 FGM parametrization

The governing processes in nonpremixed, and specifically in spray, combustion systems are the mixing of fuel and oxidizer, ignition, and the reaction progress in the diffusion flame. Hence, suitable control variables have to be chosen to adequately describe the spatial and temporal variations of these processes. The mixing process is described by the mixture fraction Z,

as defined in Section 3.1.4. The flamelet solutions of the present counter-flow flames are obtained in physical space, which is illustrated in Fig. 3.3 showing the temperature and CO profiles as a function of spatial coordinate x at various time instances. Mixture fraction is a monotonic function

(a) Temperature

(b) CO mass fraction
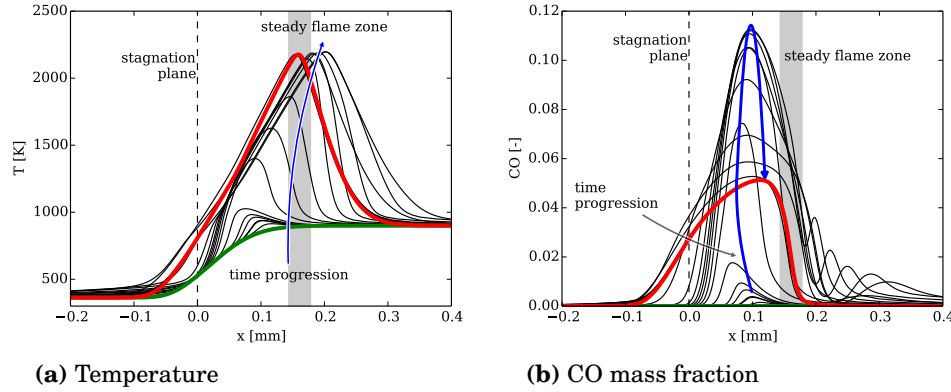
Figure 3.3 – Transient counterflow diffusion flamelet solution for n-dodecane ($T_{fu} = 363$K, $T_{ox} = 900$K, $a = 500$s^{-1}). The green and red lines mark the initial conditions and steady state, respectively. The flame zone is here determined by the location of the highest heat release in the steady state.

of spatial coordinate x, which allows a direct mapping from physical to mixture fraction space, and hence the thermochemical quantities ψ can be expressed as a function of mixture fraction $\psi = \psi(Z)$.

Ignition and the reaction progress in a diffusion flame can be described by the evolution of suitable species mass fractions. With respect to the transient behavior during igniting any chemical species which increases or decreases monotonically in time from the initial mixing solution to chemical equilibrium is suitable. However, the ignition process involves a large number of radicals and intermediate species, which generally do not exhibit a monotonic behavior throughout the transition towards chemical equilibrium. Hence, to ensure (a) a monotonic behavior and (b) to capture the ignition process as well as the steady flame sufficiently, the progress variable is constructed from a linear combination of species mass fractions:

$$\mathcal{Y} = \sum_i \gamma_i Y_i \tag{3.29}$$

The species i and weight factors γ_i have to be chosen for the particular combustion system of interest. A typical choice for hydrocarbon fuels includes the major combustion products CO_2 and CO (e.g. [105, 147–152]). To capture the early onset of ignition, formaldehyde (CH_2O) is well suited

as it is formed in relatively high concentrations during the early ignition phase [151]. The reciprocal of the species' molecular weights are chosen as weight factors, $\gamma_i = 1/M_i$, to achieve a more balanced contribution of the single species during the different phases of ignition and combustion. Hence, a time-accurate solution of the counterflow flamelet equations is obtained to describe the ignition process, which is then parametrized by $\mathcal{Y}$. It should be noted that for the unsteady flamelet the maximum value of the progress variable after ignition slightly exceeds the steady state value. After this, the progress variable decreases slightly and reaches the steady state value, as the flamelet solution approaches the chemical equilibrium. This part of the unsteady flamelet solution is omitted from the current FGM database to ensure monotonicity of the progress variable and hence a consistent FGM database.

To account for the reaction progress in the steady flame, the FGM database obtained from the unsteady flamelet solution is extended by steady state flamelets at a range of strain rates ($a = 1 \dots 500\,\mathrm{s}^{-1}$). The steady flamelet solutions are parametrized by $\mathcal{Y}$ as well, where the unsteady flamelet solution is obtained at the highest strain rate ($a = 500\,\mathrm{s}^{-1}$) to ensure a monotonic behavior over both parameters (time t and strain rate a). Figure 3.4 shows the temporal evolution of $\mathcal{Y}$ for a strain rate $a = 500\,\mathrm{s}^{-1}$, as well as the steady state solutions over a range of strain rates in a flamelet calculation relevant to the present spray combustion cases.
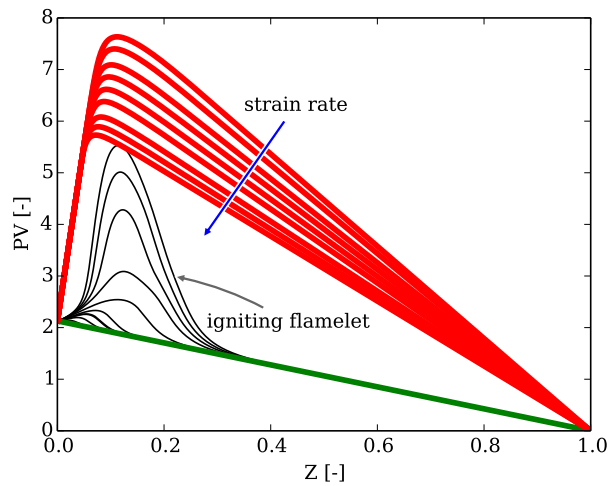
Figure 3.4 – Progress variable as function of mixture fraction for an igniting counterflow flamelet ($a = 500\mathrm{s}^{-1}$, black lines) and steady state solutions (red lines) at strain rates ranging from $a = 500 \dots 1\mathrm{s}^{-1}$. The initial mixing solution is indicated by the green line.

In summary, the flamelet solutions are obtained in physical space ($\psi =$

$\psi(x,t)$) and parametrized by mixture fraction and progress variable ($\psi = \psi(Z, \mathcal{Y})$), i.e. a low-dimensional manifold is generated based on flamelet solutions. It should be noted that all flamelet calculation are carried out with the assumption of constant pressure and conserved enthalpy, and hence variations of these quantities are not represented in the FGM database. If variations in one or more of them are expected to have a significant influence on the combustion, they would have to be included as an additional control variable and hence increase the dimension of the manifold.

3.6.2 FGM implementation

The coupling of the FGM database containing the thermochemical quantities and the multi-dimensional flow solver is described in the following. In the flow solver a transport equation for each control variable has to be solved. For nonpremixed combustion, this leads to the transport equation for mixture fraction (Eq. 3.19) and an additional transport equation for the reaction progress variable. The latter can be derived from the transport equations for species mass fraction and reads

$$\frac{\partial \rho \mathcal{Y}}{\partial t} + \frac{\partial (\rho \mathcal{Y} u_j)}{\partial x_j} = \frac{\partial}{\partial x} \left(\frac{\lambda}{c_p} \frac{\partial \mathcal{Y}}{\partial x_j} \right) + \dot{\omega}_{\mathcal{Y}} \, , \qquad (3.30)$$

where the chemical source term $\dot{\omega}_{\mathcal{Y}}$ is obtained from the FGM database. Having obtained the mixture fraction and progress variable fields as a function of spatial coordinates and time in the flow solver, the thermochemical quantities of interest as well as the progress variable source term can be retrieved from the FGM database with a multi-dimensional linear interpolation.

Various coupling strategies concerning the temperature and density changes exist, depending on the flow case and solver implementation. Here, three commonly used options are briefly introduced:

1. Update temperature, density and thermophysical (i.e. μ, λ, c_p) properties directly from the FGM database: This implies that all variations of the conserved variables are either incorporated into the FGM database or can be neglected. (This option has been used e.g. by Vreman et al. [153], Kröger et al. [154].)

2. Update a representative set of species mass fractions and calculate temperature/density subsequently: This requires the solution of the enthalpy equation and the calculation of the temperature/density

from the respective equations of state (Eqs. 3.10 and 3.11), as well as the evaluation of the thermophysical properties in the flow solver (used e.g. in [43, 155]).

3. Solve a transport equation for a representative set of species and obtain the chemical source terms from the FGM database. Temperature, density and thermophysical properties are calculated as in Option 2 (used e.g. in [42, 148]). However, compared to Option 2, this allows to take differential diffusion effects in the flow solver into account.

In the present thesis, the coupling of the FGM database with the flow solver is achieved via a representative set of species mass fractions (Option 2). In the flow solver, these species mass fractions are looked-up from the FGM database and thus no transport equations for the species mass fractions are solved. The thermophysical properties are subsequently evaluated for the representative species in the flow solver as described in Section 3.1.2. The temperature calculation is based on the absolute enthalpy (Eq. (3.9)) and mixture averaged heat capacity, which allows to account for cooling effects due to evaporation in the upstream liquid fuel spray. However, the effect of the lower temperature in the upstream fuel spray on the reaction source term is neglected in the present approach. This assumption will be further discussed in Section 4.2. The coupling approach further implies the assumption of unity Lewis number for all species.

For the combustion cases in the present thesis 15 representative species are considered out of the few hundred species in the respective chemical mechanisms. However, this subset of species does not ensure the conservation of mass, energy or thermodynamic properties, specifically during ignition or in the fuel-rich high temperature flame where many intermediate species are involved. Galpin et al. [148] proposed a procedure based on atomic mass budget considerations to ensure element mass conservation for a reduced set of species. This approach has been successfully applied in LES of methane flames [148] as well as α-methylnaphthalene/n-decane sprays [152]. The conservation of energy and thermodynamic properties, however, would not be ensured by atomic budget considerations for the present spray flames, specifically during ignition. To remedy this defect, a constrained sequential least squares programming procedure is applied to optimize the species mass fractions of the subset with respect to element mass and energy conservation. A more detailed description of this proce-

dure can be found in the Appendix of Publication II. It should be noted that not all species are subject to this optimization procedure (e.g. n-$C_{12}H_{26}$, OH and CH_2O), in order to accurately predict fuel evaporation and allow for post-processing calculations during run-time.

3.7   Turbulence chemistry interaction

In LES of non-reacting flows, equations for the mean quantities are solved, and the unclosed terms are modeled accordingly, as described in Section 3.2. For turbulent combustion, however, an additional problem arises, when the filtered transport equations for the species composition (compare Eq. (3.8)) are derived, as the filtered reaction source terms $\overline{\dot{\omega}_\alpha\left(\vec{x},t\right)}$ appear in unclosed form, and hence require modeling. The approximation to evaluate the reaction source term based on the mean quantities, $\overline{\dot{\omega}_\alpha\left(\vec{x},t\right)} = \dot{\omega}_\alpha\left(\overline{\rho\left(\vec{x},t\right)}, \widetilde{T\left(\vec{x},t\right)}, \widetilde{Y_\alpha\left(\vec{x},t\right)}\right)$, may lead to significant errors, depending on the grid resolution and filter width, as well as on the turbulent flow and combustion conditions.

   The closure model used in the present thesis is introduced next, followed by a brief description of alternative approaches.

3.7.1   Probability Density Function methods

Many models for the reaction source terms are based on expressing $\overline{\dot{\omega}_\alpha\left(\vec{x},t\right)}$ in terms of a *Probability Density Function (PDF)* [156] as

$$\overline{\dot{\omega}_\alpha\left(\vec{x},t\right)} = \int_{Y_\alpha}\int_T\int_\rho \dot{\omega}_\alpha\left(\rho,T,Y_\alpha\right)\mathcal{P}\left(\rho,T,Y_\alpha;\vec{x},t\right) d\rho\,dT\,dY_\alpha\,, \qquad (3.31)$$

where $\mathcal{P}\left(\rho,T,Y_\alpha;\vec{x},t\right))$ is either a prescribed or calculated PDF of the subgrid composition. In the latter case, a (modeled) transport equation is solved for the subgrid composition PDF. In LES this leads to the so-called *Filtered-Density Function (FDF)* approach proposed by Pope [157]. Similar models are used in the LES and RANS approaches, and are generally referred to as *transported PDF* methods; for a detailed description it is referred the comprehensive review by Haworth [158]. It should be noted at this point that even though these considerations are presented for LES with a direct evaluation of the chemical source terms, the same closure problem arises for the FGM combustion modeling approach, which can be directly seen from the definition of the reaction progress variable (compare Eqs. (3.29) and (3.30)).

   In the *presumed PDF* approach, the subgrid composition PDF is assumed

to have a certain shape and subsequently parametrized by its first and second moments, which are obtained from transport equations or algebraic models. This approach has been proven successful especially in nonpremixed flames with various chemical kinetic models [42, 142, 143, 153, 159, 160]. The presumed PDF approach has found wide adoption specifically in models based on the ILDM method, since the subgrid composition can be parametrized by a low number of variables and thus leads to a realizable joint PDF. With respect to the FGM method for nonpremixed combustion LES, this leads to a joint PDF of mixture fraction and reaction progress variable and hence the thermochemical quantities read

$$\widetilde{\psi} = \int \int \mathcal{F}_\psi(Z, \mathcal{Y}) \widetilde{P}(Z, \mathcal{Y}) \, dZ \, d\mathcal{Y} \, , \tag{3.32}$$

where $\widetilde{P}$ denotes the density weighted joint PDF and is generally unknown. Since in nonpremixed combustion $\mathcal{Y}$ is generally dependent on mixture fraction Z, a normalized progress variable $\mathcal{C}$ is defined as

$$\mathcal{C} = \frac{\mathcal{Y} - \mathcal{Y}_{\min}(Z)}{\mathcal{Y}_{\max}(Z) - \mathcal{Y}_{\min}(Z)} \, , \tag{3.33}$$

where $\mathcal{Y}_{\max}(Z)$ and $\mathcal{Y}_{\min}(Z)$ denote the minimum and maximum values of $\mathcal{Y}$ at a given mixture fraction. The definition of $\mathcal{C}$ allows the assumption of statistical independence for Z and $\mathcal{C}$ [161]. By further assuming the beta- and delta-function to approximate the marginal mixture fraction and progress variable distributions, the joint PDF simplifies to

$$\widetilde{P}(Z, \mathcal{Y}) = \widetilde{P}(Z) \widetilde{P}(\mathcal{C}) = \beta(Z; \widetilde{Z}, \widetilde{Z''^2}) \delta(\widetilde{\mathcal{C}} - \mathcal{C}) \, . \tag{3.34}$$

In LES, the mean value of mixture fraction is obtained from Eq. (3.23) and the filtered transport equation for the progress variable reads

$$\frac{\partial \left(\overline{\rho} \widetilde{\mathcal{Y}} \right)}{\partial t} + \frac{\partial \left(\overline{\rho} \widetilde{u_j} \widetilde{\mathcal{Y}} \right)}{\partial x_j} = \frac{\partial}{\partial x_j} \left(\overline{\rho} \widetilde{u_j} \widetilde{\mathcal{Y}} - \overline{\rho u_j \mathcal{Y}} + \overline{\rho} \widetilde{D} \frac{\partial \widetilde{\mathcal{Y}}}{\partial x_j} \right) + \overline{\dot{\omega}_\mathcal{Y}} \, . \tag{3.35}$$

The residual term resulting from the filter operation is modeled analog to the terms in Eqs. (3.20)–(3.22), as described in Section 3.2.

The subgrid mixture fraction variance is estimated using an algebraic model [162]

$$\widetilde{Z''^2} = \widetilde{Z^2} - \widetilde{Z}^2 = C_v \Delta^2 \left| \frac{\partial \widetilde{Z}}{\partial x_j} \right|^2 \, , \tag{3.36}$$

where C_v is a dynamically evaluated model coefficient [163] and Δ denotes the LES filter width.

3.7.2 Alternative approaches

In combustion problems, the value of the species mass fractions and temperature within the main reaction zone often appears to depend strongly on the local instantaneous value of some variable, such as mixture fraction $Z(x, t)$ in nonpremixed combustion systems. Utilizing this observation, Klimenko [164] and Bilger [165] independently derived transport equations for a conditional expectation of species mass fractions $Y_\alpha(x, t)$ and temperature $T(x, t)$, conditional on the associated value of $Z(x, t)$. The method is known as the Conditional Moment Closure (CMC) and belongs to the class of presumed PDF methods. A detailed introduction to the CMC method can be found in the comprehensive review by Klimenko and Bilger [166].

Alternatively, different types of phenomenological models can be used to approximate the filtered reaction source terms $\overline{\dot{\omega}_\alpha(\vec{x}, t)}$. Here, a very brief overview is given, introducing the Thickened Flame Model (TFM) [167–169], the Eddy Dissipation Concept (EDC) model [170] and the Partially Stirred Reactor (PaSR) model (e.g. [41, 171, 172]). The TFM model is based on an observation by O'Rourke and Bracco [173], who noted that the flame thickness can be rescale while preserving the flame speed. For LES this can be realized by increasing the diffusion coefficient D_α by a factor F, if the filtered reaction source terms $\overline{\dot{\omega}_\alpha(\vec{x}, t)}$ are decreased by the same factor F. This operation leads to a flame thickness that is multiplied by F and can be resolved in an LES. Various subgrid scale effects can be accounted for by an efficiency function [168] and the model has been extended to nonpremixed combustion by using a sensor [169] to activate the rescaling only in the reaction zone and hence avoid altering the inert mixing. The PaSR approach is based on the Eddy Dissipation Concept by Magnussen [170], and thus both models share the idea of dividing the computational cell into a reacting part and a non-reacting part. The reacting part is treated as a perfectly stirred, i.e. homogenous, reactor and the subgrid interaction with the non-reacting part is explicitly accounted for by certain submodels. The PaSR and EDC models have gain considerable popularity in RANS simulations of diesel fuel sprays, e.g. [41, 51, 100, 101, 171].

4. Results and discussion

Turbulent spray combustion involves various complex physical and chemical processes. In order to establish reliable and predictive models, it is beneficial to study the critical phenomena independently. This becomes especially important when computationally demanding models or simulation techniques are used and parameter studies would thus become cumbersome. However, due to the tight coupling of the various processes such independent studies are not always possible. In the following various aspects concerning turbulent spray combustion modeling are explored, starting with results from non-reacting spray simulations in Section 4.1. These results were earlier published in Publication I. In Section 4.2, results from canonical combustion configurations are analyzed, which are used to generate the low-dimensional manifolds for the spray combustion simulations in Publication II and III. Finally, results from turbulent spray combustion LES published in Publication II and III are discussed in Section 4.3.

4.1 Non-reacting sprays and mesh sensitivity

Non-reacting spray simulations allow to isolate and analyze effects of the various modeling assumptions in the LPT/LES approach at a reasonable computational cost. Thus, in Publication I, non-reacting simulations of the Spray A baseline case ($0\,\%$ O_2, $900\,K$, $22.8\,kg/m^3$ and $150\,MPa$) were carried out to evaluate and develop the spray modeling approach in an LES context. Also Publication III includes a parameter study of the injection pressure effects in non-reacting spray LES.

The objectives of the research for Publication I are (1) to investigate the effect of the grid resolution in high-velocity fuel spray LES, and (2) to understand the sensitivity of droplet breakup modeling to integral spray

quantities and mixture formation. Therefore, four mesh resolutions (250, 125, 62.5 and 41.67 µm) and two breakup models (ETAB and KHRT) are considered for this study.

Important global measures for high-velocity fuel sprays are:

1. Breakup length: The distance from the injection location at which the droplets have reached a stable diameter and no further breakup occurs.

2. Liquid length: The maximum penetration of the liquid phase. The liquid length marks the steady state at which the total evaporation rate equals the fuel injection rate.

3. Vapor penetration: The maximum distance to the injection location of $0.1\,\%$ vapor mass fraction

The simulated liquid length, here defined as in Publication I by the maximum distance of $95\,\%$ liquid mass to the injection location, is compared with the experimental data obtained at Sandia in Fig. 4.1. As a first observation it can be seen that the cases with a $250\,\mu m$ mesh resolution are not able to predict the liquid length correctly. The situation improves significantly for the $125\,\mu m$ mesh resolution, which leads in the case of the ETAB model to an accurate prediction of the liquid length and for the KHRT model to an overshoot of approximately $50\,\%$. The simulations with the $41.67\,\mu m$ and $62.5\,\mu m$ mesh resolution provide good results, which appear to be insensitive to the breakup model.

From further investigations of the flow fields (Fig. 4.2), it can be concluded that the $250\,\mu m$ cell size is too large to model the momentum transfer from the liquid to the gas phase correctly. Furthermore, the mesh resolution is too coarse to capture the turbulent motion of the flow. Hence, also the air entrainment and consequently the heat transfer from the gas phase to the droplets is not correctly predicted. Both effects contribute to a slower evaporation and thus the significantly over-predicted liquid length. Even though the liquid length for the $125\,\mu m$–KHRT case is also over-predicted, the mesh resolution is high enough to resolve a considerable part of the turbulent motion. Discarding the $250\,\mu m$ mesh resolution cases in what follows, a comparison of the experimental and the simulated vapor penetration is shown in Fig. 4.3. The results are in good agreement with the experimental data for both breakup models. However, it is observed that the simulations under-predict the vapor penetration slightly.

---

[4]Reprinted from Publication I with permission from Begell House, Inc.
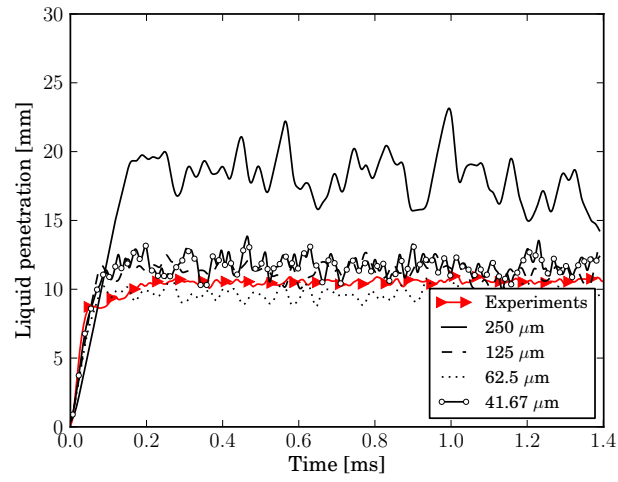
(a) ETAB
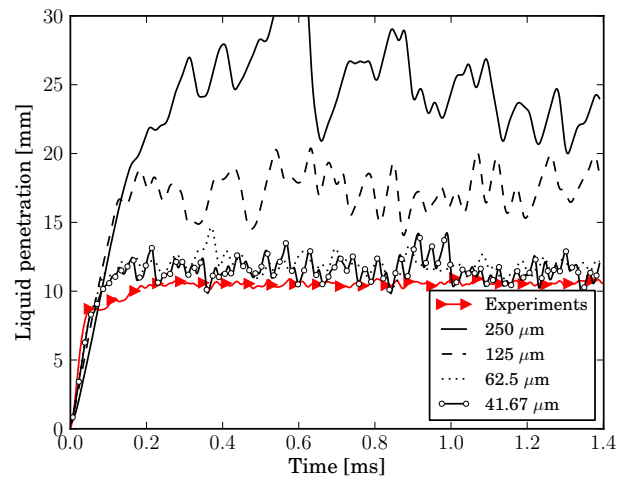
(b) KHRT

Figure 4.1 – Liquid length versus time for the four mesh sizes comparing the ETAB and KHRT breakup model.[4]

(a) 250 μm   **(b)** 125 μm   **(c)** 62.5 μm   **(d)** 41.67 μm

Figure 4.2 – Instantaneous vapor mass fraction comparing the four mesh resolutions (KHRT model).[4]

Figure 4.3 – Vapor penetration over time; KHRT: ○, ETAB: no marker[4]
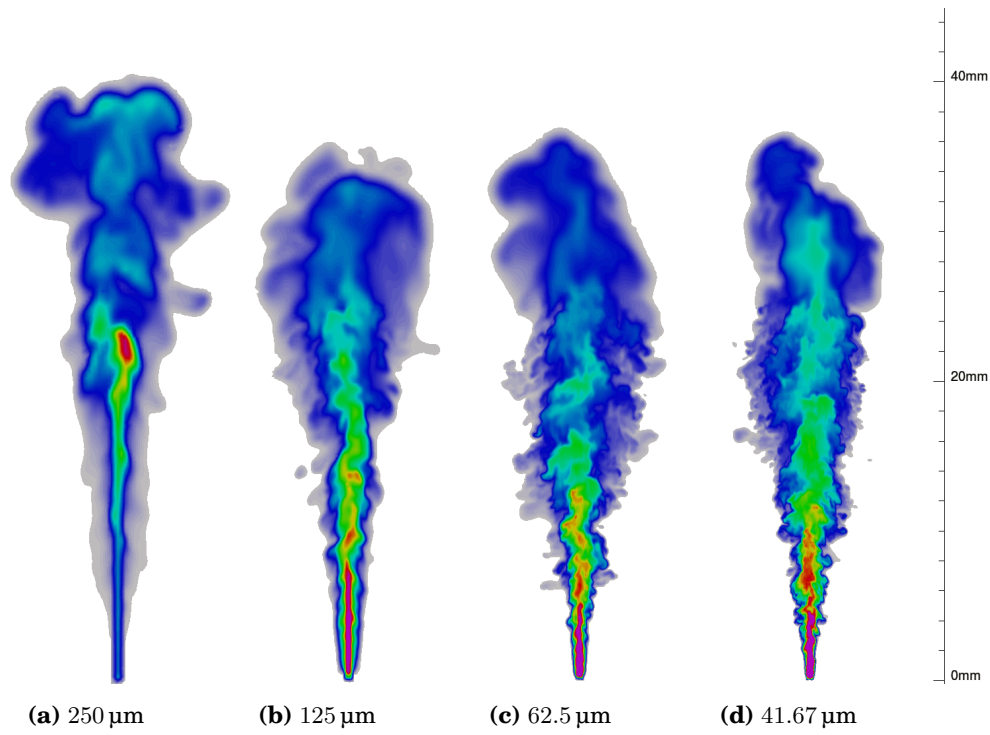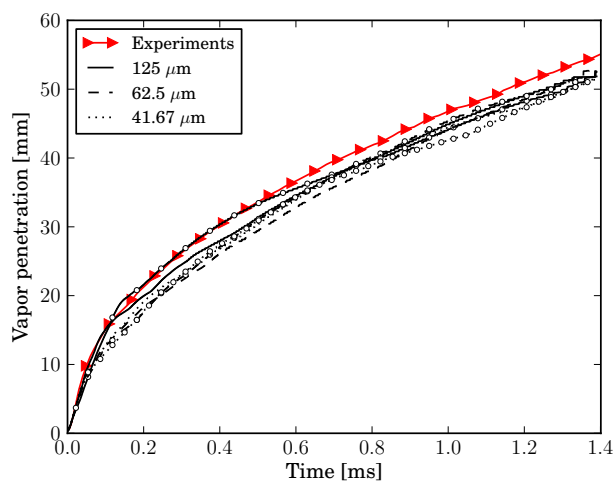
The results for liquid and vapor penetration show rather small differences between the breakup models, given a sufficient mesh resolution (i.e. 62.5 and $41.67\,\mu m$). An analysis of the Weber number in Publication I suggests that the droplet breakup occurs mainly within the first $2\,mm$ from the injection location, where the droplets reach a stable diameter. It is worth to point out that the average droplet sizes are found to be very small (between 0.3 and $1.5\,\mu m$, depending on the breakup model and mesh resolution). The droplet lifetime is thus mostly determined by the evaporation rate. Due to a rather constant injection pressure, and thus a constant initial droplet velocity, the limiting factor for the liquid length is therefore the evaporation time scale. The evaporation time scale is dependent on the droplet diameter and temperature, and thus the heat transfer from gas to liquid phase plays a crucial role. The rate of heat transfer again is limited by air entrainment, i.e. mixing, which requires a sufficient mesh resolution in order to resolve a significant part of the turbulent motion.

To conclude this subsection, LES of non-reacting sprays gives valuable insight into mesh resolution requirements and spray model implications. Most importantly, it was found that a high mesh resolution, and hence a sufficiently resolved turbulent motion, is paramount for accurate predictions of the spray characteristics and mixture formation. This is further emphasized by the mixing controlled nature of high-velocity fuel sprays. An adequate mesh resolution for the present spray case was achieved with cell sizes slightly smaller than the nozzle hole diameter. The global spray characteristics are shown to be rather insensitive to the breakup modeling approach. This holds also true for the local mixture formation after the liquid fuel has been evaporated and hence the resulting gas jets are very similar. It should be noted that the results are, at least partially, depending on the computational framework (OpenFOAM) and the underlying algorithms (FVM discretization, PISO solution algorithm, etc.). From the viewpoint of LES fuel spray modeling, the present results support the view that with the increase in mesh resolution, and the resulting resolved features of the flow, the importance of the breakup modeling decreases. The further can be assumed that a more advanced description of the thermodynamic and transport processes related to the liquid-gas phase transition may require an even finer mesh resolution than in the current study.

4.2 Canonical combustion configurations

The data obtained from flamelet calculations play a crucial role in the FGM combustion modeling approach because such datasets define the manifold which is used in the multi-dimensional turbulent combustion simulations. Typically, flamelet calculations are carried out with certain boundary conditions or further assumptions derived from the turbulent combustion conditions. Hence, an investigation of the flamelet data prior to the generation of the low-dimensional manifold and an evaluation of these assumptions based on the flamelet data can yield already valuable insight into the ignition characteristics and combustion process. The results and discussion in this section are mainly focused on the ignition delay time (IDT), a widely used measure with respect to ignition, defined as the time when $2\,\%$ of the steady state OH mass fraction is reached, unless stated otherwise. Most of the results in this section were published earlier in Publication II.

4.2.1 Flamelet boundary conditions

In the LES, fuel is injected into the combustion chamber in liquid form and evaporation is explicitly modeled. The flamelet calculations, however, consider only the gas phase and do not account for the energy required to evaporate the liquid fuel. The implications of this approach were investigated in unsteady flamelet calculations with different fuel inlet temperatures T_{fu} (Publication II). The calculations were carried out for the Spray A baseline conditions ($T_{\mathrm{ox}} = 900\,\mathrm{K}$ and $15\,\%$ O_2) using the Stanford mechanism and an applied strain rate $a = 500\,\mathrm{s}^{-1}$ (compare Eq. 3.28). The numerical investigations indicate that the fuel inlet temperature has only a small influence on the IDT, which amounts to differences of about $10\,\%$ between $T_{\mathrm{fu}} = 250\,\mathrm{K}$ and $T_{\mathrm{fu}} = 363\,\mathrm{K}$. The species composition for $Z < 0.2$ is practically unchanged and only minor differences are observed for higher Z. This is an important observation from a combustion modeling perspective, as it allows to assume a fuel inlet temperature of $363\,\mathrm{K}$ in the flamelet calculation to approximate the conditions in the combustion chamber relevant to ignition and combustion. However, it should also be noted that this is specific to the present case, also considering that evaporation and ignition take place in spatially separated locations and a flame–droplet interaction is not of primary concern.

A boundary condition in the flamelet calculations typically not known

prior to the turbulent combustion LES is the applied strain rate. Hence, the strain rate dependency of the IDT was investigated in Publication II using unsteady flamelet calculation at strain rates $a = 5 \dots 4000 \, \mathrm{s}^{-1}$. The extinction strain rate was found to be above 2000 and $3000 \, \mathrm{s}^{-1}$ for the POLIMI and Stanford mechanisms, respectively. From Fig. 4.4, showing the IDT over strain rate, it is noted that the IDT is insensitive to the strain rate for $a < 1000 \, \mathrm{s}^{-1}$, irrespective of the chemical mechanisms. The investigation showed that the strain rate has only a small effect
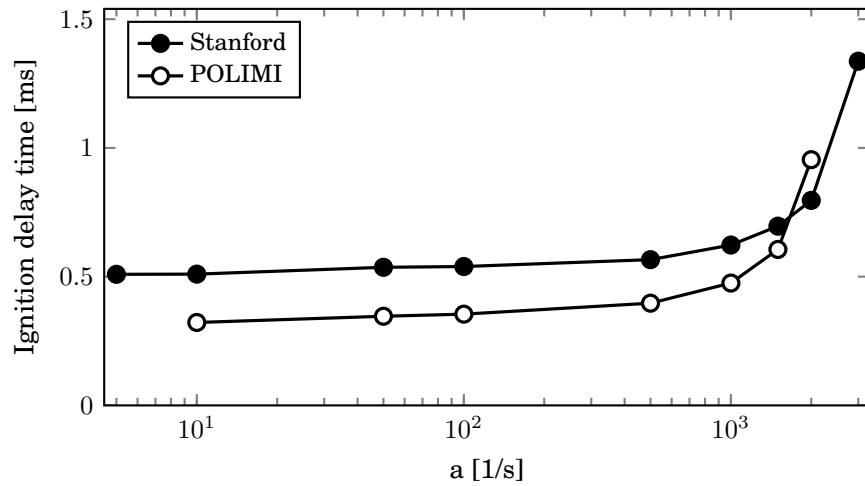
Figure 4.4 – IDT as a function of strain rate a obtained from unsteady flamelet calculations.

on the species composition in the early onset of ignition, where the first intermediate species and radicals are formed. Differences are observed towards the end of ignition when the high temperature combustion is reached, which is to be expected due to the strain rate dependency of the steady flamelets [42, 43].

4.2.2 Chemical mechanisms

The chemical mechanism used in spray combustion simulations of n-dodecane has been identified in several studies [46, 63, 67] as a source of uncertainty with respect to ignition predictions. For an evaluation of chemical mechanisms, canonical combustion configurations like homogenous reactors or flamelets are well suited, as they allow to isolate the influence of the chemistry model from turbulence effects. Therefore, in a first step, the IDTs obtained from homogenous reactor calculations with the POLIMI and Stanford mechanisms are compared in Fig. 4.5 for three ambient oxygen concentrations (see Table 2.1). The results show a consistent offset between the two mechanisms, where the absolute difference in IDT at the
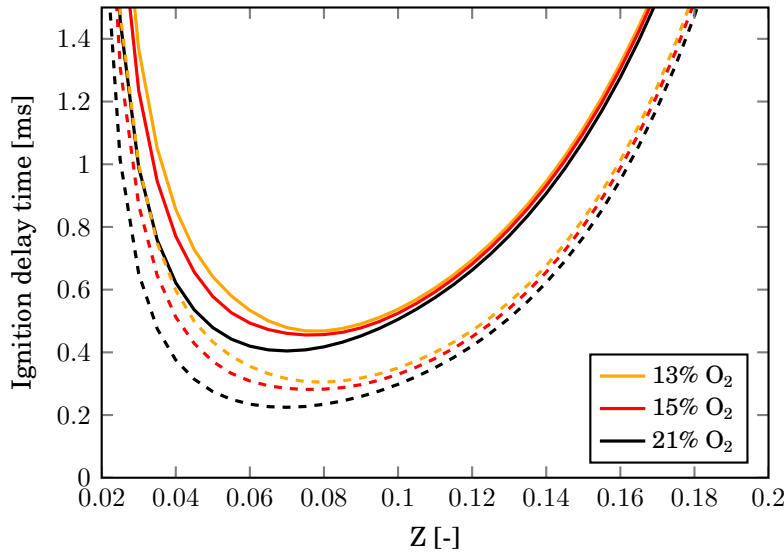
Figure 4.5 – IDT as a function of mixture fraction Z obtained from homogenous reactor calculations. Solid lines mark the Stanford and dashed lines the POLIMI mechanism.

most reactive condition is approximately $0.17\,\text{ms}$ for all the three ambient conditions.

The data from unsteady flamelet calculations ($\tau_{\text{ign}}^{\text{F}}$) were analyzed in Publication II and the IDT results show the same difference of $0.17\,\text{ms}$ for all three oxygen cases (see also the results for the $15\,\%\;O_2$ case in Fig. 4.4). However, when plotting the temperature as a function of mixture fraction at times shifted relative to the IDT ($t^* = t - \tau_{\text{ign}}^{\text{F}}$), similar flame structures are observed with both mechanisms (Fig. 4.6). Hence, the results from the homogenous reactors and flamelet calculations both imply that the differences in IDT between the mechanisms originate dominantly from the chemistry and are not significantly affected by the mixing. It is important to note that the observed absolute difference of $0.17\,\text{ms}$ translates to a relative difference of $35\,\%$ to $70\,\%$, depending on the ambient oxygen concentration.

Results from the steady state flamelet calculations at a range of strain rates ($a = 1 \ldots 500\,\text{s}^{-1}$) show a very good agreement between the mechanisms for temperature, as well as the major combustion products like CO_2 or CO (not shown here), where only small differences between the mechanisms are found for lower strain rates. This is to be expected, since both mechanisms include detailed C1–C4 submechanisms, which account for the major heat release and high temperature reactions in the steady flame.

---

[5]Reprinted from Publication II with permission from Elsevier.
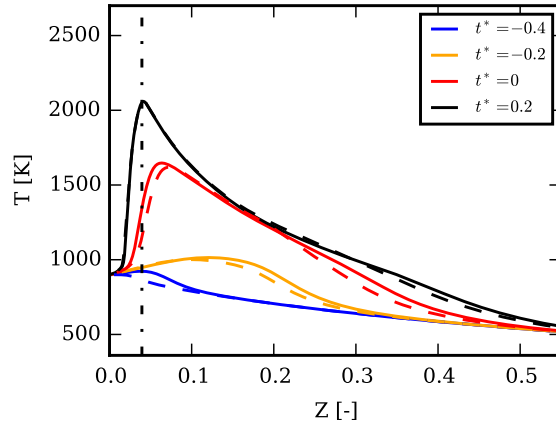
(a) 13 % O_2
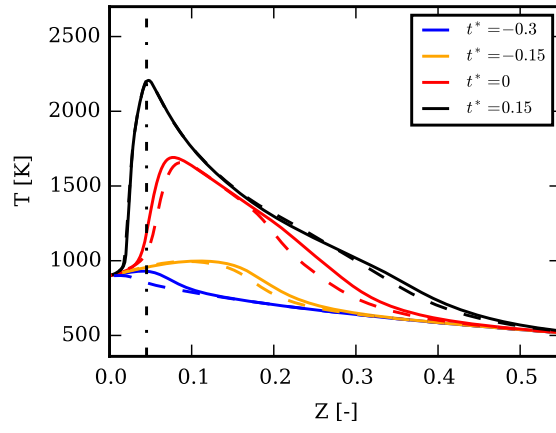
(b) 15 % O_2
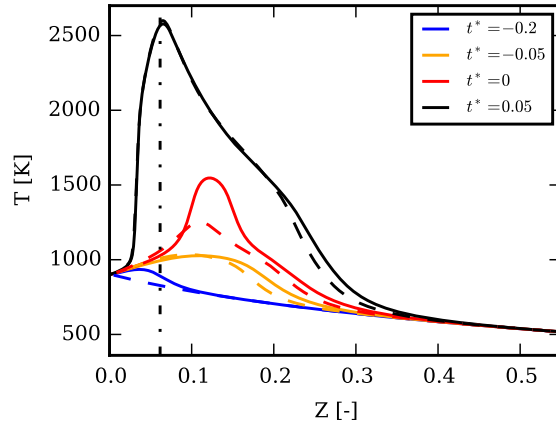
(c) 21 % O_2

Figure 4.6 – Temperature T as a function of mixture fraction Z obtained from an unsteady flamelet (strain rate $a = 500\,\mathrm{s}^{-1}$) at times shifted relative to the ignition delay time $t^* = t - \tau_{\mathrm{ign}}^{\mathrm{F}}$. Solid lines mark the Stanford and dashed lines the POLIMI mechanism. The vertical dashed-dotted line marks the stoichiometric mixture fraction.[5]

4.3 Turbulent spray combustion

In the course of this thesis, two parameter studies on Spray A were carried out: (1) A sweep in ambient oxygen concentration (Publication II) and (2) a variation of the injection pressure (Publication III). Both studies utilize the same computational setup and spray solver, but serve different purposes with respect to spray combustion research and model validation. The variation in ambient oxygen conditions leads to different reactivities of the mixture, resembling an Exhaust Gas Recirculation (EGR) as e.g. used in LTC concepts. In particular, the three reactive ambient conditions listed in Table 2.1 (corresponding to $13\,\%$, $15\,\%$ and $21\,\%$ O_2 by volume) are investigated in this study using two chemical mechanisms (Stanford and POLIMI). The injection pressure study aims at validating the spray combustion modeling approach for different flow conditions, as this variation leads to different injection velocities. It further enables an investigation of the ignition characteristics and flame stabilization mechanism under different turbulence conditions. The computational mesh and breakup modeling approach are based on the insight gained from the non-reacting spray study in Publication I. Hence, a minimum cell size of $62.5\,\mathrm{\mu m}$ in the main spray region is employed and the KHRT breakup model is used.

4.3.1 Spray ignition in physical space

Based on the results from Publication II and III, ignition of turbulent spray flames can be characterized by several stages that are directly connected to the involved physical and chemical processes. These stages can be identified in Fig. 4.7 showing a comparison of the spatial temperature distribution obtained with two chemical mechanisms (Stanford and POLIMI) for the Spray A baseline case ($15\,\%$ O_2) at several time instances.

The instantaneous temperature distribution prior to the first-stage ignition ($t = 0.15\,\mathrm{ms}$) is similar for both mechanisms, as the spray is mixing dominated at this stage and hence independent of the chemical mechanism. After favorable conditions for ignition have been formed, three stages of ignition can be observed (annotated in Fig. 4.7 with I, II and III). In the first stage (I) a rise in temperature is noted, resulting from the low temperature heat release in the premixed part of the spray. The first stage is well represented at $t \approx 0.3\,\mathrm{ms}$ for the POLIMI mechanism, whereas for the Stanford mechanism the respective time is prolonged until $t \approx 0.45\,\mathrm{ms}$. This stage is also particularly well noted from Fig. 4.8, which shows the

t = 0.15 ms

I

t = 0.30 ms

II

I

t = 0.45 ms

II

t = 0.60 ms

III

t = 0.75 ms

t = 0.90 ms

III

T [K]
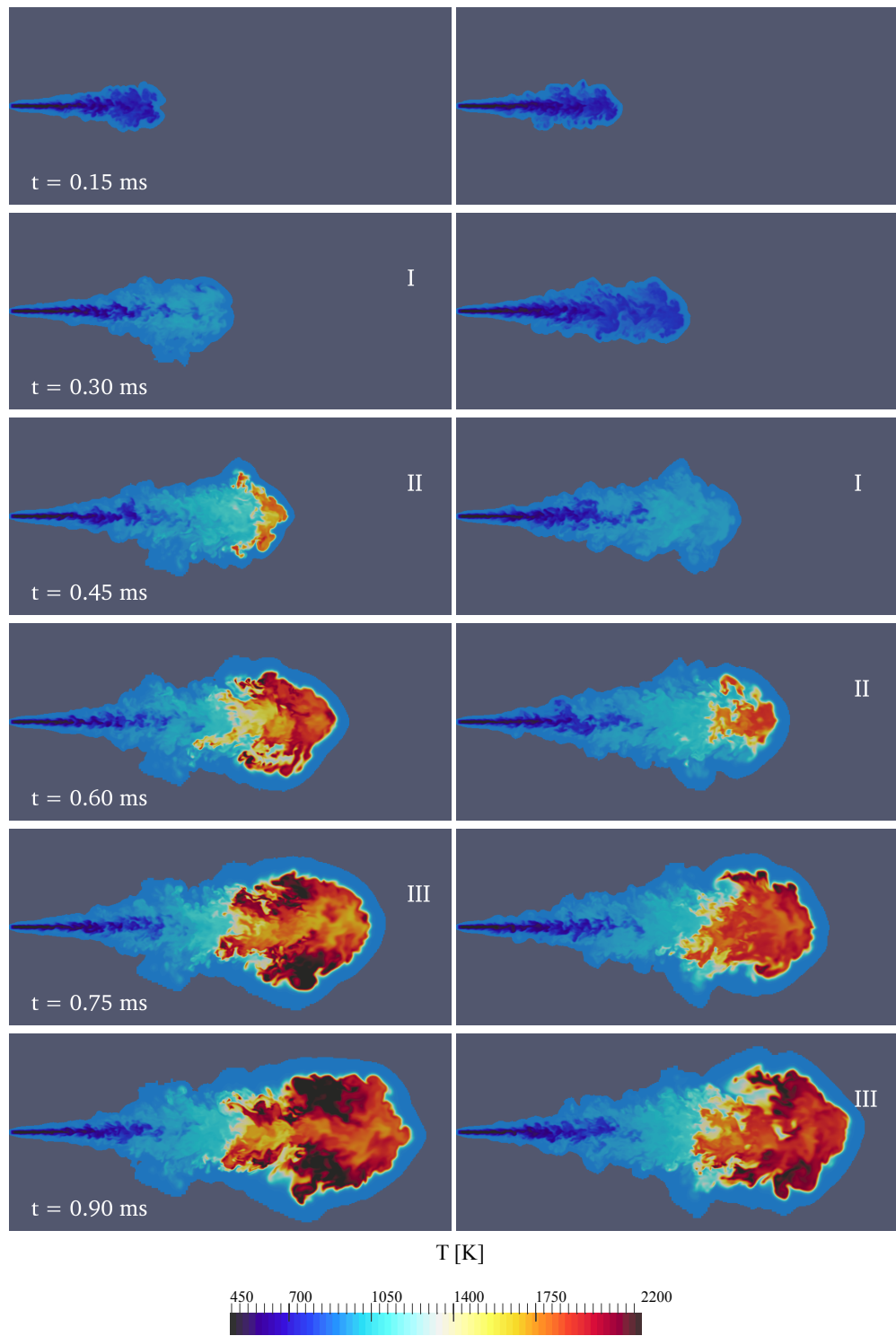
Figure 4.7 – Temporal evolution of temperature for the reacting Spray A baseline case ($15\,\%$ O$_2$). Plots on the left show simulations using the POLIMI, right the Stanford mechanism.[5]

time evolution of the maximum temperature in the simulation domain. In
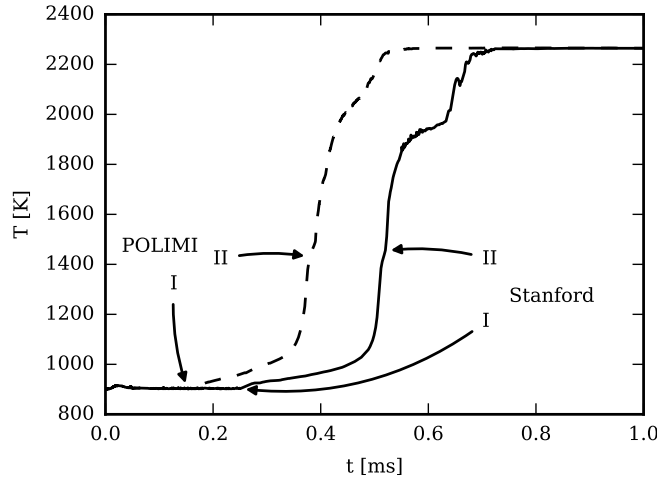
Figure 4.8 – Maximum temperature evolution for the reacting Spray A base-
line case ($15\,\%$ O_2). The first- and second-stage ignition are
indicated by (I) and (II), respectively.[5]

stage II, Fig. 4.7 reveals high temperature zones at the tip of the spray. For
the POLIMI mechanism, stage II is observed at time $t = 0.45\,\text{ms}$, whereas
for the Stanford mechanism it is only seen around $t = 0.60\,\text{ms}$. Stage II
is noted well also in Fig. 4.8 showing a steep temperature rise after the
moderate growth rate of stage I. In the last stage of ignition (III), the high
temperature region is noted to spread and expand (Fig. 4.7). It is observed
that at time $t \approx 0.90\,\text{ms}$ both mechanisms are approaching a quasi-steady
state. It is worth to mention that the observed constant time shift in
ignition stages between the two chemical mechanisms is very close to the
offset predicted in the flamelet calculations.

The presented observations on the three ignition stages are qualitatively
similar for the $13\,\%$ and $21\,\%$ oxygen concentration cases, which are not
shown here for brevity. The IDTs obtained with the POLIMI mechanism
agree well with the experimental data and are only slightly under-predicted
for the $13\,\%$ O_2 case (see Publication II). LES with the Stanford mecha-
nism leads to a similarly over-predicted IDT (approx. $0.17\,\text{ms}$) as already
observed in the canonical combustion configurations for all three ambient
oxygen concentrations. The IDTs from the LES in Publication II and III
are gathered at the end of this section (Table 4.1) and more detailed com-
parisons to the experimental data are given in the respective publications.

### 4.3.2 Spray ignition in mixture fraction space

In nonpremixed combustion configurations such as the conventional diesel combustion, the mixture formation plays a crucial role. However, also in cases where slow chemical reactions become predominant or even rate limiting, the mixture formation still has a significant influence on the local conditions. Hence, it is of interest to analyze the ignition characteristics with respect to local mixture conditions, by sampling joint PDFs of mixture fraction and temperature from the three-dimensional LES data.

From scatter plots of mixture fraction and temperature for the $15\,\%$ O_2 case at times $t = 0.4$, 0.5 and $0.6\,$ms (Fig. 4.9) it is seen that ignition takes place under fuel-rich conditions around $Z = 0.11$ with both mechanisms. The earlier observed differences during ignition between the mechanisms are also observed here, as the rise in temperature is delayed for the Stanford mechanism compared to the POLIMI mechanism. It is also observed that the spatial location of the first temperature rise is located farther downstream with the Stanford mechanism, which can be attributed to the delayed ignition timing and hence a more progressed jet penetration. It should be noted that the maximum temperatures are reached around stoichiometric conditions once a quasi-steady flame is reached at time $t \approx 1.5\,$ms, irrespective of the chemical mechanism.

4.3.3 Ambient gas composition

The effect of different ambient oxygen concentrations, as they may occur for instance in diesel engines with EGR, is illustrated by instantaneous temperature fields at several time instance in Fig. 4.10. Here the results are only shown for the POLIMI mechanism, as very similar temperatures and structures are obtained with the Stanford mechanism (see Publication II). The case with $21\,\%$ O_2 resembles a conventional diesel combustion mode, whereas the $15\,\%$ and $13\,\%$ O_2 cases are more representative for conditions used in LTC concepts. The results show that a lower oxygen concentration leads to a significantly reduced combustion temperature. The results further indicate that with a decreased ambient oxygen concentration, and thus a less reactive mixture, the flame stabilizes farther downstream than for the high reactive mixture.

The link of the variation in ambient oxygen concentration to the different diesel combustion concepts, can be analyzed in ϕ–T maps [174–176], where conditions under which undesired emissions are formed can be identified.
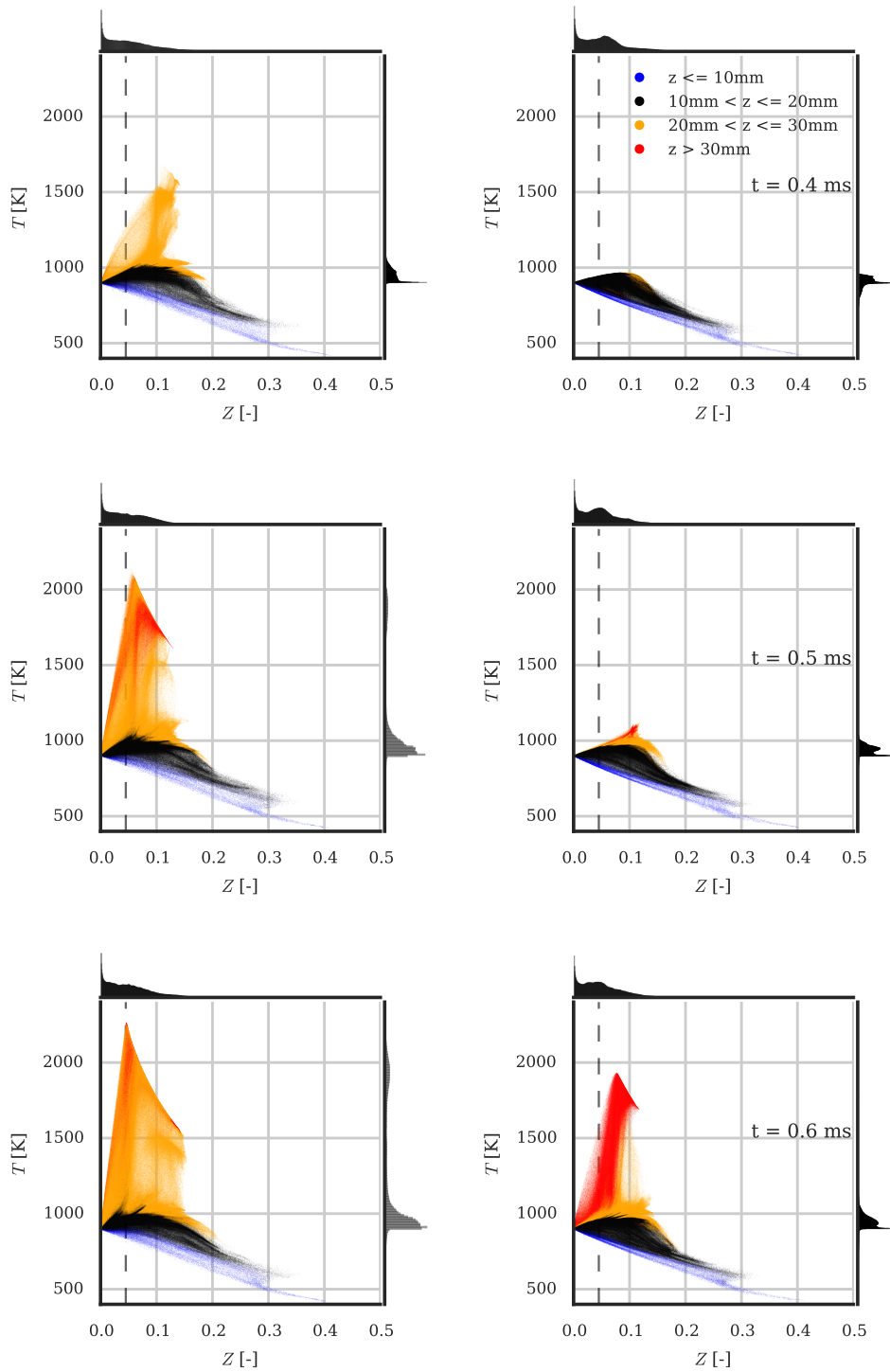
Figure 4.9 – Scatter plots and marginal PDFs of mixture fraction and temperature for the $15\,\%\,O_2$ case at $t = 0.4$, 0.5 and $0.6\,$ms. Plots on the left show simulations using the POLIMI, right the Stanford mechanism. Colors indicate spatial location along the spray axis z.[5]
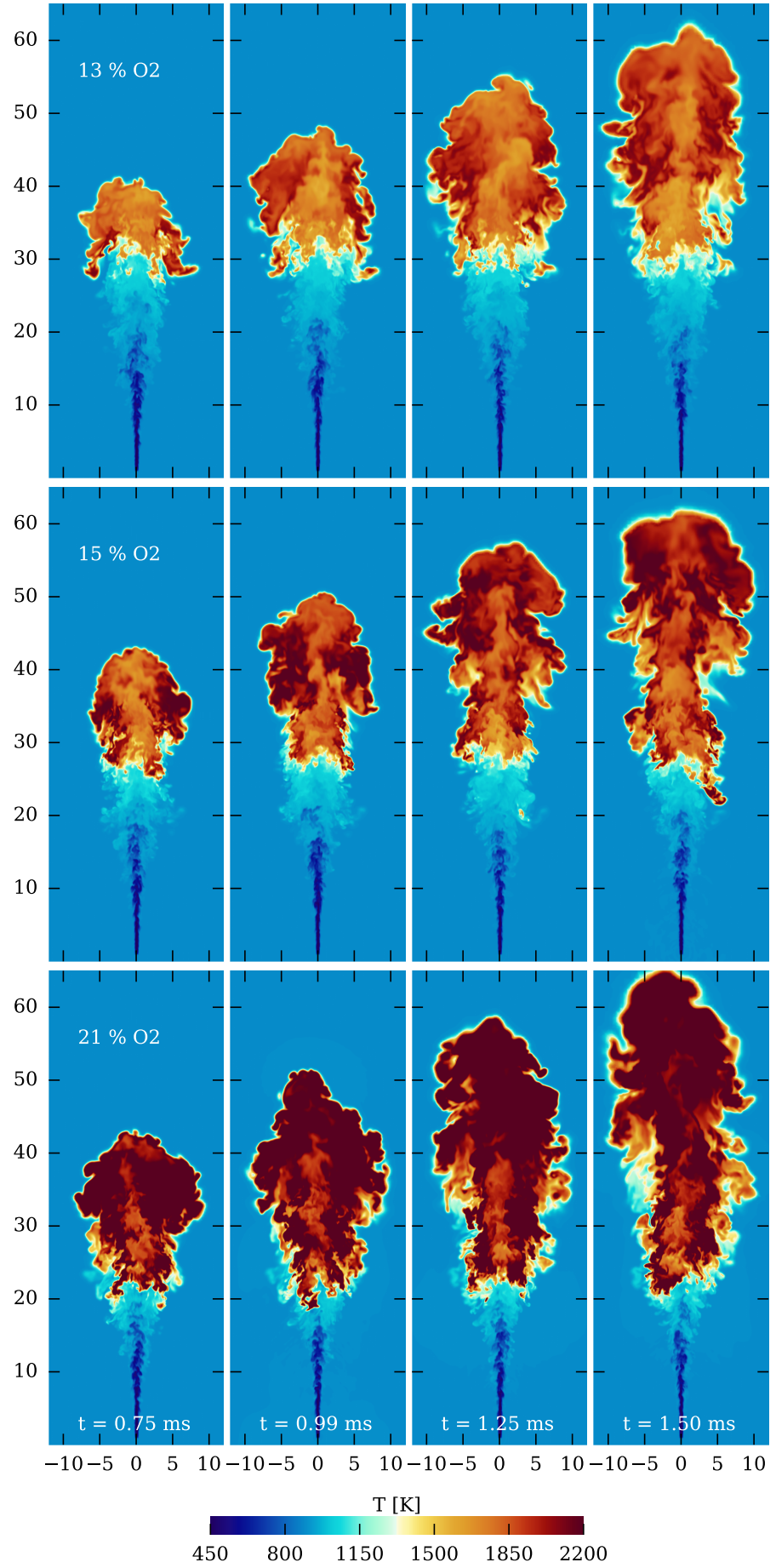
Figure 4.10 – Temperature distribution for different ambient oxygen conditions at times $t = 0.75, 0.99, 1.25$ and 1.5 ms.

The map shown in Fig. 4.11 is generated from isothermal homogenous reactor calculations for n-dodecane–air. The calculations are carried out
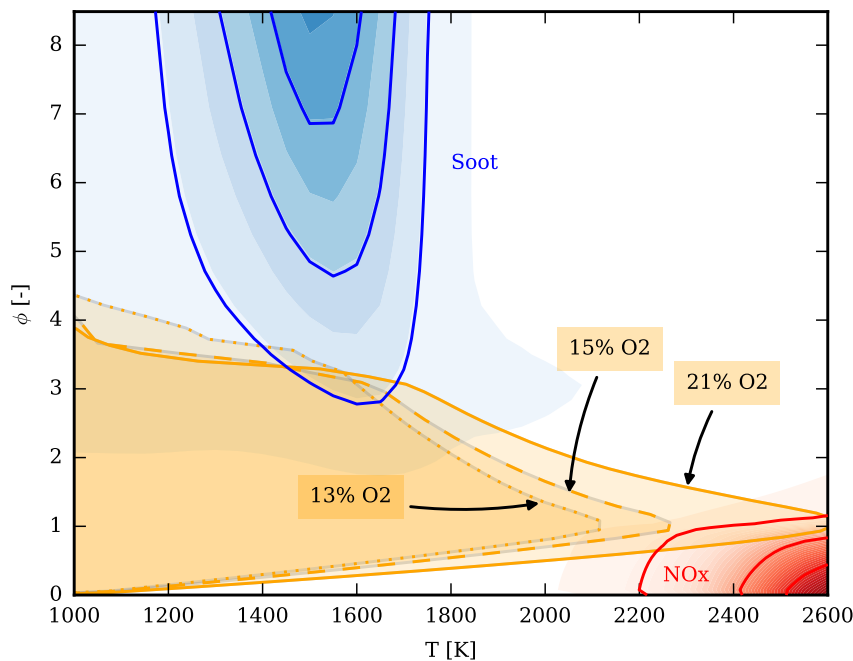
Figure 4.11 – ϕ–T maps for diesel combustion analysis. Red contours mark the NOx, blue the soot regions. The temperature and equivalence ratios observed in the spray LES at the three ambient oxygen conditions are indicated by the orange contours.

using the detailed mechanism by Ranzi et al. [29], which includes sub-mechanisms for NOx and gaseous soot precursors, i.e. Polycyclic Aromatic Hydrocarbons (PAH). The blue and red contours in Fig. 4.11 indicate the regions in the ϕ–T parameter space where soot (represented by the first two aromatic rings, benzene and pyrene) and NOx are formed. The maximum temperatures as a function of equivalence ratio obtained from the spray LES at the three ambient oxygen conditions are marked by the orange contours. In the LES, the maximum temperature for $\phi < 3$ is reached very soon after ignition and the contours represent an temporal average between $t = 1.0$ and 1.6 ms. From Fig. 4.11 it is seen that the reduced combustion temperature obtained in the low ambient oxygen cases prevents the formation of NOx, whereas the $21\,\%$ O$_2$ is prone to form significant amounts of NOx. The effect on the soot formation on the other hand is not that clear, as the results indicate that for all three oxygen levels soot is formed. However, it is observed that with $13\,\%$ ambient oxygen the high temperature region extends to higher equivalence ratios, which may have an influence on the soot formation. It should be noted at this point that

neither one of the mechanisms used for the spray LES in the present thesis includes NOx or soot chemistry, but the ϕ–T analysis here gives a first indication of the emission.

4.3.4 Flame stabilization

As a last topic, the flame stabilization mechanism is investigated, primarily in Publication III, but also in Publication II. The investigation in Publication III is facilitated by the comparison of three injection pressures (50, 100, $150\,$MPa), which lead to different flow velocities and turbulence levels, and subsequently different flow conditions in the ignition region. From the injection pressure variation a clear dependency of the flame stabilization location on the turbulent flow conditions is observed, where the ambient gas conditions are otherwise identical and correspond to the $15\,\%$ O_2 case.

In particular, the instantaneous temperature fields in Fig. 4.12 show that small ignition pockets are formed in early stages of the flame development close to the flame lift-off length (FLOL). These ignition kernels merge with other kernels and are eventually convected downstream where they merge with the main flame. A distinctive difference between the high and low injection pressures can be seen by comparing the structures indicated by I: For the $50\,$MPa case the merged kernels draw the main flame more upstream, decreasing the FLOL permanently. In contrast, the merging ignition kernels with $150\,$MPa are not stable and the upstream flame front finally breaks down into small high temperature pockets (II). Simultaneously new ignition pockets are forming upstream (III), which will go through the same evolution process as the ones before. Therefore the main flame remains farther downstream, compared to the experimental FLOL results. This analysis shows that the stabilization of the present spray flame is governed by an interaction of the turbulent flow structures and the chemical ignition characteristics, i.e. the flame stabilizes at a location where the local turbulence levels permit a formation and growth of ignition kernels.

While in principle similar processes take place in cases with higher reactivity (e.g. the $21\,\%$ O_2 case investigated in Publication II), the role of the ignition kernels is less dominant there, due to the fast chemical reactions and rapid rise of temperature to overall higher values. The results from the injection pressure variation are in line with earlier findings on similar combustion configurations like diesel sprays [177, 178] or jet-in-hot-coflow [179, 180] flames.
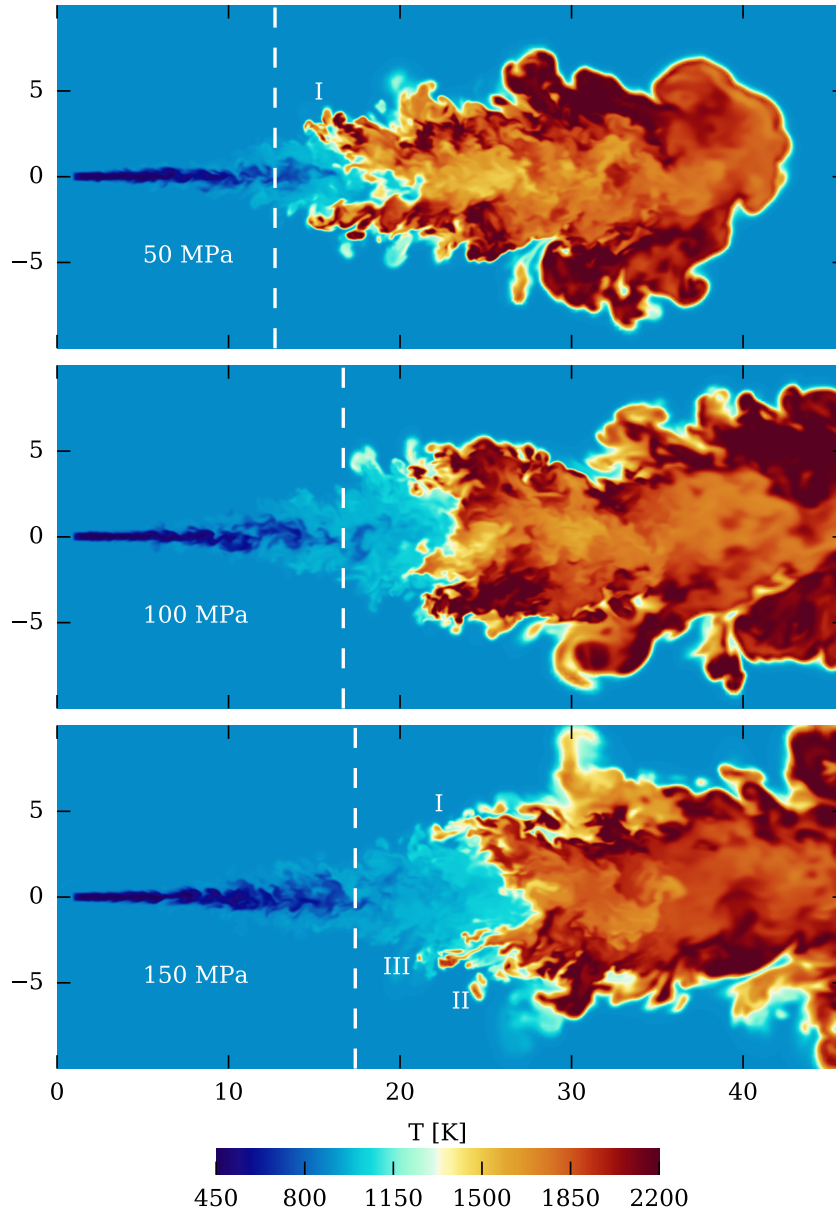
Figure 4.12 – Quasi-steady state temperature distribution for different injection pressures at time $t = 1.5\,\text{ms}$ ($15\,\%\ O_2$). The dashed horizontal line indicates the experimental FLOL measured at Eindhoven University of Technology (TU/e).

4.4 Summary of integral length scales in turbulent spray combustion

Altogether, one of the key achievements of the present research has been the development of an LES/FGM modeling approach capable of predicting various experimentally observed features of Spray A. The presented LES results cover the fuel injection, evaporation, turbulence transition and combustion, where various models are employed for the respective processes. Figure 4.13 shows a visualization of Spray A from the present LES data, highlighting several important length scales. The injection of the liquid
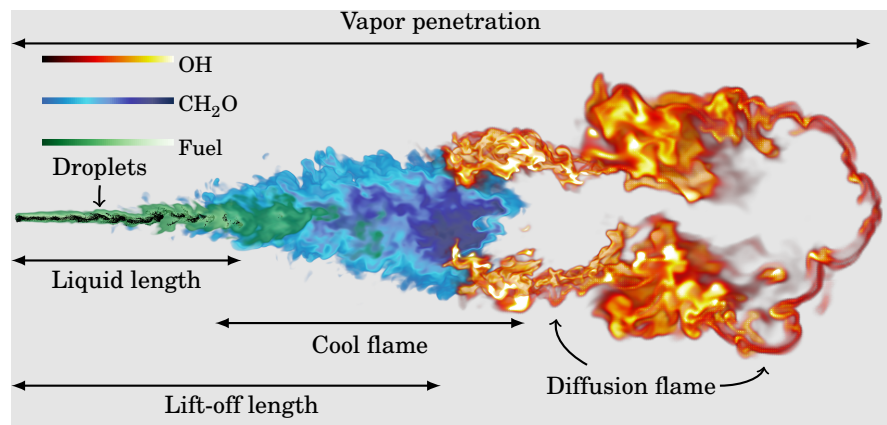
Figure 4.13 – Length scales in turbulent spray combustion.

fuel into the combustion chamber, is modeled by discrete particles, which undergo rapid atomization and evaporation, and subsequently induce a high-velocity gas jet. Thus the primary jet breakup was not explicitly modeled and relatively small droplets were injected. This assumption was further supported by the findings of Publication I that showed that the droplets reach shortly after injection a stable droplet diameter and this location was referred to as breakup length (approximately $\frac{1}{5}$ of the liquid length). The maximum penetration of the liquid phase is denoted by the liquid length (compare Fig. 4.13), which covers the region where evaporation and the turbulence transition of the induced gas jet take place. In Publication III an analysis using Proper Orthogonal Decomposition (POD) is included, which further investigates the impact of the mesh resolution on the potential core of the gas jet and the turbulence transition around the liquid length. It was found that this gas jet exhibits features similar to those found in studies on single phase gas jets, e.g. [181, 182]. However, the transition was implied to be somewhat inadequately captured with the current model.

With respect to combustion, important scales are given by the location

and size of the "cool flame", i.e. the region where the low-temperature reactions take place and form the first radicals as well as intermediate species. An intermediate species produced in significant concentrations in the low-temperature region is formaldehyde (CH_2O), which is used to indicated the cool flame in Fig. 4.13. The high-temperature diffusion flame enveloping the spray is indicated by the OH radical (yellow-red colors) in Fig. 4.13. The onset of this high-temperature diffusion flame is denoted by the lift-off length. Finally, the various integral length scales determined in Publication II and III are gathered in Table 4.1. The length scales in the spray simulations are defined following the recommendations by the ECN: The liquid length is determined by the maximum distance from the nozzle outlet to the farthest axial position for $0.1\,\%$ liquid volume fraction, the lift-off length is defined as the first axial location of the Favre-averaged OH mass fraction reaching $2\,\%$ of its maximum in the domain and the extent of the cool flame is based on a threshold of $2\,\%$ of the maximum formaldehyde mass fraction.

Table 4.1 – Liquid penetration L_{liq}, ignition delay τ_{ign}, flame lift-off length L_{off} and the axial extent of the cool flame in a quasi-steady state L_{CF} from the LES for all studied cases.

		L_{liq} (mm)	τ_{ign} (ms)	L_{off} (mm)	L_{CF} (mm)
Publication II					
	$13\,\%\ O_2$		0.56	22.0	28.1
Stanford	$15\,\%\ O_2$		0.52	19.6	26.6
	$21\,\%\ O_2$		0.46	17.7	18.9
	$13\,\%\ O_2$		0.42	21.5	27.3
POLIMI	$15\,\%\ O_2$		0.38	16.6	24.0
	$21\,\%\ O_2$		0.28	15.3	19.9
Publication III					
$50\,\text{MPa}$		9.3	0.420	13.3	17.3
$100\,\text{MPa}$		10.1	0.395	17.3	20.4
$150\,\text{MPa}$		12.2	0.383	19.9	24.1

4.5   Computational cost

As outlined in Section 2.3, a significant advantage of the current simulation approach is the low computational cost of the combustion model. The computational cost of a non-reacting Spray A simulation, using a $62.5\,\mu m$ mesh resolution with in total approximately 11.5 million cells (Publication II and III), is approximately 29 hours on 192 processors (5568 processor hours) for $1.6\,ms$ simulated time. The reacting simulations (Publication II and III) with otherwise comparable setup require approximately 50 hours on 192 processors (9600 processor hours) to reach $1.6\,ms$ simulated time. All computations were carried out on a Cray XC40 supercomputer with Intel Xeon processors (E5-2690v3, 2.6GHz) at the Finnish IT Center for Science (CSC). The comparison of the computational times shows that the reacting simulations are only about $70\,\%$ more expensive than the non-reaching simulations. Considering the complex processes in turbulent spray combustion and the accurate results obtained with the LES/FGM simulation approach, these numbers are very encouraging also with respect to a possible application to engine simulations.

Similar studies of the Spray A conditions using LES and a direct integration of the chemical kinetics may take several weeks with a similar computational setup due to the high computational requirements related to the transport of the chemical species and the chemical reactions (see e.g. [68]).

4.6   Remarks on high-velocity fuel spray modeling using LES

The various spray submodels and their subsequent parameters have a significant influence on the outcome of fuel spray simulations. Specifically the number of injected parcels as well as the breakup model constants are important parameters, which are often adjusted to match experimental droplet sizes and breakup rates. These empirical constants are well tested in a vast amount of simulations, where the majority is based on the RANS approach. RANS simulations are usually carried out with fairly large cell sizes (characteristic length of about $500\,\mu m$), e.g. [110–112, 183–185], and the models have not been tested much for LES, as noted for instance by Bharadwaj and Rutland [186]. One of the objectives of this thesis is to develop a spray model in the LES context that captures the global spray characteristics as well as the spray structure quantitatively.

In the following guidelines regarding the LPT spray modeling in an LES context are given based on the findings of the research in the present thesis.

- A statistical approach was chosen for the description of the dispersed liquid phase, where droplets of similar size are grouped in parcels. Thus, a larger number of injected parcels is expected to yield more accurate results [94, 102]. However, in order to avoid issues in the numerical computations (e.g. floating point numbers close the machine accuracy), the number of injected parcels should be chosen such that the average parcel mass is sufficiently large. For the fuel spray simulations in the present thesis an average parcel mass of approximately 3.5×10^{-12} kg was found suitable.

- Various values for the breakup model constants were tested during the course of this thesis (see e.g. Publication I) and the KHRT model with model constants listed in Table 4.2 was found to yield good results for all three injection pressures investigated in Publication III.

Table 4.2 – KHRT model constants

B_0	B_1	C_τ	C_{RT}	ms_{Lim}	We_{Lim}
0.61	7	1	0.1	0.3	6

- The primary breakup of the liquid jet is not explicitly modeled in the present approach and the liquid fuel is injected as dispersed droplets. The initial droplet diameter is determined from a size distribution with an average diameter of ≈ 6 µm, where the injection location is at a slightly downstream location from the nozzle exit and the diameter of the injection area is subsequently adjusted based on an assumed spray opening angle. A detailed discussion on the assumptions made regarding the initial droplet size distribution is given in Publication I.

- To avoid stability issues in the numerical computations, the spray source terms are filtered, i.e. averaged over several cells, close to the injection location ($z < 10D$). Special care is taken to ensure a strict conservation of mass, momentum and energy for this filtering procedure.

- As with any LES, an adequate mesh resolution was found to be paramount for the success of the spray simulations. In particular, a higher mesh resolution, and subsequently a larger resolved part

of the turbulent motion, was found to reduce the sensitivity to the breakup modeling (see Section 4.1 for a more detailed discussion).

- In the absence of detailed experimental data on the structure of the liquid phase and/or droplet sizes in such high-velocity fuel sprays, the accurate prediction of the liquid length and turbulence transition was found to be valuable measures for the success to of spray LES.

- For the scalar transport equations, such as mixture fraction and enthalpy, a discretization scheme with full TVD properties was found to be most suitable (see also Section 3.4). The discretization scheme for the velocity equation plays a crucial role with regard to the implicit LES turbulence modeling approach. Here the `Gamma` discretization scheme [116] was found to be a sensible choice for the present spray cases. The schemes and parameters used in the OpenFOAM case setup are given in Listing 4.1.

Listing 4.1 – Finite volume discretization schemes in OpenFOAM (`fvSchemes`)

```
div(phi,U)       Gauss  GammaV 0.3;
div(phi,Yi_h)    Gauss  multivariateSelection
{
    Z                    Gamma01 1;
    PV                   Gamma 1;
    ha                   Gamma 1;
};
```

- Another important factor for the success of a spray LES is the velocity-pressure-density solution scheme. In the present thesis, the PISO algorithm, as implemented in the OpenFOAM framework, was employed. Due to the high velocity and density gradients originating from the spray source terms, several corrector steps (Listing 4.2) were necessary in order to avoid mass conservation errors.

Listing 4.2 – PISO solution algorithm settings in OpenFOAM (`fvSolution`)

```
nOuterCorrectors          3;
nCorrectors               1;
nNonOrthogonalCorrectors 1;
```

Last, it should be noted that many of the spray model parameters and assumptions are based on empirical correlations and may further be specific to the implementation in the present computational framework (OpenFOAM).

5. Conclusions

5.1 Summary

This thesis addressed several research question related to combustion of fuel sprays under diesel engine conditions. The Spray A conditions defined by the Engine Combustion Network (ECN) provided the experimental reference case for the thesis. First, the implications and performance of certain models and assumptions for LES of high-velocity fuel sprays were investigated. Particularly the mesh resolution requirements were studied in detail and it was found that for the present Spray A case with a 90-µm nozzle diameter, a minimum cell size of $62.5\,\mu$m is required to capture the turbulence transition of the induced gas jet. The applicability and influence of breakup models traditionally used in RANS simulations has been explored. The numerical results showed that the induced gas jet and the local mixture formation, after the liquid fuel has been evaporated, are very similar for the KHRT and ETAB breakup models, given an adequate mesh resolution.

In order to carry out turbulent spray combustion LES, various aspects regarding the FGM combustion modeling approach have been evaluated in canonical combustion systems. The results from igniting flamelet calculations indicate that the IDT is insensitive to the applied strain rate for values below $1000\,\mathrm{s}^{-1}$. A significant influence of the chemical mechanism was found, however, for all three investigated ambient oxygen conditions. The two mechanisms considered in the present study showed a consistent offset in IDT of approximately $0.17\,$ms for homogenous reactor and flamelet calculations. With regard to the steady state flame as well as the flame structure, it was also found that the results obtained with both mechanisms are very similar.

Finally, the turbulent spray combustion research included two parameter studies on (1) different ambient oxygen conditions and (2) a variation in injection pressure. The analysis of the ignition process in physical and mixture fraction space, allowed for a deeper understanding of the two-stage ignition process of n-dodecane under turbulent flow conditions. The dependency of the ignition delay time on the chemical mechanisms was also present in the turbulent spray combustion LES, irrespective of the ambient oxygen concentration (i.e. the mixture reactivity). At the same time, the expected differences in combustion temperature due to the change in ambient mixture composition were very well captured by both mechanisms for the steady spray flame. It was further shown, that these differences in combustion temperature can be directly linked to the reduction of harmful emissions. A major finding of the second parameter study on the injection pressure variation was that the flame stabilization is governed by the formation of ignition kernels, which are modulated by the turbulent flow conditions. This is in line with earlier findings on similar combustion configurations [177–180].

With respect to combustion modeling, an important finding was that the presented LES/FGM approach is able to capture the transient and unsteady features of spray flames, as supported by experimental data. In particular, the low computational cost of the FGM combustion modeling approach offers a tractable way for the otherwise demanding description of the chemical kinetics of long-chained hydrocarbon fuels. This subsequently allows a high spatial and temporal resolution in LES and hence the possibility to study the local and unsteady processes in greater detail. An important achievement of this work is the implementation of the FGM method in the open-source CFD framework OpenFOAM [113]. Also various thermodynamic, transport and mixture models, as well as libraries and utilities for post-processing were implemented either in OpenFOAM or the python scripting language [187–190].

The research questions raised in the introduction are addressed in the following:

1. Implications of modeling fuel sprays in LES:

   - For LES of high-velocity fuel sprays such as Spray A ($90\,\mu m$ nozzle diameter, $150\,MPa$ injection pressure), the required mesh resolution to capture the turbulence transition was found to be $62.5\,\mu m$ with the present computational approach. The interpre-

tation of the results in an LES context becomes questionable for much coarser mesh resolutions. It should however be noted that other computational approaches may require an even higher resolution.

- An adequate mesh resolution, and hence a sufficiently resolved turbulence transition, lead to better results, especially regarding the mixture formation. The mixture formation was found to be crucial regarding the liquid length predictions, due to the diminished influence of the breakup modeling and hence a stronger dependency on the evaporation rate.

2. Turbulent combustion simulation of n-dodecane fuel sprays:

- The two investigated chemical mechanisms were both found to be suitable for the Spray A cases, specifically because both predict similar flame structures and results for a steady flame at three different ambient conditions.

- The temporal offset with respect to the transient ignition characteristics and ignition delay times however, indicates that more work is needed on the validation and development of mechanisms for transport fuels, such as n-dodecane, under engine relevant conditions.

- The selected parameter study on different ambient oxygen concentrations showed that the combustion temperatures significantly decreased for the lower oxygen levels. A peak combustion temperature of $2100\,\mathrm{K}$ for the $13\,\%\,\mathrm{O_2}$ case, compared to $2600\,\mathrm{K}$ for the $21\,\%\,\mathrm{O_2}$ case, was directly linked to possible reductions of harmful emissions.

- The FGM combustion modeling approach is suitable for a detailed modeling of spray ignition and combustion, as implied by comparison to experimental data and novel PLIF imaging (see Publication II).

3. Effect of flow and turbulence on ignition and flame stabilization:

- The present LES/FGM approach was shown to be capable of capturing the transient flame stabilization mechanism governed by ignition and the local turbulent flow conditions.

- This can mainly be attributed to the sufficient mesh resolution, which allows to capture the turbulence transition reasonably

well under all considered turbulence levels.

5.2 Limitations

The spray modeling approach in the present thesis is, in a sense, only a coarse approximation of (1) the liquid fuel injection and atomization using LPT and (2) the description of the fluid motion in the very early stages of the liquid jet. Hence, the modeling approach imposes certain limitations to the analysis of the results for $z < L_{\mathrm{liq}}$. However, despite of this, the liquid length can be reproduced with the present numerical model which can be considered as evidence of a relatively well captured overall mixing rate and the associated turbulence transition process with right order of magnitude. The situation could be improved by an increase in mesh resolution. However, in this case the applicability of the LPT approach becomes questionable and a more sophisticated description of the multiphase thermodynamics could be required. The work carried out in the course of the present thesis on the other hand, explored and established a modeling approach which allows to investigate high-velocity fuel sprays, and specifically their ignition and combustion characteristics farther away from the near-nozzle region ($z > L_{\mathrm{liq}}$).

Another limitation comes from the FGM combustion modeling approach: The combustion event in the current setup is solely described by, and hence constrained to, a three-dimensional manifold spanned by mixture fraction, mixture fraction variance and a reaction progress variable. This restriction may have an influence on minor species predictions and remains to be investigated further in future studies.

The direct applicability of the present results to diesel fuel sprays, as they occur in modern internal combustion engines, is limited by some of the simplifications of the investigated reference cases. For instance, the usage of n-dodecane as a surrogate for diesel fuel imposes an approximation that still remains to be quantified. Also the fact that the liquid fuel is injected into a quiescent gas mixture may not represent the flow conditions in an internal combustion engine, where gas is typically in a swirling motion. While the results allow for a better understanding of certain phenomena, some of the simplifications may lead to the omission of features that are present in real world engines. The results of the present thesis should hence be interpreted with caution specifically when more complex

configurations are studied.

5.3 Future directions

The research conducted in the course of the present doctoral thesis comprised two main topics. First, the modeling of high-velocity fuel sprays in LES was investigated. In order to gain deeper insight into the mechanical and thermodynamical processes related to high-velocity fuel sprays, and hence further confidence in the modeling approach, more detailed simulations are indicated. Specifically the thermodynamic models employed in the spray submodels need to be further evaluated, as recent research [76–83] shows that real gas thermodynamics may be needed in order to describe diesel fuel sprays accurately. Real gas thermodynamics adds however an additional level of complexity and may increase the computational cost. Hence, a quantification of the error connected to the present thermodynamic models would help to further understand the implications of the LPT approach with respect to high-velocity fuel sprays. In the meantime, the presented LPT spray modeling approach offers a tractable and reasonably accurate route for spray combustion simulation, if the very early stages of the liquid fuel injection are not of primary concern. For future studies, both directions should be considered.

The second major topic was the turbulent combustion simulation of such fuel sprays. Regarding the combustion modeling, the present study showed that the FGM approach was able to capture, and to accurately predict many important features present in turbulent spray combustion. A drawback can be seen in the knowledge and experience needed to generate and parametrize the low-dimensional manifolds. In the present thesis adhoc definitions of the reaction progress variable have been used, which may not be optimal to represent all of the complex stages during spray ignition and flame stabilization accurately. A systematic definition of the progress variables and the respective low-dimensional manifolds using optimization or statistical methods, such as the Principal Component Analysis (PCA), may proof of advantage. Recent studies [191–194] have shown that systematically defined progress variables may also improve the overall accuracy of the manifold. These systematic methods further allow for a consistent definition of additional progress variables, which may further increase the representation of the high-dimensional state space by the low-dimensional manifold.

Further, the role of turbulence modeling in combustion LES, and specifically the turbulence chemistry interaction, comprises an interesting and important topic for further research. The problem of modeling the unresolved scales in combustion simulation is twofold: First the turbulent fluctuations need to be estimated and secondly their influence on the chemical reactions needs to be taken into account. Regarding the description of the turbulence chemistry interaction by the means of a presumed PDF, the determination of the scalar variance (e.g. $\widetilde{Z''^2}$) from a transport equation for either variance [195] or the second moment [196] could be further investigated.

A. Flame stretch transport equation

The one-dimensional formulation of the opposed flow strained flame problem is described in the following. Kee et al. [144] showed that the two-dimensional Navier–Stokes equations can be reformulated in one space coordinate with two independent parameters, namely the tangential pressure gradient and the divergence of the flow field at the burner nozzle for a steady state flow. Stahl and Warnatz [137] extended the applicability of this approach to unsteady problems, under certain assumptions, which are as follows:

1. The temperature and mass fractions of all species solely are a function of the coordinate normal to the flame x

2. The normal velocity component u solely is a function of x;

3. The tangential velocity component v is proportional to the coordinate tangential to the flame y; the tangential velocity gradient $\frac{\partial v}{\partial y} = f(x)$ therefore is solely dependent on x

4. The solutions are considered along the x axis ($y = 0$).

The conservative form of the unsteady two-dimensional Navier–Stokes in Cartesian coordinates reads

$$\frac{\partial \rho}{\partial t} + \frac{\partial \rho u}{\partial x} + \frac{\partial \rho v}{\partial y} = 0 \tag{1.1}$$

$$\frac{\partial \rho u}{\partial t} + \frac{\partial \left(\rho u^2 + p\right)}{\partial x} + \frac{\partial \rho v u}{\partial y} = \frac{\partial}{\partial x}\left(\frac{2}{3}\mu\left(2\frac{\partial u}{\partial x} + \frac{\partial v}{\partial y}\right)\right) + \frac{\partial}{\partial y}\left(\mu\left(\frac{\partial u}{\partial y} + \frac{\partial v}{\partial x}\right)\right) \tag{1.2}$$

$$\frac{\partial \rho v}{\partial t} + \frac{\partial \rho u v}{\partial x} + \frac{\partial \left(\rho v^2 + p\right)}{\partial y} = \frac{\partial}{\partial x}\left(\mu\left(\frac{\partial u}{\partial y} + \frac{\partial v}{\partial x}\right)\right) + \frac{\partial}{\partial y}\left(\frac{2}{3}\mu\left(2\frac{\partial v}{\partial y} + \frac{\partial u}{\partial x}\right)\right) \ . \tag{1.3}$$

Applying the definition of the flame stretch rate

$$K(x,t) := \frac{\partial v(x, y, t)}{\partial y} \tag{1.4}$$

and the above introduced assumptions $\left(\frac{\partial \rho}{\partial y} = \frac{\partial u}{\partial y} = \frac{\partial^2 v}{\partial y^2} = 0\right)$ to the v-momentum equation (1.3) yields

$$\frac{\partial \rho v}{\partial t} + \frac{\partial \rho u v}{\partial x} + 2\rho v K + \frac{\partial p}{\partial y} = \frac{\partial}{\partial x}\left(\mu \frac{\partial v}{\partial x}\right) .$$

Integrating equation (1.4) with respect to y gives

$$v(x, y, t) = yK(x, t) + C ,$$

where the integration constant $C = 0$, due to the initial assumptions $(v(x, 0, t) = 0)$. A transport equation for the flame stretch rate is then obtained as:

$$\frac{\partial \rho K}{\partial t} + \frac{\partial \rho u K}{\partial x} + 2\rho K^2 + \frac{1}{y}\frac{\partial p}{\partial y} = \frac{\partial}{\partial x}\left(\mu \frac{\partial K}{\partial x}\right) \qquad (1.5)$$

Similarly, the u-momentum equation reads

$$\frac{\partial \rho u}{\partial t} + \frac{\partial \left(\rho u^2 + p\right)}{\partial x} + \rho u K = \frac{\partial}{\partial x}\left(\frac{2}{3}\mu\left(2\frac{\partial u}{\partial x} + K\right)\right) + \mu\frac{\partial K}{\partial x}$$

and can be further simplified by using the continuity equation

$$\frac{\partial \rho}{\partial t} + \frac{\partial \rho u}{\partial x} = -\rho K$$

to

$$\rho\frac{\partial u}{\partial t} + \rho u\frac{\partial u}{\partial x} + \frac{\partial p}{\partial x} = \frac{\partial}{\partial x}\left(\frac{2}{3}\mu\left(2\frac{\partial u}{\partial x} + K\right)\right) + \mu\frac{\partial K}{\partial x} . \qquad (1.6)$$

Deriving equation (1.6) with respect to y, and subsequently dividing by y, yields

$$\frac{1}{y}\frac{\partial}{\partial y}\left(\frac{\partial p}{\partial x}\right) = \frac{1}{y}\frac{\partial}{\partial x}\left(\frac{\partial p}{\partial y}\right) = 0 ,$$

and hence the remaining pressure term in the flame stretch equation (1.5) is merrily a function of time. Stahl and Warnatz [137] further showed that the one-dimensional formulation leads to a potential flow assumptions in the far field, where the flame stretch rate becomes only a function of time

$$\left.\frac{\partial K(x, t)}{\partial x}\right|_{x=\pm\infty} = \left.\frac{\partial^2 K(x, t)}{\partial x^2}\right|_{x=\pm\infty} = 0 .$$

Furthermore, defining a prescribed strain rate at the oxidizer boundary $a(t) := K_{ox}(t)$, equation (1.5) reduces to

$$\frac{1}{y}\frac{\partial p}{\partial y} = -\rho_{ox}\left(\frac{\partial a(t)}{\partial t} + a(t)^2\right) .$$

The final transport equation for the flame stretch reads

$$\frac{\partial \rho K}{\partial t} + \frac{\partial \rho u K}{\partial x} = \frac{\partial}{\partial x}\left(\mu \frac{\partial K}{\partial x}\right) + \rho_{ox}\left(\frac{\partial a(t)}{\partial t} + a(t)^2\right) - 2\rho K^2 . \qquad (1.7)$$

References

[1] International Energy Agency, editor. *World Energy Outlook 2011*. OECD, Paris, 2011. ISBN 978-92-64-12413-4.

[2] European Parliament and Council of the European Union. Regulation (EC) No 715/2007, June 2007.

[3] T. A. Boden, R. J. Andres, and G. Marland. Global, Regional, and National Fossil-Fuel CO2 Emissions. Technical report, Carbon Dioxide Information Analysis Center, Oak Ridge National Laboratory, U.S. Department of Energy, Oak Ridge, Tenn., U.S.A., 2015.

[4] Rolf D. Reitz. Directions in internal combustion engine research. *Combustion and Flame*, 160(1):1–8, January 2013. doi: 10.1016/j.combustflame.2012.11.002.

[5] Rolf D. Reitz. Combustion and ignition chemistry in internal combustion engines. *International Journal of Engine Research*, 14(5):411–415, October 2013. doi: 10.1177/1468087413498047.

[6] Mark P. B. Musculus, Paul C. Miles, and Lyle M. Pickett. Conceptual models for partially premixed low-temperature diesel combustion. *Progress in Energy and Combustion Science*, 39(2–3):246–283, April 2013. doi: 10.1016/j.pecs.2012.09.001.

[7] John B. Heywood. *Internal combustion engine fundamentals*. McGraw-Hill, 1988.

[8] Klaus Mollenhauer and Helmut Tschöke. *Handbuch Dieselmotoren*. VDI-Buch. Springer Berlin Heidelberg, Berlin, Heidelberg, 2007. ISBN 978-3-540-72164-2.

[9] Nasser Ashgriz, editor. *Handbook of Atomization and Sprays*. Springer US, Boston, MA, 2011. ISBN 978-1-4419-7264-4.

[10] A.H. Lefebvre. *Atomization and sprays*. CRC press, 1989. ISBN 0-89116-603-3.

[11] Gunnar Stiesch. *Modeling Engine Spray and Combustion Processes*. Heat and Mass Transfer. Springer Berlin Heidelberg, Berlin, Heidelberg, 2003. ISBN 978-3-642-05629-1.

[12] John E. Dec. A Conceptual Model of DI Diesel Combustion Based on Laser-Sheet Imaging. SAE Technical Paper 970873, SAE International, Warrendale, PA, 1997.

[13] John E. Dec. Advanced compression-ignition engines–understanding the in-cylinder processes. *Proceedings of the Combustion Institute*, 32(2):2727–2742, 2009. doi: 10.1016/j.proci.2008.08.008.

[14] A. N. Kolmogorov. The Local Structure of Turbulence in Incompressible Viscous Fluid for Very Large Reynolds Numbers. *Doklady Akademiia Nauk SSSR*, 30(4):299–303, 1941.

[15] A. N. Kolmogorov. Dissipation of Energy in the Locally Isotropic Turbulence. *Doklady Akademiia Nauk SSSR*, 32(1):19–21, 1941.

[16] Stephen B. Pope. *Turbulent Flows*. Cambridge University Press, 2000. ISBN 978-0-521-59886-6.

[17] Martin Schmitt, Christos E. Frouzakis, Ananias G. Tomboulides, Yuri M. Wright, and Konstantinos Boulouchos. Direct numerical simulation of the effect of compression on the flow, temperature and composition under engine-like conditions. *Proceedings of the Combustion Institute*, 2014. doi: 10.1016/j.proci.2014.06.097.

[18] Pijush K. Kundu and Ira M. Cohen. *Fluid Mechanics*. Academic Press, fourth edition, 2008.

[19] G. I. Taylor and A. E. Green. Mechanism of the Production of Small Eddies from Large Ones. *Proceedings of the Royal Society of London A: Mathematical, Physical and Engineering Sciences*, 158(895):499–521, February 1937. doi: 10.1098/rspa.1937.0036.

[20] Charles Hirsch. *Numerical Computation of Internal and External Flows: The Fundamentals of Computational Fluid Dynamics*. Butterworth-Heinemann, Oxford; Burlington, MA, 2nd edition, August 2007. ISBN 978-0-7506-6594-0.

[21] J. Smagorinsky. General Circulation Experiments with the Primitive Equations: I. the Basic Experiment. *Monthly Weather Review*, 91(3):99–164, March 1963. doi: 10.1175/1520-0493(1963)091<0099:GCEWTP>2.3.CO;2.

[22] James W. Deardorff. A numerical study of three-dimensional turbulent channel flow at large Reynolds numbers. *Journal of Fluid Mechanics*, 41 (02):453–480, April 1970. doi: 10.1017/S0022112070000691.

[23] Jürgen Warnatz, Ulrich Maas, and Robert W. Dibble. *Combustion - Physical and Chemical Fundamentals, Modeling and Simulation, Experiments, Pollutant*. Springer Berlin Heidelberg New York, 2 edition, 2001. ISBN 978-3-540-65228-0.

[24] Norbert Peters. *Turbulent Combustion*. Cambridge University Press, 2000. ISBN 978-0-511-61270-1.

[25] Marcus Ó Conaire, Henry J. Curran, John M. Simmie, William J. Pitz, and Charles K. Westbrook. A comprehensive modeling study of hydrogen oxidation. *International Journal of Chemical Kinetics*, 36(11):603–622, 2004. doi: 10.1002/kin.20036.

[26] Gregory P. Smith, David M. Golden, Michael Frenklach, Nigel W. Moriarty, Boris Eiteneer, Mikhail Goldenberg, C. Thomas Bowman, Ronald K. Hanson, Soonho Song, Jr. William C. Gardiner, Vitali V. Lissianski, and Zhiwei Qin. GRI 3.0. `http://www.me.berkeley.edu/gri_mech/`, July 1999.

[27] S. M. Sarathy, C. K. Westbrook, M. Mehl, W. J. Pitz, C. Togbe, P. Dagaut, H. Wang, M. A. Oehlschlaeger, U. Niemann, K. Seshadri, P. S. Veloo, C. Ji, F. N. Egolfopoulos, and T. Lu. Comprehensive chemical kinetic modeling of the oxidation of 2-methylalkanes from C7 to C20. *Combustion and Flame*, 158(12):2338 – 2357, 2011. doi: 10.1016/j.combustflame.2011.05.007.

[28] S. M. Sarathy, C. Yeung, C. K. Westbrook, W. J. Pitz, M. Mehl, and M. J. Thomson. An experimental and kinetic modeling study of n-octane and 2-methylheptane in an opposed-flow diffusion flame. *Combustion and Flame*, 158(7):1277–1287, July 2011. doi: 10.1016/j.combustflame.2010.11.008.

[29] E. Ranzi, A. Frassoldati, R. Grana, A. Cuoci, T. Faravelli, A. P. Kelley, and C. K. Law. Hierarchical and comparative kinetic modeling of laminar flame speeds of hydrocarbon and oxygenated fuels. *Progress in Energy and Combustion Science*, 38(4):468–501, August 2012. doi: 10.1016/j.pecs.2012.03.004.

[30] Tianfeng Lu and Chung K. Law. Toward accommodating realistic fuel chemistry in large-scale computations. *Progress in Energy and Combustion Science*, 35(2):192 – 215, 2009. doi: 10.1016/j.pecs.2008.10.002.

[31] K. Radhakrishnan. Comparison of numerical techniques for integration of stiff ordinary differential equations arising in combustion chemistry. NASA Technical Report 2372, October 1984.

[32] Christopher P. Stone and Fabrizio Bisetti. Comparison of ODE Solver for Chemical Kinetics and Reactive CFD Applications. In *52nd Aerospace Sciences Meeting*. American Institute of Aeronautics and Astronautics, 2014.

[33] Turbulent Nonpremixed Flames. International Workshop on Measurement and Computation of Turbulent Nonpremixed Flames. `http://www.sandia.gov/TNF/`, 2015.

[34] Engine Combustion Network. "Spray A" Operating Condition. `http://www.sandia.gov/ecn/cvdata/sprayA.php`, March 2015.

[35] H. J. Curran, P. Gaffuri, W. J. Pitz, and C. K. Westbrook. A comprehensive modeling study of iso-octane oxidation. *Combustion and Flame*, 129(3): 253–280, May 2002. doi: 10.1016/S0010-2180(01)00373-X.

[36] Dennis Siebers and Brian Higgins. Flame Lift-Off on Direct-Injection Diesel Sprays Under Quiescent Conditions. SAE Technical Paper 2001-01-0530, SAE International, Warrendale, PA, March 2001.

[37] Dennis L. Siebers, Brian Higgins, and Lyle Pickett. Flame Lift-Off on Direct-Injection Diesel Fuel Jets: Oxygen Concentration Effects. SAE Technical Paper 2002-01-0890, SAE International, Warrendale, PA, March 2002.

[38] Lyle M. Pickett and Dennis L. Siebers. Orifice Diameter Effects on Diesel Fuel Jet Flame Structure. *Journal of Engineering for Gas Turbines and Power*, 127(1):187–196, 2005. doi: 10.1115/1.1760525.

[39] John Abraham and Lyle M. Pickett. Computed and Measured Fuel Vapor Distribution in a Diesel Spray. *Atomization and Sprays*, 20(3):241–250, 2010. doi: 10.1615/AtomizSpr.v20.i3.50.

[40] Ulaş Egüz, Sridhar Ayyapureddi, Cemil Bekdemir, Bart Somers, and Philip de Goey. Modeling Fuel Spray Auto-ignition using the FGM Approach: Effect of Tabulation Method. SAE Technical Paper 2012-01-0157, SAE International, Warrendale, PA, April 2012.

[41] Anne Kösters, Valeri Golovitchev, and Anders Karlsson. A Numerical Study of the Effect of EGR on Flame Lift-off in n-Heptane Sprays Using a Novel PaSR Model Implemented in OpenFOAM. *SAE International Journal of Fuels and Lubricants*, 5(2):604–610, April 2012. doi: 10.4271/2012-01-0153.

[42] C. Bekdemir, L. M. T. Somers, L. P. H. de Goey, J. Tillou, and C. Angelberger. Predicting diesel combustion characteristics with Large-Eddy Simulations including tabulated chemical kinetics. *Proceedings of the Combustion Institute*, 34(2):3067 – 3074, 2013. doi: 10.1016/j.proci.2012.06.160.

[43] Ulaş Egüz, Sridhar Ayyapureddi, Cemil Bekdemir, Bart Somers, and Philip de Goey. Manifold resolution study of the FGM method for an igniting diesel spray. *Fuel*, 113(0):228 – 238, 2013. doi: 10.1016/j.fuel.2013.05.090.

[44] Yuanjiang Pei, Evatt R. Hawkes, and Sanghoon Kook. Transported probability density function modelling of the vapour phase of an n-heptane jet at diesel engine conditions. *Proceedings of the Combustion Institute*, 34(2): 3039–3047, 2013. doi: 10.1016/j.proci.2012.07.033.

[45] Yuanjiang Pei, Evatt R. Hawkes, and Sanghoon Kook. A Comprehensive Study of Effects of Mixing and Chemical Kinetic Models on Predictions of n-heptane Jet Ignitions with the PDF Method. *Flow, Turbulence and Combustion*, 91(2):249–280, September 2013. doi: 10.1007/s10494-013-9454-z.

[46] Subhasish Bhattacharjee and Daniel C. Haworth. Simulations of transient n-heptane and n-dodecane spray flames under engine-relevant conditions using a transported PDF method. *Combustion and Flame*, 160(10):2083 – 2102, 2013. doi: 10.1016/j.combustflame.2013.05.003.

[47] Chetan Bajaj, Muhsin Ameen, and John Abraham. Evaluation of an Unsteady Flamelet Progress Variable Model for Autoignition and Flame Lift-Off in Diesel Jets. *Combustion Science and Technology*, 185(3):454–472, 2013. doi: 10.1080/00102202.2012.726667.

[48] J. Tillou, J.-B. Michel, C. Angelberger, C. Bekdemir, and D. Veynante. Large-Eddy Simulation of Diesel Spray Combustion with Exhaust Gas Recirculation. *Oil & Gas Science and Technology – Revue d'IFP Energies nouvelles*, 69(1):155–165, January 2014. doi: 10.2516/ogst/2013139.

[49] Michele Bolla, Daniele Farrace, Yuri M. Wright, Konstantinos Boulouchos, and Epaminondas Mastorakos. Influence of turbulence–chemistry interaction for n-heptane spray combustion under diesel engine conditions with emphasis on soot formation and oxidation. *Combustion Theory and Modelling*, 18(2):330–360, March 2014. doi: 10.1080/13647830.2014.898795.

[50] Abolfazl Irannejad, Araz Banaeizadeh, and Farhad Jaberi. Large eddy simulation of turbulent spray combustion. *Combustion and Flame*, 162(2): 431–450, February 2015. doi: 10.1016/j.combustflame.2014.07.029.

[51] Anne Kösters, Anders Karlsson, Michael Oevermann, Gianluca D'Errico, and Tommaso Lucchini. RANS predictions of turbulent diffusion flames: comparison of a reactor and a flamelet combustion model to the well stirred approach. *Combustion Theory and Modelling*, 19(1):81–106, January 2015. doi: 10.1080/13647830.2014.982342.

[52] J. T. Farrell, N. P. Cernansky, F. L. Dryer, C. K. Law, D. G. Friend, C. A. Hergart, R. M. McDavid, A. K. Patel, Charles J. Mueller, and H. Pitsch. Development of an Experimental Database and Kinetic Models for Surrogate Diesel Fuels. SAE Technical Paper 2007-01-0201, SAE International, Warrendale, PA, April 2007.

[53] Lyle M. Pickett, Caroline L. Genzale, Gilles Bruneaux, Louis-Marie Malbec, Laurent Hermant, Caspar Christiansen, and Jesper Schramm. Comparison of Diesel Spray Combustion in Different High-Temperature, High-Pressure Facilities. *SAE International Journal of Engines*, 3(2):156–181, October 2010. doi: 10.4271/2010-01-2106.

[54] Lyle M. Pickett, Julien Manin, Caroline L. Genzale, Dennis L. Siebers, Mark P. B. Musculus, and Cherian A. Idicheria. Relationship Between Diesel Fuel Spray Vapor Penetration/Dispersion and Local Fuel Mixture Fraction. *SAE International Journal of Engines*, 4(1):764–799, April 2011. doi: 10.4271/2011-01-0686.

[55] Raul Payri, Jose M. García-Oliver, Michele Bardi, and Julien Manin. Fuel temperature influence on diesel sprays in inert and reacting conditions. *Applied Thermal Engineering*, 35:185–195, March 2012. doi: 10.1016/j.applthermaleng.2011.10.027.

[56] Maarten Meijer, Bart Somers, Jaclyn Johnson, Jeffrey Naber, Seong-Young Lee, Louis Marie Malbec, Gilles Bruneaux, Lyle M. Pickett, Michele Bardi, Raul Payri, and Tim Bazyn. Engine Combustion Network (ECN): Characterization and Comparison of Boundary Conditions for Different Combustion Vessels. *Atomization and Sprays*, 22(9):777–806, 2012. doi: 10.1615/AtomizSpr.2012006083.

[57] Michele Bardi, Raul Payri, Louis Marie Malbec, Gilles Bruneaux, Lyle M. Pickett, Julien Manin, Tim Bazyn, and Caroline Genzale. Engine Combustion Network: Comparison of Spray Development, Vaporization, and Combustion in Different Combustion Vessels. *Atomization and Sprays*, 22 (10):807–842, 2012. doi: 10.1615/AtomizSpr.2013005837.

[58] Maarten Meijer, Jonas Galle, L. M. T. Somers, J. G. H. Griensven, and Sebastian Verhelst. High-Speed Characterization of ECN Spray A Using Various Diagnostic Techniques. *SAE International Journal of Engines*, 6(2): 1238–1248, April 2013. doi: 10.4271/2013-01-1616.

[59] Jesús Benajes, Raúl Payri, Michele Bardi, and Pedro Martí-Aldaraví. Experimental characterization of diesel ignition and lift-off length using a single-hole ECN injector. *Applied Thermal Engineering*, 58(1–2):554–563, September 2013. doi: 10.1016/j.applthermaleng.2013.04.044.

[60] Scott A. Skeen, Julien Manin, and Lyle M. Pickett. Simultaneous formaldehyde PLIF and high-speed schlieren imaging for ignition visualization in high-pressure spray flames. *Proceedings of the Combustion Institute*, 35(3): 3167–3174, 2015. doi: 10.1016/j.proci.2014.06.040.

[61] S. Som, D. E. Longman, Z. Luo, M. Plomer, and T. Lu. Three dimensional simulations of diesel sprays using n-dodecane as a surrogate. In *Fall Technical Meeting of the Eastern States Section of the Combustion Institute*, 2011.

[62] Zhaoyu Luo, Sibendu Som, S. Mani Sarathy, Max Plomer, William J. Pitz, Douglas E. Longman, and Tianfeng Lu. Development and validation of an n-dodecane skeletal mechanism for spray combustion applications. *Combustion Theory and Modelling*, 18(2):187–203, March 2014. doi: 10.1080/13647830.2013.872807.

[63] G. D'Errico, T. Lucchini, F. Contino, M. Jangi, and X.-S. Bai. Comparison of well-mixed and multiple representative interactive flamelet approaches for diesel spray combustion modelling. *Combustion Theory and Modelling*, 18 (1):65–88, January 2014. doi: 10.1080/13647830.2013.860238.

[64] Prithwish Kundu, Yuanjiang Pei, Mingjie Wang, Raju Mandhapati, and Sibendu Som. Evaluation of Turbulence-Chemistry Interaction Under Diesel Engine Conditions with Multi-Flamelet RIF Model. *Atomization and Sprays*, 24(9):779–800, 2014. doi: 10.1615/AtomizSpr.2014010506.

[65] M. A. Chishty, Y. Pei, E. R. Hawkes, M. Bolla, and S. Kook. Investigation of the Flame Structure of Spray-A Using the Transported Probability Density Function. Melbourne, Australia, 2014.

[66] Yuanjiang Pei, Evatt R. Hawkes, Sanghoon Kook, Graham M. Goldin, and Tianfeng Lu. Modelling n-dodecane spray and combustion with the transported probability density function method. *Combustion and Flame*, 162(5):2006–2019, May 2015. doi: 10.1016/j.combustflame.2014.12.019.

[67] Cheng Gong, Mehdi Jangi, Tommaso Lucchini, Gianluca D'Errico, and Xue-Song Bai. Large Eddy Simulation of Air Entrainment and Mixing in Reacting and Non-Reacting Diesel Sprays. *Flow, Turbulence and Combustion*, 93(3):385–404, October 2014. doi: 10.1007/s10494-014-9566-0.

[68] Yuanjiang Pei, Sibendu Som, Eric Pomraning, Peter K. Senecal, Scott A. Skeen, Julien Manin, and Lyle M. Pickett. Large eddy simulation of a reacting spray flame with multiple realizations under compression ignition engine conditions. *Combustion and Flame*, 162(12):4442–4455, December 2015. doi: 10.1016/j.combustflame.2015.08.010.

[69] Layal Hakim, Guilhem Lacaze, and Joseph Oefelein. Large Eddy Simulation of Autoignition Transients in a Model Diesel Injector Configuration. *SAE International Journal of Fuels and Lubricants*, 9(1):165–176, April 2016. doi: 10.4271/2016-01-0872.

[70] Krithika Narayanaswamy, Perrine Pepiot, and Heinz Pitsch. A chemical mechanism for low to high temperature oxidation of n-dodecane as a component of transportation fuel surrogates. *Combustion and Flame*, 161(4): 866–884, April 2014. doi: 10.1016/j.combustflame.2013.10.012.

[71] Eliseo Ranzi, Alessio Frassoldati, Alessandro Stagni, Matteo Pelucchi, Alberto Cuoci, and Tiziano Faravelli. Reduced Kinetic Schemes of Complex Reaction Systems: Fossil and Biomass-Derived Transportation Fuels. *International Journal of Chemical Kinetics*, 46(9):512–542, September 2014. doi: 10.1002/kin.20867.

[72] Charles K. Westbrook, William J. Pitz, Olivier Herbinet, Henry J. Curran, and Emma J. Silke. A comprehensive detailed chemical kinetic reaction mechanism for combustion of n-alkane hydrocarbons from n-octane to n-hexadecane. *Combustion and Flame*, 156(1):181 – 199, 2009. doi: 10.1016/j.combustflame.2008.07.014.

[73] Muhsin M. Ameen and John Abraham. RANS and LES Study of Lift-Off Physics in Reacting Diesel Jets. SAE Technical Paper 2014-01-1118, SAE International, Warrendale, PA, April 2014.

[74] V. Moureau, G. Lartigue, Y. Sommerer, C. Angelberger, O. Colin, and T. Poinsot. Numerical methods for unsteady compressible multi-component reacting flows on fixed and moving grids. *Journal of Computational Physics*, 202(2):710–736, January 2005. doi: 10.1016/j.jcp.2004.08.003.

[75] Thierry Poinsot and Denis Veynante. *Theoretical and Numerical Combustion*. Third edition, 2012.

[76] Rainer N. Dahms, Julien Manin, Lyle M. Pickett, and Joseph C. Oefelein. Understanding high-pressure gas-liquid interface phenomena in Diesel engines. *Proceedings of the Combustion Institute*, 34(1):1667 – 1675, 2013. doi: 10.1016/j.proci.2012.06.169.

[77] Rainer N. Dahms and Joseph C. Oefelein. On the transition between two-phase and single-phase interface dynamics in multicomponent fluids at supercritical pressures. *Physics of Fluids (1994-present)*, 25(9):092103, September 2013. doi: 10.1063/1.4820346.

[78] Rainer N. Dahms and Joseph C. Oefelein. Non-equilibrium gas–liquid interface dynamics in high-pressure liquid injection systems. *Proceedings of the Combustion Institute*, 35(2):1587–1594, 2015. doi: 10.1016/j.proci.2014.05.155.

[79] Rainer N. Dahms and Joseph C. Oefelein. Liquid jet breakup regimes at supercritical pressures. *Combustion and Flame*, 162(10):3648–3657, October 2015. doi: 10.1016/j.combustflame.2015.07.004.

[80] Joseph Oefelein, Rainer Dahms, and Guilhem Lacaze. Detailed Modeling and Simulation of High-Pressure Fuel Injection Processes in Diesel Engines. *SAE International Journal of Engines*, 5(3):1410–1419, April 2012. doi: 10.4271/2012-01-1258.

[81] Joseph Oefelein, Guilhem Lacaze, Rainer Dahms, Anthony Ruiz, and Antony Misdariis. Effects of Real-Fluid Thermodynamics on High-Pressure Fuel Injection Processes. *SAE International Journal of Engines*, 7(3):1125–1136, April 2014. doi: 10.4271/2014-01-1429.

[82] J. Manin, M. Bardi, L. M. Pickett, R. N. Dahms, and J. C. Oefelein. Microscopic investigation of the atomization and mixing processes of diesel sprays injected into high pressure and temperature environments. *Fuel*, 134:531–543, October 2014. doi: 10.1016/j.fuel.2014.05.060.

[83] Guilhem Lacaze, Antony Misdariis, Anthony Ruiz, and Joseph C. Oefelein. Analysis of high-pressure Diesel fuel injection processes using LES with real-fluid thermodynamics and transport. *Proceedings of the Combustion Institute*, 35(2):1603–1611, 2015. doi: 10.1016/j.proci.2014.06.072.

[84] C. R. Wilke. A Viscosity Equation for Gas Mixtures. *The Journal of Chemical Physics*, 18(4):517–519, 1950. doi: 10.1063/1.1747673.

[85] S. Mathur and S. C. Saxena. Viscosity of polar gas mixtures: Wilke's method. *Applied Scientific Research, Section A*, 15(1):404–410, January 1966. doi: 10.1007/BF00411574.

[86] Alexander Burcat and Branko Ruscic. Extended Third Millenium Ideal Gas and Condensed Phase Thermochemical Database for Combustion with Updates from Active Thermochemical Tables. Technical Report ANL-05/20 TAE 960, Argonne National Laboratory, 2005.

[87] R. W. Bilger, S. H. Stårner, and R. J. Kee. On reduced mechanisms for methane-air combustion in nonpremixed flames. *Combustion and Flame*, 80(2):135 – 149, 1990. doi: 10.1016/0010-2180(90)90122-8.

[88] Eric Garnier, Nikolaus Adams, and Pierre Sagaut. *Large Eddy Simulation for Compressible Flows*. Scientific Computation. Springer, 2009. ISBN 978-90-481-2819-8.

[89] Len G. Margolin and William J. Rider. A rationale for implicit turbulence modelling. *International Journal for Numerical Methods in Fluids*, 39(9): 821–841, July 2002. doi: 10.1002/fld.331.

[90] F. F. Grinstein, L. G. Margolin, and W. J. Rider. *Implicit Large Eddy Simulation*. Cambridge University Press, 2007. ISBN 978-0-521-86982-9.

[91] Fernando F. Grinstein and Christer Fureby. On Flux-Limiting-Based Implicit Large Eddy Simulation. *Journal of Fluids Engineering*, 129(12): 1483–1492, July 2007. doi: 10.1115/1.2801684.

[92] Christer Fureby and Fernando F. Grinstein. Large Eddy Simulation of High-Reynolds-Number Free and Wall-Bounded Flows. *Journal of Computational Physics*, 181(1):68–97, September 2002. doi: 10.1006/jcph.2002.7119.

[93] Fernando Franklin Grinstein. Recent Progress on Monotone Integrated Large Eddy Simulation of Free Jets. *JSME International Journal Series B Fluids and Thermal Engineering*, 49(4):890–898, 2006. doi: 10.1299/jsmeb.49.890.

[94] Ville Anton Vuorinen, Harri Hillamo, Ossi Kaario, Mika Nuutinen, Martti Larmi, and Laszlo Fuchs. Effect of Droplet Size and Atomization on Spray Formation: A Priori Study Using Large-Eddy Simulation. *Flow, Turbulence and Combustion*, 86(3-4):533–561, April 2011. doi: 10.1007/s10494-010-9266-3.

[95] V. Vuorinen, M. Larmi, P. Schlatter, L. Fuchs, and B. J. Boersma. A low-dissipative, scale-selective discretization scheme for the Navier–Stokes equations. *Computers & Fluids*, 70:195–205, November 2012. doi: 10.1016/j.compfluid.2012.09.022.

[96] V. Vuorinen, J. Yu, S. Tirunagari, O. Kaario, M. Larmi, C. Duwig, and B. J. Boersma. Large-eddy simulation of highly underexpanded transient gas jets. *Physics of Fluids*, 25(1):016101, 2013. doi: 10.1063/1.4772192.

[97] Ville Vuorinen, Armin Wehrfritz, Christophe Duwig, and B. J. Boersma. Large-eddy simulation on the effect of injection pressure and density on fuel jet mixing in gas engines. *Fuel*, 130:241–250, August 2014. doi: 10.1016/j.fuel.2014.04.045.

[98] John K. Dukowicz. A particle-fluid numerical model for liquid sprays. *Journal of Computational Physics*, 35(2):229–253, April 1980. doi: 10.1016/0021-9991(80)90087-X.

[99] Dennis L. Siebers. Liquid-Phase Fuel Penetration in Diesel Sprays. SAE Technical Paper 980809, SAE International, Warrendale, PA, February 1998.

[100] Ossi Kaario, Martti Larmi, and Franz Tanner. Relating Integral Length Scale to Turbulent Time Scale and Comparing k-ϵ and RNG k-ϵ Turbulence Models in Diesel Combustion Simulation. SAE Technical Paper 2002-01-1117, SAE International, March 2002.

[101] Ossi Kaario, Martti Larmi, and Franz Tanner. Comparing Single-Step and Multi-Step Chemistry Using The Laminar and Turbulent Characteristic Time Combustion Model In Two Diesel Engines. SAE Technical Paper 2002-01-1749, SAE International, May 2002.

[102] Ville Vuorinen, Harri Hillamo, Ossi Kaario, Martti Larmi, and L. Fuchs. Large Eddy Simulation of Droplet Stokes Number Effects on Turbulent Spray Shape. *Atomization and Sprays*, 20(2):93–114, 2010. doi: 10.1615/AtomizSpr.v20.i2.

[103] Ossi Kaario, Ville Vuorinen, Tuomo Hulkkonen, K. Keskinen, M. Nuutinen, Martti Larmi, and Franz X. Tanner. Large Eddy Simulation of High Gas Density Effects in Fuel Sprays. *Atomization and Sprays*, 23(4):297–325, 2013. doi: 10.1615/AtomizSpr.2013006784.

[104] Qingluan Xue, Sibendu Som, Peter K. Senecal, and E. Pomraning. Large Eddy Simulation of Fuel-Spray Under Non-Reacting IC Engine Conditions. *Atomization and Sprays*, 23(10):925–955, 2013. doi: 10.1615/AtomizSpr.2013008320.

[105] Edward Knudsen, Shashank, and Heinz Pitsch. Modeling partially premixed combustion behavior in multiphase LES. *Combustion and Flame*, 162(1):159–180, January 2015. doi: 10.1016/j.combustflame.2014.07.013.

[106] N. Frössling. Über die Verdunstung fallender Tropfen. *Gerlands Beiträge zur Geophysik*, 52:170–216, 1938.

[107] W. E. Ranz and W. R. J. Marshall. Evaporation from Drops, Part I. *Chemical Engineering Progress*, 48(3):141–146, 1952.

[108] W. E. Ranz and W. R. J. Marshall. Evaporation from Drops, Part II. *Chemical Engineering Progress*, 48(3):173–180, 1952.

[109] Jennifer C. Beale and Rolf D. Reitz. Modeling Spray Atomization with the Kelvin-Helmholtz/Rayleigh-Taylor Hybrid Model. *Atomization and Sprays*, 9(6):623–650, 1999. doi: 10.1615/AtomizSpr.v9.i6.40.

[110] Rolf D. Reitz. Modeling Atomization Processes in High-Pressure Vaporizing Sprays. *Atomisation and Spray Technology*, 3:309–337, 1987.

[111] F. X. Tanner. Liquid Jet Atomization and Droplet Breakup Modeling of Non-Evaporating Diesel Fuel Sprays. SAE Technical Paper 970050, February 1997.

[112] Peter J. O'Rourke and Anthony A. Amsden. The TAB Method for Numerical Calculation of Spray Droplet Breakup. SAE Technical Paper 872089, SAE International, Warrendale, PA, November 1987.

[113] OpenFOAM Foundation. OpenFOAM® - The Open Source Computational Fluid Dynamics (CFD) Toolbox. http://www.openfoam.org/, 2014.

[114] H. G. Weller, G. Tabor, H. Jasak, and C. Fureby. A tensorial approach to computational continuum mechanics using object-oriented techniques. *Computers in Physics*, 12(6):620–631, November 1998. doi: 10.1063/1.168744.

[115] Jukka-Pekka Keskinen. *Large Eddy Simulation of In-Cylinder Flows*. PhD thesis, Aalto University, Espoo, Finland, 2016.

[116] H. Jasak, H. G. Weller, and A. D. Gosman. High resolution NVD differencing scheme for arbitrarily unstructured meshes. *International Journal for Numerical Methods in Fluids*, 31(2):431–449, September 1999. doi: 10.1002/(SICI)1097-0363(19990930)31:2<431::AID-FLD884>3.0.CO;2-T.

[117] H. Pitsch and H. Steiner. Large-eddy simulation of a turbulent piloted methane/air diffusion flame (Sandia flame D). *Physics of Fluids (1994-present)*, 12(10):2541–2554, October 2000. doi: 10.1063/1.1288493.

[118] N. Branley and W. P. Jones. Large Eddy simulation of a turbulent non-premixed flame. *Combustion and Flame*, 127(1–2):1914 – 1934, 2001. doi: 10.1016/S0010-2180(01)00298-X.

[119] A. M. Kempf, B. J. Geurts, and J. C. Oefelein. Error analysis of large-eddy simulation of the turbulent non-premixed sydney bluff-body flame. *Combustion and Flame*, 158(12):2408–2419, December 2011. doi: 10.1016/j.combustflame.2011.04.012.

[120] M. Chrigui, A.R. Masri, A. Sadiki, and J. Janicka. Large Eddy Simulation of a Polydisperse Ethanol Spray Flame. *Flow, Turbulence and Combustion*, 90(4):813–832, 2013. doi: 10.1007/s10494-013-9449-9.

[121] Ilias A. Dodoulas and Salvador Navarro-Martinez. Analysis of extinction in a non-premixed turbulent flame using large eddy simulation and the chemical explosion mode analysis. *Combustion Theory and Modelling*, 19 (1):107–129, January 2015. doi: 10.1080/13647830.2014.993713.

[122] R. I. Issa, B. Ahmadi-Befrui, K. R. Beshay, and A. D. Gosman. Solution of the implicitly discretised reacting flow equations by operator-splitting. *Journal of Computational Physics*, 93(2):388 – 410, 1991. doi: 10.1016/0021-9991(91)90191-M.

[123] U. Maas and S. B. Pope. Simplifying chemical kinetics: Intrinsic low-dimensional manifolds in composition space. *Combustion and Flame*, 88 (3–4):239–264, March 1992. doi: 10.1016/0010-2180(92)90034-M.

[124] V. Bykov and U. Maas. Extension of the ILDM method to the domain of slow chemistry. *Proceedings of the Combustion Institute*, 31(1):465 – 472, 2007. doi: 10.1016/j.proci.2006.08.104.

[125] V. Bykov and U. Maas. The extension of the ILDM concept to reaction–diffusion manifolds. *Combustion Theory and Modelling*, 11(6):839–862, 2007. doi: 10.1080/13647830701242531.

[126] V. Bykov and U. Maas. Problem adapted reduced models based on Reaction-Diffusion Manifolds (REDIMs). *Proceedings of the Combustion Institute*, 32 (1):561 – 568, 2009. doi: 10.1016/j.proci.2008.06.186.

[127] U. Maas and V. Bykov. The extension of the reaction/diffusion manifold concept to systems with detailed transport models. *Proceedings of the Combustion Institute*, 33(1):1253–1259, 2011. doi: 10.1016/j.proci.2010.06.117.

[128] Zhuyin Ren, Stephen B. Pope, Alexander Vladimirsky, and John M. Guckenheimer. The invariant constrained equilibrium edge preimage curve method for the dimension reduction of chemical kinetics. *The Journal of Chemical Physics*, 124(11):114111, 2006. doi: 10.1063/1.2177243.

[129] F. A. Williams. Recent Advances in Theoretical Descriptions of Turbulent Diffusion Flames. In S. N. B. Murthy, editor, *Turbulent Mixing in Nonreactive and Reactive Flows*, pages 189–208. Springer New York, January 1975. ISBN 978-1-4615-8740-8.

[130] Norbert Peters. Local Quenching of Diffusion Flamelets and Non-Premixed Turbulent Combustion. Technical Report WSS 80-4, Combustion Institute, Irvine, CA, 1980.

[131] V. R. Kuznetsov. Influence of turbulence on the formation of high nonequilibrium concentrations of atoms and free radicals in diffusion flames. *Fluid Dynamics*, 17(6):815–820, November 1982. doi: 10.1007/BF01090372.

[132] N. Peters. Laminar flamelet concepts in turbulent combustion. *Symposium (International) on Combustion*, 21(1):1231 – 1250, 1988. doi: 10.1016/S0082-0784(88)80355-2.

[133] K. N. C. Bray and N. Peters. Laminar flamelets in turbulent flames. In P. A. Libby and F. A. Williams, editors, *Turbulent reacting flows*, pages 63–113. 1994.

[134] G. Dixon-Lewis, T. David, P. H. Gaskell, S. Fukutani, H. Jinno, J. A. Miller, R. J. Kee, M. D. Smooke, N. Peters, E. Effelsberg, J. Warnatz, and F. Behrendt. Calculation of the structure and extinction limit of a methane-air counterflow diffusion flame in the forward stagnation region of a porous cylinder. *Symposium (International) on Combustion*, 20(1):1893 – 1904, 1985. doi: 10.1016/S0082-0784(85)80688-3.

[135] Robert J. Kee, James A. Miller, Gregory H. Evans, and Graham Dixon-Lewis. A computational model of the structure and extinction of strained, opposed flow, premixed methane-air flames. *Symposium (International) on Combustion*, 22(1):1479 – 1494, 1989. doi: 10.1016/S0082-0784(89)80158-4.

[136] Graham Dixon-Lewis. Structure of laminar flames. *Twenty-Third Symposium (International) on Combustion*, 23(1):305–324, January 1991. doi: 10.1016/S0082-0784(06)80274-2.

[137] G. Stahl and J. Warnatz. Numerical investigation of time-dependent properties and extinction of strained methane- and propane-air flamelets. *Combustion and Flame*, 85(3–4):285 – 299, 1991. doi: 10.1016/0010-2180(91)90134-W.

[138] F. Williams. Turbulent Combustion. In *The Mathematics of Combustion*, Frontiers in Applied Mathematics, pages 97–131. Society for Industrial and Applied Mathematics, January 1985. ISBN 978-0-89871-053-3.

[139] H. Pitsch, H. Barths, and N. Peters. Three-Dimensional Modeling of NOx and Soot Formation in DI-Diesel Engines Using Detailed Chemistry Based on the Interactive Flamelet Approach. SAE Technical Paper 962057, SAE International, Warrendale, PA, October 1996.

[140] J. A. van Oijen and L. P. H. de Goey. Modelling of Premixed Laminar Flames using Flamelet-Generated Manifolds. *Combustion Science and Technology*, 161(1):113–137, December 2000. doi: 10.1080/00102200008935814.

[141] Olivier Gicquel, Nasser Darabiha, and Dominique Thévenin. Laminar premixed hydrogen/air counterflow flame simulations using flame prolongation of ILDM with differential diffusion. *Proceedings of the Combustion Institute*, 28(2):1901 – 1908, 2000. doi: 10.1016/S0082-0784(00)80594-9.

[142] Charles D. Pierce and Parviz Moin. Progress-variable approach for large-eddy simulation of non-premixed turbulent combustion. *Journal of Fluid Mechanics*, 504:73–97, April 2004. doi: 10.1017/S0022112004008213.

[143] Matthias Ihme, Chong M. Cha, and Heinz Pitsch. Prediction of local extinction and re-ignition effects in non-premixed turbulent combustion using a flamelet/progress variable approach. *Proceedings of the Combustion Institute*, 30(1):793–800, January 2005. doi: 10.1016/j.proci.2004.08.260.

[144] Robert J. Kee, Graham Dixon-Lewis, Jürgen Warnatz, Michael E. Coltrin, and James A. Miller. A Fortran Computer Code Package For The Evaluation Of Gas-Phase, Multicomponent Transport Properties. Technical Report SAND86-8246, 1986.

[145] CHEM1D. A one-dimensional laminar flame code. `http://www.combustion.tue.nl`, 2014.

[146] L. M. T. Somers. *The Simulation of Flat Flames with Detailed and Reduced Chemical Models*. PhD thesis, Eindhoven University of Technology, Eindhoven, 1994.

[147] B. Fiorina, O. Gicquel, L. Vervisch, S. Carpentier, and N. Darabiha. Approximating the chemical structure of partially premixed and diffusion counterflow flames using FPI flamelet tabulation. *Combustion and Flame*, 140(3):147 – 160, 2005. doi: 10.1016/j.combustflame.2004.11.002.

[148] Jéremy Galpin, Alexandre Naudin, Luc Vervisch, Christian Angelberger, Olivier Colin, and Pascale Domingo. Large-eddy simulation of a fuel-lean premixed turbulent swirl-burner. *Combustion and Flame*, 155(1–2):247 – 266, 2008. doi: 10.1016/j.combustflame.2008.04.004.

[149] L. M. Verhoeven, W. J. S. Ramaekers, J. A. van Oijen, and L. P. H. de Goey. Modeling non-premixed laminar co-flow flames using flamelet-generated manifolds. *Combustion and Flame*, 159(1):230 – 241, 2012. doi: 10.1016/j.combustflame.2011.07.011.

[150] Cemil Bekdemir. *Tabulated chemical kinetics for efficient and detailed simulations of diesel engine combustion*. PhD thesis, Technische Universiteit Eindhoven, Eindhoven, 2012.

[151] Cemil Bekdemir, Bart Somers, and Philip de Goey. DNS with detailed and tabulated chemistry of engine relevant igniting systems. *Combustion and Flame*, 161(1):210–221, January 2014. doi: 10.1016/j.combustflame.2013.08.022.

[152] J. Tillou, J. B. Michel, C. Angelberger, and D. Veynante. Assessing LES models based on tabulated chemistry for the simulation of Diesel spray combustion. *Combustion and Flame*, 161(2):525–540, February 2014. doi: 10.1016/j.combustflame.2013.09.006.

[153] A. W. Vreman, B. A. Albrecht, J. A. van Oijen, L. P. H. de Goey, and R. J. M. Bastiaans. Premixed and nonpremixed generated manifolds in large-eddy simulation of Sandia flame D and F. *Combustion and Flame*, 153(3):394–416, May 2008. doi: 10.1016/j.combustflame.2008.01.009.

[154] Hannes Kröger, Egon Hassel, Nikolai Kornev, and Detlef Wendig. LES of Premixed Flame Propagation in a Free Straight Vortex. *Flow, Turbulence and Combustion*, 84(3):513–541, April 2010. doi: 10.1007/s10494-009-9242-y.

[155] C. Bekdemir, L. M. T. Somers, and L. P. H. de Goey. Modeling diesel engine combustion using pressure dependent Flamelet Generated Manifolds. *Proceedings of the Combustion Institute*, 33(2):2887–2894, 2011. doi: 10.1016/j.proci.2010.07.091.

[156] Peyman Givi. Model-free simulations of turbulent reactive flows. *Progress in Energy and Combustion Science*, 15(1):1–107, January 1989. doi: 10.1016/0360-1285(89)90006-3.

[157] S. B. Pope. Computations of turbulent combustion: Progress and challenges. *Twenty-Third Symposium (International) on Combustion*, 23(1):591–612, January 1991. doi: 10.1016/S0082-0784(06)80307-3.

[158] D. C. Haworth. Progress in probability density function methods for turbulent reacting flows. *Progress in Energy and Combustion Science*, 36(2):168 – 259, 2010. doi: 10.1016/j.pecs.2009.09.003.

[159] J. Janicka and W. Kollmann. A two-variables formalism for the treatment of chemical reactions in turbulent H2—Air diffusion flames. *Seventeenth Symposium (International) on Combustion*, 17(1):421–430, January 1979. doi: 10.1016/S0082-0784(79)80043-0.

[160] Jean-Baptiste Michel, Olivier Colin, Christian Angelberger, and Denis Veynante. Using the tabulated diffusion flamelet model ADF-PCM to simulate a lifted methane–air jet flame. *Combustion and Flame*, 156(7): 1318 – 1331, 2009. doi: 10.1016/j.combustflame.2008.12.012.

[161] Luc Vervisch, Raphaël Hauguel, Pascale Domingo, and Matthieu Rullaud. Three facets of turbulent combustion modelling: DNS of premixed V-flame, LES of lifted nonpremixed flame and RANS of jet-flame. *Journal of Turbulence*, 5:1–36, 2004. doi: 10.1088/1468-5248/5/1/004.

[162] Charles D. Pierce and Parviz Moin. A dynamic model for subgrid-scale variance and dissipation rate of a conserved scalar. *Physics of Fluids (1994-present)*, 10(12):3041–3044, 1998. doi: 10.1063/1.869832.

[163] G. Balarac, H. Pitsch, and V. Raman. Development of a dynamic model for the subfilter scalar variance using the concept of optimal estimators. *Physics of Fluids (1994-present)*, 20(3):035114, March 2008. doi: 10.1063/1.2896287.

[164] A. Yu Klimenko. Multicomponent diffusion of various admixtures in turbulent flow. *Fluid Dynamics*, 25(3):327–334, May 1990. doi: 10.1007/BF01049811.

[165] R. W. Bilger. Conditional moment closure for turbulent reacting flow. *Physics of Fluids A: Fluid Dynamics (1989-1993)*, 5(2):436–444, February 1993. doi: 10.1063/1.858867.

[166] A. Y. Klimenko and R. W. Bilger. Conditional moment closure for turbulent combustion. *Progress in Energy and Combustion Science*, 25(6):595–687, December 1999. doi: 10.1016/S0360-1285(99)00006-4.

[167] C. Angelberger, D. Veynante, F. Egolfopoulos, and T. Poinsot. Large eddy simulations of combustion instabilities in premixed flames. In *Proc. of the Summer Program*, pages 61–82. Citeseer, 1998.

[168] O. Colin, F. Ducros, D. Veynante, and T. Poinsot. A thickened flame model for large eddy simulations of turbulent premixed combustion. *Physics of Fluids (1994-present)*, 12(7):1843–1863, July 2000. doi: 10.1063/1.870436.

[169] J.-Ph Légier, T. Poinsot, and D. Veynante. Dynamically thickened flame LES model for premixed and non-premixed turbulent combustion. In *Proc. of the summer program*, pages 157–168. Citeseer, 2000.

[170] B. Magnussen. On the structure of turbulence and a generalized eddy dissipation concept for chemical reaction in turbulent flow. In *19th Aerospace Sciences Meeting*. American Institute of Aeronautics and Astronautics, 1981. doi: 10.2514/6.1981-42.

[171] Jery Chomiak and Anders Karlsson. Flame liftoff in diesel sprays. *Symposium (International) on Combustion*, 26(2):2557–2564, 1996. doi: 10.1016/S0082-0784(96)80088-9.

[172] M. Berglund, E. Fedina, C. Fureby, J. Tegnér, and V. Sabel'nikov. Finite Rate Chemistry Large-Eddy Simulation of Self-Ignition in Supersonic Combustion Ramjet. *AIAA Journal*, 48(3):540–550, 2010. doi: 10.2514/1.43746.

[173] P. J O'Rourke and F. V Bracco. Two scaling transformations for the numerical computation of multidimensional unsteady laminar flames. *Journal of Computational Physics*, 33(2):185–203, November 1979. doi: 10.1016/0021-9991(79)90015-9.

[174] Kazuhiro Akihama, Yoshiki Takatori, Kazuhisa Inagaki, Shizuo Sasaki, and Anthony M. Dean. Mechanism of the Smokeless Rich Diesel Combustion by Reducing Temperature. SAE Technical Paper 2001-01-0655, SAE International, Warrendale, PA, March 2001.

[175] T. Kitamura, T. Ito, J. Senda, and H. Fujimoto. Mechanism of smokeless diesel combustion with oxygenated fuels based on the dependence of the equivalence ration and temperature on soot particle formation. *International Journal of Engine Research*, 3(4):223–248, August 2002. doi: 10.1243/146808702762230923.

[176] Ossi Kaario, Anders Brink, Armin Wehrfritz, and Martti Larmi. Analyzing Local Combustion Environment with a Flamelet Model and Detailed Chemistry. SAE Technical Paper 2012-01-0150, SAE International, Warrendale, PA, April 2012.

[177] Lyle M. Pickett, Dennis L. Siebers, and Cherian A. Idicheria. Relationship Between Ignition Processes and the Lift-Off Length of Diesel Fuel Jets. SAE Technical Paper 2005-01-3843, SAE Technical Paper, Warrendale, PA, October 2005.

[178] Lyle M. Pickett, Sanghoon Kook, Helena Persson, and Öivind Andersson. Diesel fuel jet lift-off stabilization in the presence of laser-induced plasma ignition. *Proceedings of the Combustion Institute*, 32(2):2793–2800, 2009. doi: 10.1016/j.proci.2008.06.082.

[179] E. Oldenhof, M.J. Tummers, E.H. van Veen, and D.J.E.M. Roekaerts. Ignition kernel formation and lift-off behaviour of jet-in-hot-coflow flames. *Combustion and Flame*, 157(6):1167–1178, June 2010. doi: 10.1016/j.combustflame.2010.01.002.

[180] E. Oldenhof, M. J. Tummers, E. H. van Veen, and D. J. E. M. Roekaerts. Role of entrainment in the stabilisation of jet-in-hot-coflow flames. *Combustion and Flame*, 158(8):1553–1563, August 2011. doi: 10.1016/j.combustflame.2010.12.018.

[181] M. Olsson and L. Fuchs. Large eddy simulation of the proximal region of a spatially developing circular jet. *Physics of Fluids*, 8(8):2125, 1996. doi: 10.1063/1.868987.

[182] Ville Vuorinen, Armin Wehrfritz, Jingzhou Yu, Ossi Kaario, Martti Larmi, and Bendiks Jan Boersma. Large-Eddy Simulation of Subsonic Jets. *Journal of Physics: Conference Series*, 318(3):032052, December 2011. doi: 10.1088/1742-6596/318/3/032052.

[183] Ossi Kaario, Martti Larmi, and Franz X. Tanner. Non-Evaporating Liquid Spray Simulations with the ETAB and WAVE Droplet Breakup Models. In *ILASS-Europe*, Zaragoza, 2002.

[184] Gianmarco Pizza, Yuri Martin Wright, German Weisser, and Konstantinos Boulouchos. Evaporating and non-evaporating diesel spray simulation: comparison between the ETAB and wave breakup model. *International Journal of Vehicle Design*, 45(1/2):80, 2007. doi: 10.1504/IJVD.2007.013672.

[185] S. Som and S. K. Aggarwal. Effects of primary breakup modeling on spray and combustion characteristics of compression ignition

engines. *Combustion and Flame*, 157(6):1179 – 1193, 2010. doi: 10.1016/j.combustflame.2010.02.018.

[186] Nidheesh Bharadwaj and Christopher J. Rutland. A Large-Eddy Simulation Study of Sub-Grid Two-Phase Interaction in Particle-Laden Flows and Diesel Engine Sprays. *Atomization and Sprays*, 20(8):673–695, 2010.

[187] Python Software Foundation. Python Language Reference, version 2.7. http://www.python.org, 1991–.

[188] Eric Jones, Travis Oliphant, Pearu Peterson, and others. SciPy: Open source scientific tools for Python. http://www.scipy.org/, 2001–.

[189] Stéfan van der Walt, S. Chris Colbert, and Gaël Varoquaux. The NumPy Array: A Structure for Efficient Numerical Computation. *Computing in Science & Engineering*, 13(2):22–30, March 2011. doi: 10.1109/MCSE.2011.37.

[190] Travis E. Oliphant. Python for Scientific Computing. *Computing in Science & Engineering*, 9(3):10–20, May 2007. doi: 10.1109/MCSE.2007.58.

[191] Alireza Najafi-Yazdi, Benedicte Cuenot, and Luc Mongeau. Systematic definition of progress variables and Intrinsically Low-Dimensional, Flamelet Generated Manifolds for chemistry tabulation. *Combustion and Flame*, 159 (3):1197–1204, March 2012. doi: 10.1016/j.combustflame.2011.10.003.

[192] Matthias Ihme, Lee Shunn, and Jian Zhang. Regularization of reaction progress variable for application to flamelet-based combustion models. *Journal of Computational Physics*, 231(23):7715–7721, October 2012. doi: 10.1016/j.jcp.2012.06.029.

[193] Yi-Shuai Niu, Luc Vervisch, and Pham Dinh Tao. An optimization-based approach to detailed chemistry tabulation: Automated progress variable definition. *Combustion and Flame*, 160(4):776–785, April 2013. doi: 10.1016/j.combustflame.2012.11.015.

[194] Uwe Prüfert, Sandra Hartl, Franziska Hunger, Danny Messig, Michael Eiermann, and Christian Hasse. A Constrained Control Approach for the Automated Choice of an Optimal Progress Variable for Chemistry Tabulation. *Flow, Turbulence and Combustion*, 94(3):593–617, February 2015. doi: 10.1007/s10494-015-9595-3.

[195] Cécile Pera, Julien Réveillon, Luc Vervisch, and Pascale Domingo. Modeling subgrid scale mixture fraction variance in LES of evaporating spray. *Combustion and Flame*, 146(4):635 – 648, 2006. doi: 10.1016/j.combustflame.2006.07.003.

[196] C. M. Kaul, V. Raman, G. Balarac, and H. Pitsch. Numerical errors in the computation of subfilter scalar variance in large eddy simulations. *Physics of Fluids (1994-present)*, 21(5):055102, 2009. doi: 10.1063/1.3123531.

This dissertation is concerned with the study of turbulent spray combustion in the context of diesel engines using Large Eddy Simulation (LES). A challenge arises from the description of the complex chemical reactions that take place during the oxidation of fuels used in such engines. The approach to address this in the present work is based on the Flamelet Generated Manifold (FGM) method. The objectives of the dissertation are to explore and implement modeling approaches which allow to investigate high-velocity fuel sprays, and specifically their ignition and combustion characteristics, in LES. The investigated spray combustion cases correspond to Spray A, a reference case defined within the Engine Combustion Network (ECN). The results show that the chosen approach towards the simulation of turbulent spray flames is suitable and allows for a detailed analysis of the unsteady processes.

**BUSINESS +
ECONOMY**

**ART +
DESIGN +
ARCHITECTURE**

**SCIENCE +
TECHNOLOGY**

CROSSOVER

**DOCTORAL
DISSERTATIONS**